DYNAMICS MODEL FOR PREDICTING MAXIMUM AND TYPICAL ACCELERATION RATES OF PASSENGER VEHICLES

Matthew C. Snare

Thesis submitted to the Faculty of the Virginia Polytechnic Institute and State University
in partial fulfillment of the requirements for the degree of

Master of Science
in
Civil Engineering

Dr. Hesham Rakha, Chair
Dr. Francois Dion
Dr. Pushkin Kachroo

August 26, 2002
Blacksburg, Virginia

Keywords: Vehicle Acceleration, Vehicle Dynamics Models, Traffic Simulation,
Car-Following Behavior

DYNAMICS MODEL FOR PREDICTING MAXIMUM AND TYPICAL ACCELERATION RATES OF PASSENGER VEHICLES

Matthew C. Snare

Abstract

Effectively modeling the acceleration behavior of vehicles is an important consideration in a variety of transportation engineering applications. The acceleration profiles of vehicles are important in the geometric design of roadways and are used to model vehicle behavior in simulation software packages. The acceleration profile of the vehicle is also a critical parameter in fuel consumption and emissions models. This paper develops and validates a vehicle dynamics model to predict the maximum acceleration rates of passenger vehicles. The model is shown to be superior to other similar models in that it accurately predicts speed and acceleration profiles in all domains and for a variety of vehicle types. The paper also modifies the model by introducing a reduction factor, which enables the model to predict the typical acceleration patterns for different driver types. The reduction factors for the driving population are shown to follow a normal distribution with a mean of 0.60 and a standard deviation of 0.08. The paper also provides new data sets containing maximum and typical acceleration profiles for thirteen different vehicles and twenty different drivers.

Acknowledgements

I would like to take this opportunity to thank the many people that helped me throughout the process of creating this thesis. First and foremost, I thank my advisor Dr. Hesham Rakha, who guided me through the research process and was also instrumental in my decision to choose traffic engineering as a career. I would also like to thank the other members of my committee, Dr. Francois Dion and Dr. Pushkin Kachroo, for their support. I would also like to acknowledge the test drivers who volunteered their time towards my data collection. In addition, I thank the Charles Edward Via family for the generous fellowship I received that enabled me to pursue my graduate education. Finally, I am grateful towards my future wife, Miriam, who lifted my spirits when times got rough.

Table of Contents

List of Tables

List of Figures

Chapter One: Introduction

1.1 Background Information

Vehicle behavior is one of the most important -- yet surprisingly one of the most often overlooked -- factors relating to safe and efficient flow of traffic. Donald Drew points out that "the traffic engineer, paradoxically, has done little to study and understand the very element that is responsible for his professional existence [the vehicle]" (1968). Vehicle acceleration in particular has a significant impact on several factors in traffic engineering. These include the analysis of signalized intersections, the application of microsimulation traffic modeling, and the design of roadway characteristics. The acceleration capability of a vehicle is also an important factor in the investigation of certain road accidents. In addition, accurate models of typical acceleration behavior of vehicles are an essential component for some of the state-of-the-art emissions models being developed (Rakha and Ahn, 2002). However, due to the wide variety of vehicle types on the road and the wide variety of driver behavior exhibited on our roadways, it is difficult to model the acceleration behavior of vehicles when considering all these factors. This paper serves to address some of these issues.

1.2 Problem Definition

Existing acceleration models in the literature typically use kinematics to describe acceleration behavior and therefore tend to generalize all personal vehicles into one category. Simply dividing traffic into trucks and cars is no longer sufficient to properly model the differences between the wide variety of vehicles on the road. Also, many of the models only describe maximum acceleration behavior or do not accurately describe typical driver acceleration behavior in the field, other than to give it a fixed percentage of the maximum acceleration value. Furthermore, no complete model has been systematically developed and verified to describe acceleration behavior of personal automobiles based on the forces acting on the vehicle, i.e. vehicle dynamics.

1.3 Thesis Objectives

The objective of this thesis is to develop a vehicle dynamics model to predict acceleration patterns of vehicles ranging from compact cars to SUV's for both maximum acceleration behavior and typical driver behavior, and to test the model through studies in both a controlled environment (Smart Road test facility) and in actual driving conditions.

1.4 Thesis Contributions

The thesis makes several significant contributions:

- First, the thesis validates a constant power and a variable power vehicle dynamics model to predict the acceleration behavior of personal automobiles. The models are calibrated to describe both maximum acceleration behavior and typical acceleration behavior. The models will be useful for several purposes. They will help to define vehicle acceleration patterns in microsimulation software packages, and can also be used in other models -- such as emissions models -- whose variables are related to acceleration rates.

- Second, the thesis examines the effect of various variables on the accuracy of the models. These variables include vehicle type, vehicle age, vehicle weight, driver gender, and driver age. The paper addresses how the vehicle and driver characteristics affect the dispersion of the vehicle speed data.

- Third, the thesis provides a fresh set of vehicle acceleration data. Much of the data used to verify existing models is outdated or extrapolated to reflect current conditions. The thesis provides vehicle speed and position data collected by GPS units every second for vehicles that were actually in-use during the year 2001. The data is also categorized by vehicle type, vehicle properties, and driver characteristics. This new data can be used to compare model effectiveness, and test the validity of previously extrapolated data.

1.5 Thesis Layout

The thesis consists of six chapters. It first presents a literature review, followed by a description of the research methodology applied. Subsequently, constant power and variable power vehicle dynamics models are presented and verified for maximum vehicle acceleration and for typical acceleration behavior. Finally, conclusions are drawn, and recommendations for further research are presented.

Chapter 2 discusses the existing models for predicting vehicle acceleration behavior in the literature and documents where existing research is lacking.

Chapter 3 describes the research approach taken. The section outlines the model development procedure, summarizes the vehicle testing that was performed, and discusses how the models were validated.

Chapter 4 presents a constant power model and a variable power model for predicting maximum vehicle acceleration behavior and compares the models to field data collected for a variety of vehicles.

Chapter 5 presents variations to the constant power and variable power models presented in Chapter 4 to reflect typical driver behavior, and compares the results to field data obtained for different driver types.

Chapter 6 provides a summary of the findings and recommends future research actions.

Chapter Two: Literature Review

2.1 Introduction

Effectively modeling the acceleration behavior of vehicles is an important component in a variety of traffic engineering applications. The AASHTO Geometric Design of Highways and Streets points out that the acceleration rates of vehicles are often critical parameters in determining highway design (1994). They are important in dimensioning intersections, ramps, climbing lanes, and other roadway features. Acceleration models are also an integral part of microscopic traffic simulation models. The fundamental movement of the vehicles throughout a simulation network is based on acceleration models. Determining vehicle acceleration capability is also sometimes important when investigating road accidents (Searle, 1999). In addition, predicting fuel consumption is dependent on the vehicle's acceleration rate (Akcelik, 1987). The vehicle's acceleration rate also has a significant impact on vehicle emissions rates, and therefore effective acceleration models are needed in the development of state-of-the-art emissions models (Rakha and Ahn, 2002).

Consequently, several researchers have developed models in an attempt to predict the speed and acceleration profiles of the different vehicles on the roadway to be used for the various purposes described above. Essentially, these models can be broken down into two types -- models that predict behavior based on kinematics of motion, and models that incorporate vehicle dynamics. The following sections describe these existing models, their intended applications, and their strengths and weaknesses, followed by a conclusions section that documents where the existing research is lacking.

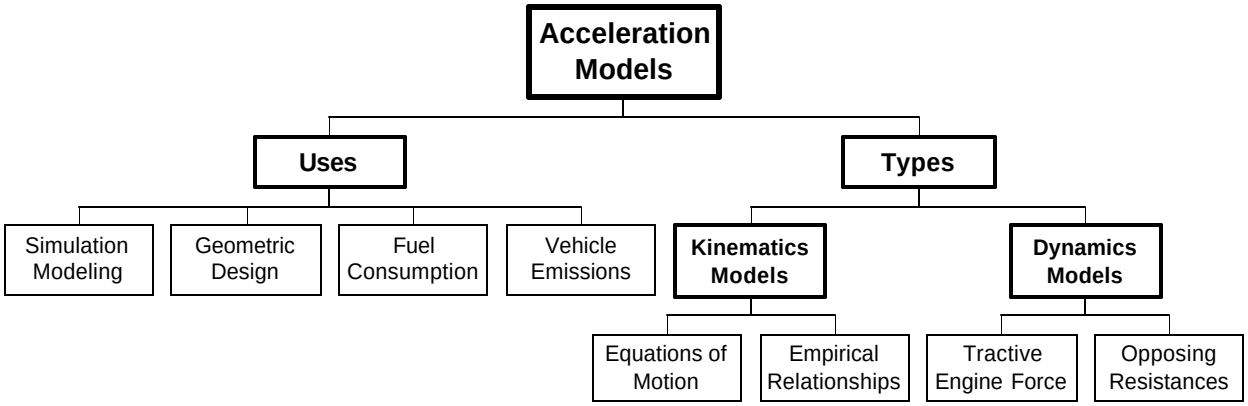

Figure 2-1: Acceleration Models Flow Chart

2.2 Modeling Using Kinematics

Kinematics models take into account the mathematical relationship between acceleration, speed, and distance traveled of any moving object. The most basic of these models is the constant acceleration model. In this model, the acceleration of the vehicle is assumed to be constant for the entire period in which the vehicle is accelerating. Because acceleration is the derivative of speed, and speed is the derivative of distance, the following relationships can be generated: (Drew, 1968)

$$\frac{dv}{dt} = a \qquad [2\text{-}1]$$

$$\int_{v_0}^{v} dv = \int_{0}^{t} a \; dt \qquad [2\text{-}2]$$

$$v = v_0 + at \qquad [2\text{-}3]$$

$$\int_{0}^{x} dx = \int_{0}^{t} (v_0 + at)dt \qquad [2\text{-}4]$$

$$x = v_0 t + \frac{1}{2}at^2 \qquad [2\text{-}5]$$

Where: $a =$ acceleration
$v =$ speed
$v_0 =$ initial speed
$x =$ distance
$t =$ time

While this is the oldest and most commonly used model, it is evident from field research that vehicle behavior does not exhibit constant acceleration, and that the assumption of constant acceleration in a model produces erroneous results when compared to field data. However, because of its simplicity, the constant acceleration model is still used in several traffic simulation packages.

Field studies have shown that vehicles can accelerate at a higher rate when traveling at lower speeds. Therefore, Bham and Benekohal developed a dual-regime model (2002). This model is similar to the constant acceleration model, except that two different acceleration rates are used -- one for low speeds and another for high speeds. The two acceleration rates can be found from the average speed profile of vehicles from the field data. Based on two sets of field data, it was determined that the second regime begins at a speed of approximately 13 m/s. It is unclear how this value was determined or if different cutoff speeds would be calculated for different data sets. This model is used in the traffic simulation model ILLISIM/CELLSIM.

In an attempt to more accurately describe actual vehicle behavior, a linear decay model was developed (also known as the non-uniform acceleration model). This model assumes that acceleration rates vary inversely with speed (Drew, 1968). In this model, vehicles obtain their maximum acceleration at a speed of 0, and the acceleration rate decreases

linearly to a value of 0 at the maximum speed. The vehicle's acceleration behavior is represented by the following relationship.

$$a = a - bv \qquad [2\text{-}6]$$

In this formulation, α is a constant representing the maximum acceleration rate, and the ratio α/β represents the maximum speed that can be attained. Using the fundamental equations of kinematics, the following relationships can be determined from the linear decay model that relate speed and distance traveled to time.

$$v = \frac{a}{b}(1 - e^{-bt}) + v_0 e^{-bt} \qquad [2\text{-}7]$$

$$x = \frac{a}{b}t - \frac{a}{b^2}(1 - e^{-bt}) + \frac{v_0}{b}(1 - e^{-bt}) \qquad [2\text{-}8]$$

Long has compiled a list of typical values for α and β from various sources as they relate to different vehicle types and driver behavior (2000). He found that values for β are similar for each vehicle type, and the values for α increase with decreasing weight-to-horsepower ratios. His research was primarily focused on geometric design considerations.

A similar model to the linear decreasing model, known as the linear acceleration model, has also been developed. In this model, acceleration decreases as a function of time rather than as a function of speed (Lee, 1977). Acceleration of the vehicle is described in this model as:

$$a = a_0 + b\,t \qquad [2\text{-}9]$$

Where: β = acceleration slope

The speed and distance relationships derived from the model are:

$$v = v_0 + a_0 t + 0.5 b\,t^2 \qquad [2\text{-}10]$$

$$x = x_0 + v_0 t + 0.5 a_0 t^2 + 0.167 b\,t^3 \qquad [2\text{-}11]$$

This model is used in the traffic simulation models INTELSIM and TEXAS. However, Bham and Benekohal have found a much stronger relationship between acceleration and speed than acceleration and time, and do not recommend the use of this model (2002).

Further study of the acceleration patterns of vehicles revealed some additional characteristics of the speed profile. Studies showed that the rate of acceleration was not maximum at time 0, as the linear decreasing and linear acceleration models suggest, but rather equaled 0 at time 0 and increased rapidly to its maximum value at a time after t = 0 (Dockerty, 1966). After additional study of speed-time data collected by the Sydney University, Akcelik noted the following three requirements for an acceleration model (1987).

- The speed profiles should indicate an S-shape.
- Acceleration rate must equal 0 at the start and end of acceleration.
- Jerk (da/dt) should equal 0 at the start and end of acceleration.

Akcelik developed three kinematics acceleration models primarily to assist in fuel consumption modeling based on these criteria (1987). The first of the three models developed is the two-term sinusoidal model. This model presents an empirical mathematical relationship for acceleration as a function of time as described by the series of equations below:

$$a(t) = Ca_m(\sin pq + B\sin 2pq) \quad [2\text{-}12]$$

$$B = \lfloor 4(v_a - v_0)/(v_f - v_0) \rfloor - 2 \quad [2\text{-}13]$$

$$1/C = \sin pq_m + B\sin 2pq_m \quad [2\text{-}14]$$

$$q_m = \frac{t_m}{t_f} = \frac{1}{p}\cos^{-1}[(-1 + (1 + 32B^2)^{\frac{1}{2}})/8B] \quad [2\text{-}15]$$

Where: a_m = maximum acceleration

v_a = average speed during acceleration

v_f = final speed

t_m = time to reach maximum acceleration

t_f = total acceleration time

To ensure that acceleration is greater than zero, the value of B is restricted to values between –1/2 and 1/2. This condition also restricts the value of θ_m to values between 1/3 and 2/3. This means that the maximum acceleration can only occur at times between 1/3 and 2/3 of the total acceleration time. Speed and distance can be calculated from the model as follows:

$$v(t) = v_0 + 0.5(v_f - v_0)[(1 + 0.5B) - \cos pq + 0.5B\cos 2pq] \quad [2\text{-}16]$$

$$x(t) = tv_0 + 0.5(v_f - v_0)[(1 + 0.5B)t - 0.318t_f \sin pq - 0.07996Bt_f \sin 2pq] \quad [2\text{-}17]$$

This model does satisfy the condition of zero acceleration at the start and end of acceleration, but does not account for the condition of zero jerk. To account for this, Akcelik developed a three-term sinusoidal model. This model describes acceleration as:

$$a(t) = Ra_m(0.5 - P\cos pq - 0.5\cos 2pq + P\cos 3pq) \quad [2\text{-}18]$$

$$P = (9p^2/32)(-0.5 + (v_f - v_a)/(v_f - v_0)) \quad [2\text{-}19]$$

$$q_m = \frac{1}{p}\cos^{-1}(1 - (1 + 48P^2)^{\frac{1}{2}})/12P),\ P \neq 0 \quad [2\text{-}20]$$

$$q_m = 0.5, P = 0$$

$$R = (1 - 3\cos^2 g)/(\sin^4 g) \quad [2\text{-}21]$$

$$g = pq_m \quad [2\text{-}22]$$

Like the two-term sinusoidal model, this model is subject to several restrictions and is therefore limited in its application. The value of P is restricted to values between –0.25 and 0.25. This equates to a restriction on θ_m to values between 0.392 and 0.608. This restriction is more severe than the restriction in the two-term model. Equations for speed and distance associated with the three-term sinusoidal model are as follows:

$$v(t) = v_0 + \frac{Ra_m t_f}{p}\left[0.5pq - P\sin pq - 0.25\sin 2pq + \frac{P}{3}\sin 3pq\right] \quad [2\text{-}23]$$

$$x(t) = tv_0 + \frac{Ra_m t_f}{p}\left[\frac{0.785t^2}{t_f} + 0.318Pt_f\cos pq + 0.0398t_f\cos 2pq - 0.035Pt_f\cos 3pq\right] \quad [2\text{-}24]$$

Bham and Benekohal found that the distance calculated in the three-term sinusoidal model becomes negative when P values other than –0.14068 are used (2002). The model therefore needs modification to allow different values of P to be used. Akcelik feels his best model is the polynomial model (1987). This model generates a peak in the acceleration profile near the beginning of the acceleration period, which more closely matches the field results. Acceleration using the polynomial model is defined as:

$$a(t) = ra_m q(1-q^m)^2 \quad (m > -0.5) \quad [2\text{-}25]$$

$$m = \frac{15 - 27r + (81r^2 - 138r + 73)^{0.5}}{12r - 4} \quad [2\text{-}26]$$

$$r = \frac{v_a - v_0}{v_f - v_0} \quad [2\text{-}27]$$

$$ra_m = \frac{2(m+1)(m+2)}{m^2}a_{avg} \quad [2\text{-}28]$$

Relationships for speed and distance traveled are calculated as follows:

$$v(t) = v_0 + t_f ra_m q^2\left[0.5 - \frac{2q_m}{m+2} + \frac{q^{2m}}{2m+2}\right] \quad [2\text{-}29]$$

$$x(t) = v_0 t + t_f^2 ra_m q\left[\frac{1}{6} - \frac{2q^m}{(m+2)(m+3)} + \frac{q^{2m}}{(2m+2)(2m+3)}\right] \quad [2\text{-}30]$$

The three models developed by Akcelik require that the total distance traveled be known in order to calculate the acceleration rates. This restricts the use of the model when this value is not known or cannot be approximated easily (Bham, 2002).

Varat and Husher have developed three models that also attempt to replicate acceleration curves observed in field data by using mathematical functions (2000). These three models include the haversine model, the sinusoidal model, and the triangular model. Each of these models predicts that maximum acceleration will occur at the center of the acceleration profile, but each describes the acceleration behavior of the vehicle in a slightly different way. Acceleration in the haversine model is described as:

$$a(t) = a\sin^2 q = a\sin^2\left(\frac{pt}{t_t}\right) \quad [2\text{-}31]$$

In this model, α represents the maximum acceleration rate as it did in the linear decreasing model. From this relationship, values for speed and distance are calculated as:

$$v(t) = v_0 + \frac{a}{4p}\left[2pt - t_f \sin\left(\frac{2pt}{t_f}\right)\right] \quad [2\text{-}32]$$

$$x(t) = \frac{t(at + 4v_0)}{4} + \frac{t_f^2}{8p^2}\left[\cos\left(\frac{2pt}{t_f}\right) - 1\right] \quad [2\text{-}33]$$

Similarly, the sinusoidal model describes acceleration, speed, and distance as:

$$a(t) = a \sin\left(\frac{pt}{t_t}\right) \quad [2\text{-}34]$$

$$a = \frac{p\,(v_f - v_0)}{2t_f} \quad [2\text{-}35]$$

$$v(t) = v_0 + \frac{t_f a}{p}\left[a - \cos\left(\frac{pt}{t_f}\right)\right] \quad [2\text{-}36]$$

$$x(t) = v_0 t + \frac{t_f a}{p}\left[t - \frac{t_f \sin(pt/t_f)}{p}\right] \quad [2\text{-}37]$$

The triangular model models acceleration in the shape of an isosceles triangle. The peak representing maximum acceleration occurs at time $t_f/2$, and the acceleration profile is broken into two regimes as follows:

$$a(t) = \frac{2at}{t_f},\ 0 \le t \le \frac{t_f}{2} \quad [2\text{-}38]$$

$$a(t) = 2a - \frac{2at}{t_f},\ \frac{t_f}{2} \le t \le t_f \quad [2\text{-}39]$$

Equations for speed and distance are defined as:

$$v(t) = v_0 + \frac{at^2}{t_f},\ 0 \le t \le \frac{t_f}{2} \quad [2\text{-}40]$$

$$v(t) = v_0 + 2at - \frac{at^2}{t_f} - \frac{at_f}{2},\ \frac{t_f}{2} \le t \le t_f \quad [2\text{-}41]$$

$$x(t) = v_0 t + \frac{at^3}{3t_f},\ 0 \le t \le \frac{t_f}{2} \quad [2\text{-}42]$$

$$x(t) = v_0 t + at^2 - \frac{at^3}{3t_f} - \frac{att_f}{2} + \frac{at^2}{12},\ \frac{t_f}{2} \le t \le t_f \quad [2\text{-}43]$$

The assumption that the maximum acceleration occurs in the middle of the acceleration profile, as required in the three models described by Varat and Husher, is not consistent with field data. As a result, these models produce unrealistic acceleration and speed

profiles (Bham, 2002). Bham and Benekohal have tried to address this problem by modifying the triangular model to vary the location of the maximum acceleration. Instead of introducing the second regime at time $t/2$, they use the observed time of maximum acceleration as the break point. However, it is very difficult to accurately predict the time of maximum acceleration due to the variety of vehicle capabilities. Therefore, the application of the modified triangular model is limited.

Bham and Benekohal also developed their own model based on the gamma statistical density function (2002). They chose this function because it had a similar shape to the FHWA data acceleration profile. The gamma model describes acceleration from a stopped position as follows:

$$a(t) = \frac{b^{-a} t_i^{a-1} e^{\frac{-t_i}{b}}}{\Gamma(a)} * h,\ a > 0, b > 0 \qquad [2\text{-}44]$$

$$\ln a + y(a) = \frac{\sum_{i=1}^{n} \ln t_i}{n} \qquad [2\text{-}45]$$

$$a\,b = \bar{t}(n) \qquad [2\text{-}46]$$

Where: $\psi(\alpha)$ = digamma function
$\Gamma(\alpha)$ = gamma function
n = total number of observations in field data
t_i = time in seconds
$\bar{t}(n)$ = average duration of time field data was observed

While the gamma model has been shown to perform well for certain data sets, the extensive calibration required and the complexity of the model are limitations.

The kinematics models presented in this section attempt to empirically develop mathematical expressions to describe the acceleration patterns of the vehicle. In doing so, the actual components that go into providing the motion of the vehicle – the tractive force provided by the engine and the opposing resistance forces affecting the vehicle – have essentially been ignored. Therefore, a reasonable fit to field data cannot be expected from these kinematics models in each of the plots of acceleration versus time, speed versus time, and speed versus distance. To better account for the actual physics of motion involved with an accelerating vehicle, vehicle dynamics models have been developed. These models are described in the following section.

2.3 Modeling Using Vehicle Dynamics

Vehicle dynamics describes the forces acting on the vehicle that result in its motion. Tractive effort and resistance are the two primary opposing forces that determine the performance characteristics of road vehicles (Mannering, 1990). The engine in the vehicle supplies the tractive-effort force, and the magnitude of this force is restricted by

internal friction losses. This force is opposed by the forces of air resistance, rolling resistance, grade resistance, and friction resistance (Drew, 1968).

Only a few acceleration models have been developed that incorporate vehicle dynamics. Rakha *et al.* put forth a constant power model and a variable power model to determine the performance of trucks (2001). Their research is the basis for this thesis, and these models are described fully in the following chapter.

Searle also utilized vehicle dynamics when he prepared equations for speed, time, and distance of vehicles under maximum acceleration to help with the investigation of road accidents (1999). The model does not account for the specific effects of the resistances on the vehicle, but rather predicts vehicle performance based on the ratio of engine output to the weight of the vehicle by generating a power constant, k.

$$k = \frac{7.9 * h * P_{\max}}{M} \qquad [2\text{-}47]$$

where: k = power constant, bhp/ton (kilowatt/ton)
η = acceleration efficiency
P_{max} = maximum engine power, bhp (kilowatts)
M = mass of vehicle, tonnes

The acceleration efficiency term (η) accounts for losses in the transmission as well as resistances to motion, such as air resistance. The power constant, k, is then used to predict the speed of the vehicle and distance traveled, as given in the following equations.

$$v^2 = v_0^2 + 2kt \qquad [2\text{-}48]$$

$$v^3 = v_0^3 + 3kx \qquad [2\text{-}49]$$

$$x = \frac{[(v_0^2 + 2kt)^{\frac{3}{2}} - v_0^3]}{3k} \qquad [2\text{-}50]$$

The Searle model provides a reasonable approximation of speeds that can be obtained by vehicles within a specific time frame or over a certain distance. This is useful when trying to recreate accidents for investigations. However, the model is not as useful in describing the overall acceleration behavior of vehicles, as is required in simulation software packages. It does not accurately describe the motion of the vehicle at the beginning of acceleration from a stop or at high speeds.

Bham and Benekohal also found that the model overestimates speed during the initial stages of acceleration because it was formulated to represent maximum acceleration capability (2002). They also found that the model overestimates the distance profile. Therefore, they recommended a modification to the Searle model that would be a better fit to field data. In their model, three different values of the power constant, k, are used during different time periods. The k values can be calculated from field data as follows:

$$k = \frac{v^2 - v_0^2}{2t} = \frac{9x^2}{8t^3} = \frac{v^3}{3x} \qquad [2\text{-}51]$$

Using this model provided a good fit to the field data. However, it is difficult to determine appropriate breaking points for the different regimes, and these breaking points vary for different data sets. This model also requires extensive calibration and is not very easy to use.

2.4 Maximum vs. Typical Acceleration

The majority of these models only predict the maximum acceleration capabilities of a vehicle. However, drivers rarely use the full capabilities of the vehicle while driving in their everyday lives. The maximum acceleration characteristics are not useful in design except as bounding values (Long, 2000). Therefore, it is important to predict the typical driver acceleration behavior exhibited by drivers. However, due to large number of variables -- vehicle type, driver gender, driver age, driver's mood, etc. -- a limited amount of research has been done in this area.

Searle recognized that drivers use only a portion of the potential capability of their vehicle under normal driving conditions (1999). He also noted that because the driver controls the acceleration pattern, there is no guarantee that the acceleration curve will follow the same shape as that for maximum performance. He concluded that the only way to properly account for acceleration at everyday levels was to observe and measure actual vehicles.

Searle observed subject vehicles starting at an intersection and heading along a long straightaway with a speed limit of 60 mph. The vehicles did not know they were participating in the experiment. Searle used a radar gun to track the vehicle's speed as it accelerated away, and recorded its make and model. Results from six subject vehicles are presented in his work. It is unclear if these were the only six vehicles tested or if these were selected as ones that best fit his model. From these tests, he concluded that normal driving behavior followed a similar path as maximum performance, but was less aggressive. This resulted in a linear relationship between velocity squared and time, as his model suggests, but with smaller slopes than for the maximum acceleration behavior. However, the paper did not try to develop a mathematical relationship between the maximum and typical acceleration values.

Several researchers have taken the typical acceleration behavior of drivers to be some fixed percentage of the maximum acceleration capability throughout the acceleration period. Based on a series of road tests in the 1930's, Loutzenheiser concluded that the normal acceleration rate for drivers was about two-thirds of the maximum value (1938). The 1954 Blue Book declared that the acceleration rate of the average driver was about 60% of the maximum rate for the vehicle (AASHTO). Data presented by Long showed that this approximation was inconsistent with field data (2000). The slope of the acceleration curve was too flat and the maximum acceleration rate is underestimated. In general, Long recommends using a linearly decreasing acceleration model with $\alpha = 2$ and $\beta = 0.12$ to estimate normal driver behavior.

2.5 Comparison of Existing Models

Several sources in the literature have attempted to compare different existing acceleration models using various data sets.

Akcelik compared the three models he developed to the constant and linear decreasing acceleration models using the data extracted from the Sydney field tests (1987). He compared the models based on their ability to predict the acceleration distance and fuel consumption of the vehicles, based on their corresponding relative errors. He broke down the comparisons into three different driving environments, including central business district, urban, and non-urban. He compared the models under three sets of conditions:

- Acceleration time and distance known
- Acceleration time known but distance unknown
- Acceleration time and distance unknown

The percentage errors in distance and fuel consumption were found for each of the models. The mean and standard deviation of the percentage errors were also calculated. Akcelik noted that the standard deviation for percentage errors varied only slightly, and could therefore be attributed to driver behavior. The mean percentage error therefore represents the bias in the model.

After conducting the statistical evaluation of the models, Akcelik concluded that the polynomial model was the best overall and outperformed the other models in predicting acceleration distance and fuel consumption.

Bham and Benekohal performed an extensive comparison of fourteen models (2002). These models included existing kinematics and dynamics models, models they developed, and modifications to existing models that they proposed. A list of the models analyzed is given below:

- Gamma Model
- Single-Regime Model (constant acceleration)
- Dual-Regime Model
- Searle Model
- Modified Searle Model
- Non-Uniform Acceleration Model (linearly decreasing acceleration)
- Linear Acceleration Model
- Polynomial Model
- Two-Term Sinusoidal Model
- Three-Term Sinusoidal Model
- Haversine Model
- Sinusoidal Model
- Triangular Model
- Modified Triangular Model

A variety of statistical tests were used to compare the different acceleration models based on their compliance with data collected by FHWA in 1983. The paired t-test, and six error tests including root mean square percent error, root mean square error, mean percent error, positive and negative mean percent errors, and maximum absolute error were applied as they related to the speed profile. The authors chose to perform a variety of tests because the strength of each model varied depending on the test applied. The goal was to find the models that performed consistently better than the other models. Based on their tests, the three models that performed the best overall were the modified Searle, gamma, and dual-regime models. The authors note that the modified Searle model and the gamma model require detailed calibration and are very difficult to use. Therefore, despite their ability to match field data, these models are not recommended. The authors recommend the use of the dual regime model for use in traffic simulation models.

It should be noted that the polynomial model, which was determined to perform best by Akcelik against the single-regime model, the non-uniform model, the two-term sinusoidal model, and the three-term sinusoidal model, consistently ranked between fifth and seventh out of the fourteen models for the various error tests performed by Bham and Benekohal. The polynomial model was outperformed by the single-regime model in four of the six error tests using the FHWA data, and was outperformed by the non-uniform, two-term sinusoidal, and three-term sinusoidal models in the paired t-test. This demonstrates that the effectiveness of each of these models is dependant on the data set used and the comparison test applied, which suggests that empirical mathematical models based on one data set may not be the most effective way to model vehicle acceleration behavior.

2.6 Conclusions

Several attempts have been made to model the acceleration patterns of vehicles and drivers. The models range from simplistic approximations of constant acceleration to elaborate statistical distributions designed in an attempt to duplicate the intricate pattern of acceleration profiles observed in field data. Comparison studies show that the effectiveness of these models often varies depending on the set of field data used or the comparison test applied. This is partly because the majority of the models attempt to use empirical kinematics relationships to model a system that is governed by physics. The literature is lacking a complete dynamics model for vehicles that calculates acceleration based on the actual forces and resistances that are responsible for providing the motion. Insufficient study has also been done to relate the typical acceleration patterns of drivers to the maximum capabilities of their vehicles.

A survey of the literature also shows that many of the data sets used to validate or compare models are outdated. Data is lacking that is current, thorough, uses modern vehicles, and contains information on vehicle and driver type. Much of the data collected is from a traffic stream, where acceleration is limited by car following. Using this data, there is also no way to determine the type of cars involved, the roadway conditions, or other features that contribute to the acceleration behavior of the vehicle, such as roadway

grade. Fresh data, complete with vehicle and driver information, collected in a controlled environment with unopposed acceleration is necessary to validate these acceleration models.

It is evident from everyday driving that the acceleration patterns of the various vehicles and driver types traveling on the roadways have large variations. However, no existing model has attempted to address dispersion in the speed profile. An acceleration model that can readily generate a distribution of acceleration and speed profiles for various vehicle and driver types that is based on updated data from modern vehicles would be a valuable tool in simulation modeling and in other applications.

Chapter Three:
Research Methodology

3.1 Introduction

The following research approach has been developed in an attempt to create a vehicle acceleration model that overcomes the shortcomings of prior research efforts. The previous chapter addressed some of the problems with existing acceleration models -- their reliance on outdated data, their dependence on empirical relationships, and their inability to predict the typical acceleration patterns of drivers. The research methodology of this thesis involves four primary tasks that have been designed to address some of the problems seen in existing research efforts. The first task involves establishing a new database through field tests. The second task involves creating a model to predict the maximum acceleration rates of vehicles based on the vehicle and roadway characteristics. The third task involves modifying the model to replicate the typical acceleration behavior of various drivers. The final task involves comparing the models developed within this thesis to other existing models using various data sets. These four tasks are described completely in the following sections.

3.2 Establishing a New Database

The first task in this research effort was to establish a new database of vehicle acceleration data. A fresh set of data was necessary for several reasons. First, the available data in the literature is out-dated. In their comparison study of existing models, Bham and Benekohal (2002) were forced to use data sets that were collected in 1968 and 1983. These sets were used because more recent data sets were not extensive enough and did not capture the acceleration behavior of vehicles for a sufficient amount of time. Obviously, the acceleration capabilities of vehicles have changed dramatically since these data sets were collected. Bham and Benekohal tried to overcome this by extrapolating the trend from the 1968 data through the 1983 data to account for modern vehicle capabilities. The field tests developed for this thesis will create a new data set for modern vehicles and therefore eliminate the need to extrapolate results from old data. Another limitation of existing data is that there is rarely information available on the vehicle types, roadway characteristics, and drivers involved in the data collection. The speed and acceleration data is just grouped together for all vehicles traveling along various grades on different pavement types. Common sense suggests that the acceleration behavior of a vehicle is greatly affected by the power the vehicle can generate, the grade the vehicle is traveling on, and the resistance encountered by the vehicle. However, the existing data sets do not address these issues. The speed and acceleration data collected for this research will be complete with vehicle data, pavement data, and driver data. Finally, the existing data sets are often collected from a traffic stream, where acceleration is limited by car following behavior. The field tests performed here will enable the collection of speed data from vehicles in a controlled environment, where the acceleration is not limited by external factors other than the

vehicle capability and the driver's desire to accelerate at a given level. This is appropriate because the models developed in this thesis are designed to represent the lead vehicle accelerating from a stop line. Many car-following models have been developed to predict the acceleration behavior of vehicles behind the lead vehicle, which is outside the scope of this paper.

3.2.1 *Smart Road Testing*

The following section describes the procedures followed during the first set of field tests of vehicles for the purposes of data collection.

3.2.1.1 *Study Section Description*

The first set of testing was performed during summer 2001 on the Smart Road test facility at the Virginia Tech Transportation Institute in Blacksburg, Virginia. Currently, the Smart Road is a 1.5-km (0.9 mile) roadway that will be expanded to a 3.2-km experimental highway in southwest Virginia that spans varied terrain, from in-town to mountain passes. The horizontal layout of the test section is fairly straight with some minor horizontal curvature that does not impact vehicle speeds. The vertical layout of the section demonstrates a substantial upgrade that ranges from 6% at the leftmost end to 2.8% at the rightmost end, as illustrated in Figure 3-1. In constructing the vertical profile of the test section the elevation of 35 stations were surveyed, as indicated in Figure 3-1. The vertical profile of the test section was then generated by interpolating between station elevations using a cubic spline interpolation procedure at 1-m (3.28-ft) increments. The cubic spline interpolation ensures that the elevations, the slopes, and the rate of change of slopes are identical at the boundary conditions (in this case every meter). The grade was computed for each 1-m (3.28-ft) section and was found to vary considerably, as illustrated in Figure 3-1 (thin line). A polynomial regression relationship was fit to the grade data (R^2 of 0.951) for two reasons. First, this ensured a smooth transition in the roadway grade while maintaining the same vertical profile. Second, it also facilitated the solution of the ODE because it ensures that the grade function is continuous. The modified grade and vertical elevation, which are illustrated in Figure 3-1 (thick line), demonstrate an almost identical vertical profile with much smoother grade transitions when compared to the direct interpolation.

Apart from a 150-m (492-ft) segment of the roadway that was a rigid pavement, the entire roadway surface was asphalt. Consequently, a rolling resistance coefficient for asphalt pavement only was utilized. The quality of the road surface was fair at the time the test runs were conducted. These factors were important in identifying the road surface rolling resistance coefficients.

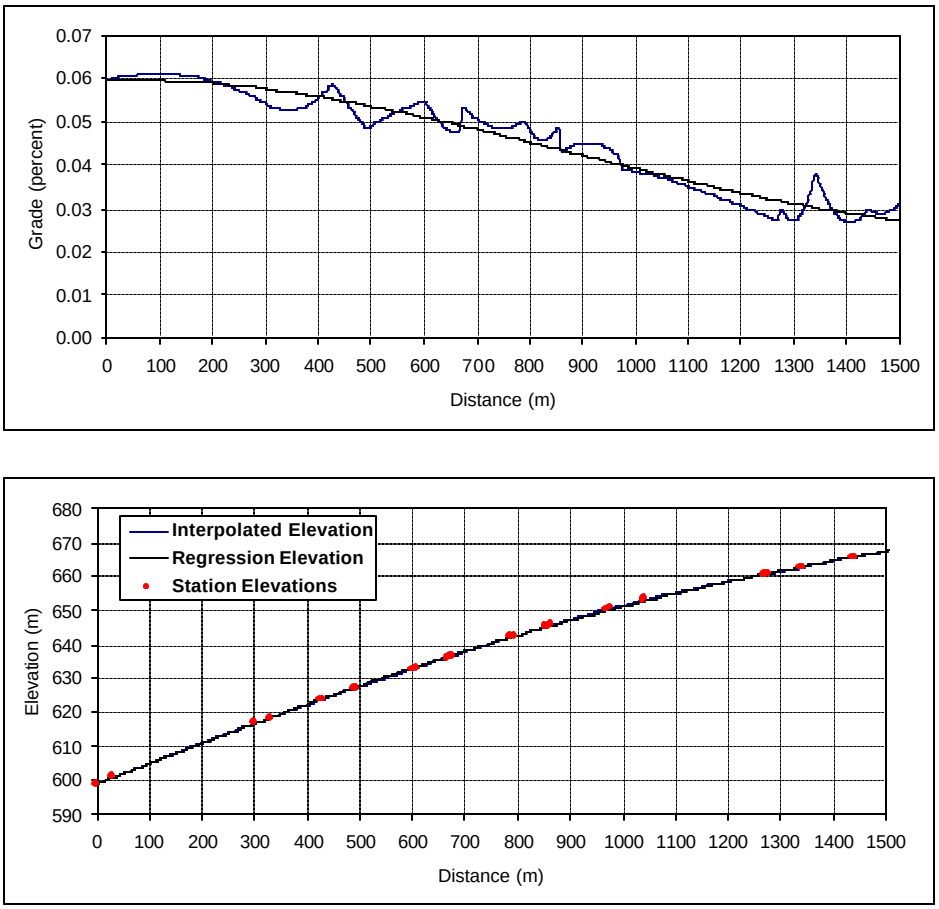

Figure 3-1: Smart Road Vertical Profile

3.2.1.2. *Speed Measurements*

Before each run, test vehicles were equipped with a Global Positioning System (GPS) unit that measured the vehicle speed to an accuracy of 0.1 m/s. (0.305 ft/sec). GPS is a worldwide, satellite-based radio-navigation system that can determine with certain accuracy the position and velocity of any object equipped with a GPS receiver.

Typical output data from GPS receivers include latitude, longitude, altitude, speed, heading, and time. The GPS receivers used were able to update these parameters once every second. Nominal position accuracy is specified with a 25-m (82-ft) spherical error probability, while nominal velocity accuracy is specified within 0.1 m/s (0.31 ft/sec) error probability. These inaccuracies are attributed to a number of sources of error. The majority of these errors are linked to the way the distance between a satellite and a GPS receiver is measured. Within the system, distances are measured by calculating the time it takes for a signal to travel between a satellite and a receiver. Consequently, any delay in the signal transmission then results in distance overestimation and inaccuracies in the estimated position of the object.

3.2.1.3 *Vehicle Descriptions*

Fourteen vehicles were chosen for use in our field tests (See Table 3-1). These vehicles were chosen to reflect the population of passenger vehicles on the roads in the year 2001. Vehicles were chosen from faculty and students at the Virginia Tech Transportation Institute, and therefore constitute the various types of automobiles that were in use at the time. The vehicles represent a wide range of sizes and a variety of EPA vehicle classes including subcompact cars, compact cars, midsize cars, large cars, sport utility vehicles, pickup trucks, and minivans. Many characteristics of each vehicle were recorded including weight, length, frontal area, type of tires, engine type and power, and air drag coefficient. This data, as well as the performance data from the vehicle testing, will be discussed further and analyzed in Chapters 4 and 5.

Table 3-1: Test Vehicles

- **1995 Acura Integra SE**
- **1995 Chevy Blazer**
- **1995 Chevy S10**
- **1995 Dodge Intrepid**
- **1995 Saturn SL**
- **1995 BMW 740I**
- **1996 Geo Metro Hatchback**
- **1998 Ford Windstar**
- **1998 Ford Taurus**
- **1998 Honda Accord**
- **1999 Ford Crown Victoria**
- **2001 Mazda Protégé LX 2.0**
- **2001 Plymouth Neon**

3.2.1.4 *Test Run Description*

Each of the fourteen vehicles was subjected to the same set of tests. The test runs involved accelerating the vehicles from a stop at the start of the test section up to various ending speeds. The tests were performed twice for each set of speeds. First, the drivers accelerated at the maximum possible acceleration rate up to the desired speed. Next, the drivers performed the test while accelerating at typical rates as if they were driving their own vehicles in town. The three speed ranges involved accelerating the vehicle from 0 mph to 35 mph, 0 mph to 55 mph, and 0 mph to the maximum speed that could be achieved by the end of the test section. Depending on the type of vehicle, maximum speeds attained by the end of the test section were between 65 mph and 100 mph. In conducting the study, a minimum of 5 repetitions were executed for each test set in order to provide a sufficient sample size for the validation analysis. This generated a total of 30 test runs for each vehicle. Please see Table 3-2 for a summary of the test runs.

Table 3-2: Summary of Test Runs

	Maximum Acceleration	Typical Acceleration
0 - 35 mph	5 trials	5 trials
0 - 55 mph	5 trials	5 trials
0 – Max	5 trials	5 trials

3.2.2 *Driver Behavior Testing*

A second set of testing was performed in spring 2002 to test the effect of driver characteristics on typical acceleration behavior. For this test, the same vehicle (1999 Ford Crown Victoria) was used for all the trial runs to serve as the control in the experiment. Approximately twenty different drivers were selected for the test, and the drivers were broken down into the following age brackets: 20 to 29 years old, 30 to 39 years old, 40 to 49 years old, and 50 years of age and older. Several drivers were chosen from each age group, and an even split of men and women was chosen.

The test section used was a relatively flat and straight strip of roadway in Blacksburg, Virginia that is controlled by a stop sign and subject to very light traffic volumes, therefore eliminating the effect of car following behavior. The vehicle was equipped with the same GPS receiver as was used during the Smart Road testing. Drivers were instructed to come to a stop at the stop sign and then accelerate from that point, as they would normally until the end of the test section marked by a cone. The test section was approximately 1100 feet in length and typical speeds reached at the end of the test section ranged from 50mph to 70mph, depending on the driver. The driver would then come back to the start line and continue performing twenty-five trial runs so that sufficient sample data could be obtained. The total testing time was approximately one hour. The data from these tests are analyzed in Chapter 5.

3.3 Predicting Maximum Acceleration Rates

After the new database is established, the next task was to develop a model to predict the maximum acceleration rates of different vehicles. The maximum acceleration rate for a vehicle can be determined readily based on several vehicle and roadway characteristics, as proposed by Rakha *et al.* (2001) and described in the following section. As was discussed in the previous chapter, drivers rarely accelerate at the maximum rate available to them. However, it is still important to determine the maximum acceleration rate as a starting point before attempting to apply typical driver behavior to the model.

3.3.1 *Truck Dynamics Model*

The acceleration model presented in this report is an adaptation of a previous model developed at Virginia Tech (Rakha *et al.*, 2001). The Rakha model, as it will be referred to in this text, is a vehicle dynamics model designed to predict the acceleration

characteristics of trucks. This model computes the maximum acceleration based on the resultant force, as indicated in Equation 3-1. Given that acceleration is the second derivative of distance with respect to time, Equation 3-1 resolves to a second-order Ordinary Differential Equation (ODE) of the form indicated in Equation 3-2. The ODE is a function of the first derivative of distance (vehicle speed) because the tractive effort, the rolling resistance, and aerodynamic resistance forces are all functions of the vehicle speed. In addition, the ODE may be a function of the distance traveled if the roadway grade changes along the study section. It should be noted at this point that because the tractive effort includes a minimum operand, the derivative of acceleration becomes a non-continuous function.

$$a = \frac{F - R}{M} \qquad [3\text{-}1]$$

$$\ddot{x} = f(\dot{x}, x) \qquad [3\text{-}2]$$

Where:
F: residual force acting on the truck (N),
M: vehicle mass (kg), and
R: total resistance force (N).

3.3.2 *Tractive Force*

The state-of-practice vehicle dynamics models estimate the vehicle tractive effort using Equation 3-3 with a maximum value based on Equation 3-4, as demonstrated in Equation 3-5. Equation 3-4 accounts for the maximum friction force that can be maintained between the tires of the vehicle's tractive axle and the roadway surface. The use of Equation 3-5 ensures that the tractive effort does not approach infinity at low vehicle speeds.

Equation 3-3 indicates that the tractive force F_t is a function of the ratio between the vehicle speed u and the engine power P. The model assumes the vehicle power to be constant and equal to the maximum potential power. The model considers two main sources of power loss that degrade the tractive effort produced by the truck engine. The first source of power loss is caused by engine accessories including the fan, generator, water pump, magneto, distributor, fuel pump and compressor. The second source of power loss occurs in the transmission system. Typical transmission efficiencies of trucks are assumed to be constant and range from 0.89 to 0.94 depending on the type of transmission (SAE J2188, 1996).

The maximum tractive force is a function of the proportion of the vehicle mass on the tractive axle. Typical axle mass distributions for different truck types and typical axle mass distributions were described in Rakha *et al*. (2001) to range between 30 to 40 percent. Alternatively, the percentage mass on the tractive axle typically ranges from 50 to 65 percent for light duty vehicles.

$$F_t = 3600\, h\, \frac{P}{u} \qquad [3\text{-}3]$$

$$F_{max} = 9.8066\ M_{ta}\ m \quad [3\text{-}4]$$

$$F = \min(F_t, F_{max}) \quad [3\text{-}5]$$

Where:
F: tractive force acting on the truck (N),
F_{max}: maximum tractive force (N),
F_t: tractive force (N),
M_{ta}: vehicle mass on tractive axle, $M \times perc_{ta}$ (kg),
$perc_{ta}$: percentage of vehicle mass on tractive axle (%),
M: vehicle mass (kg),
P: engine power (kW),
u: vehicle speed (km/h),
η: power transmission efficiency (ranges from 0.89 to 0.94), and
μ: coefficient of friction between tires and pavement.

3.3.3 *Aerodynamic Resistance*

State-of-the-art vehicle dynamics models consider three major types of resistance forces, including aerodynamic, rolling, and grade resistances as suggested in the literature (Mannering and Kilareski, 1990; Fitch, 1994; Archilla and De Cieza, 1999; Rakha *et al*., 2001). The total resistance force is computed as the sum of the three resistance components, as summarized in Equation 3-6.

The aerodynamic resistance, or air drag, is a function of the vehicle frontal area, the altitude, the truck drag coefficient, and the square of speed of the vehicle, as indicated in Equations 3-7 and 3-8. The constant c_1 accounts for the air density at sea level at a temperature of 15°C (59ºF). Typical values of vehicle frontal areas for different vehicle types and typical drag coefficients are provided in the literature (Rakha *et al*., 2001). Equation 3-8 is a linear approximation that was derived from a more complex formulation (Watanada *et al*., 1987). The linear approximation was found to provide similar results to the more complex formulation for altitudes in the range of 0 to 5000 m.

$$R = R_a + R_r + R_g \quad [3\text{-}6]$$

$$R_a = c_1 C_d C_h A u^2 \quad [3\text{-}7]$$

$$C_h = 1 - 8.5 \times 10^{-5} H \quad [3\text{-}8]$$

Where:
R_a: aerodynamic resistance (N),
R_r: rolling resistance (N),
R_g: grade resistance (N),
A: frontal area (m^2),
C_d: air drag coefficient,
C_h: altitude coefficient,
H: altitude (m), and
c_1: constant = 0.047285.

3.3.4 *Rolling Resistance*

The rolling resistance is a linear function of the vehicle speed and mass, as indicated in Equation 3-9. Typical values for rolling coefficients (C_r, c_1, *and* c_2), as a function of the road surface type, condition, and vehicle tires, are provided in the literature (Rakha *et al.*, 2001). Generally, radial tires provide a resistance that is 25 percent less than that for bias ply tires.

$$R_r = 9.8066\, C_r\, (c_2 u + c_3)\, \frac{M}{1000} \qquad [3\text{-}9]$$

Where:

M: vehicle mass (kg).

u: vehicle speed (km/h).

C_r, c_2, c_3: rolling resistance constants.

3.3.5 *Grade Resistance*

The grade resistance is a constant that varies as a function of the vehicle's total mass and the percent grade that the vehicle travels along, as indicated in Equation 3-10. The grade resistance accounts for the proportion of the vehicle weight that resists the movement of the vehicle:

$$R_g = 9.8066\, M\, i \qquad [3\text{-}10]$$

Where:

M: vehicle mass (kg).

i: grade magnitude (m/100 m).

3.3.6 *Applying the Truck Model to Cars*

In their research, Rakha *et al*. (2001) showed that the relationships presented herein would give a reasonable approximation of the maximum acceleration rates of trucks for a variety of weight to power ratios. The first goal of this thesis will be to determine if the maximum acceleration behavior of passenger vehicles can also be determined using this model by comparing the speed and acceleration values predicted by the model to the data collected in our field tests for the fourteen test vehicles. Figure 3-2 demonstrates the good fit between the constant power model and field data collected for the Dodge Intrepid during this research effort.

Although the model developed by Rakha *et al.* showed reasonable correlation to field data, it did tend to overestimate speeds at the beginning of the acceleration profile for trucks. They determined that this was due to the loss of power at the beginning of acceleration caused by gear shifting. To account for this, Rakha and Lucic developed a variable power model, which is described in the following section (2002).

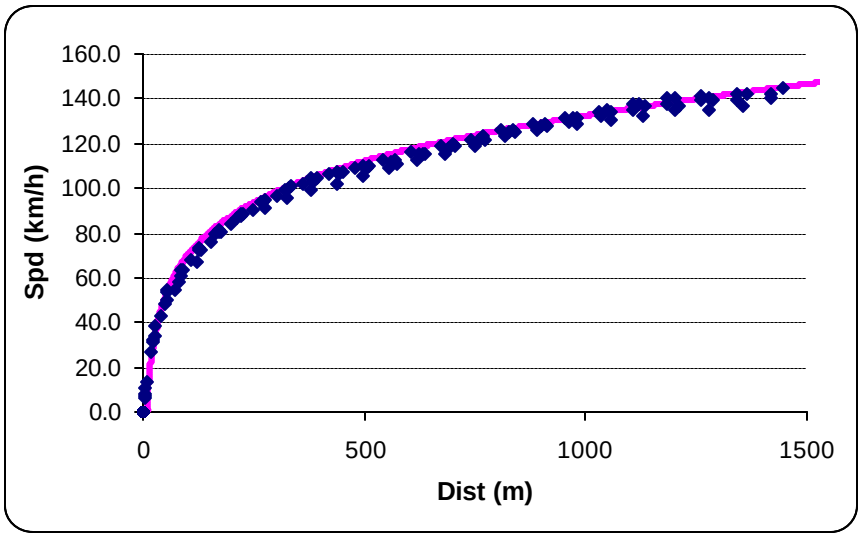

Figure 3-2: Constant Power Model Fit to Field Data for the Dodge Intrepid

3.3.7 *Variable Power Model*

Rakha and Lucic (2002) proposed the use of a variable power efficiency factor that is dependent on the vehicle speed, as opposed to a constant transmission efficiency factor that is currently utilized in state-of-the-art vehicle dynamics models. The power is assumed to increase linearly from an intercept of zero to a maximum value of 1.0 at a speed u_0, as demonstrated in Equation 3-11. In order to ensure that the vehicle has sufficient power to accelerate from a speed of zero, a vehicle power lower bound is computed using a speed of 1 km/h, as demonstrated in Equation 3-11. The adjustment factor is then multiplied by the vehicle power and incorporated in Equation 3-3 to compute the tractive force, as demonstrated in Equation 3-12.

The estimation of the variable power factor "b" requires the calibration two parameters, namely, the minimum power and the speed at optimum power. Given that the proposed model assumes the minimum power to be a function of the optimum speed, as demonstrated in Equation 3-11, only one parameter is calibrated, namely the speed at which the vehicle attains its optimum power. These parameters have been calibrated for trucks and research is currently underway to calibrate similar relationships for light duty vehicles. Specifically, the parameters were calibrated for engine powers ranging from 260 to 375 kW (350 to 500 hp), each involving ten weight configurations. The calibration demonstrated that higher weight-to-power ratios required a lower optimum speed and a higher minimum power. The proposed power model addresses this need for a variable lower bound while maintaining a single calibration parameter.

Figure 3-3 illustrates the variation in the vehicle power and the resulting vehicle acceleration by incorporating the power adjustment factor that is presented in Equation 3-11. As illustrated in the figure, the modification reduces the vehicle acceleration levels at

lower speeds with a minor alteration of vehicle speeds at high speeds. It should be noted that the use of exponential smoothing ensures that the acceleration increases gradually as the vehicle accelerates from a complete stop.

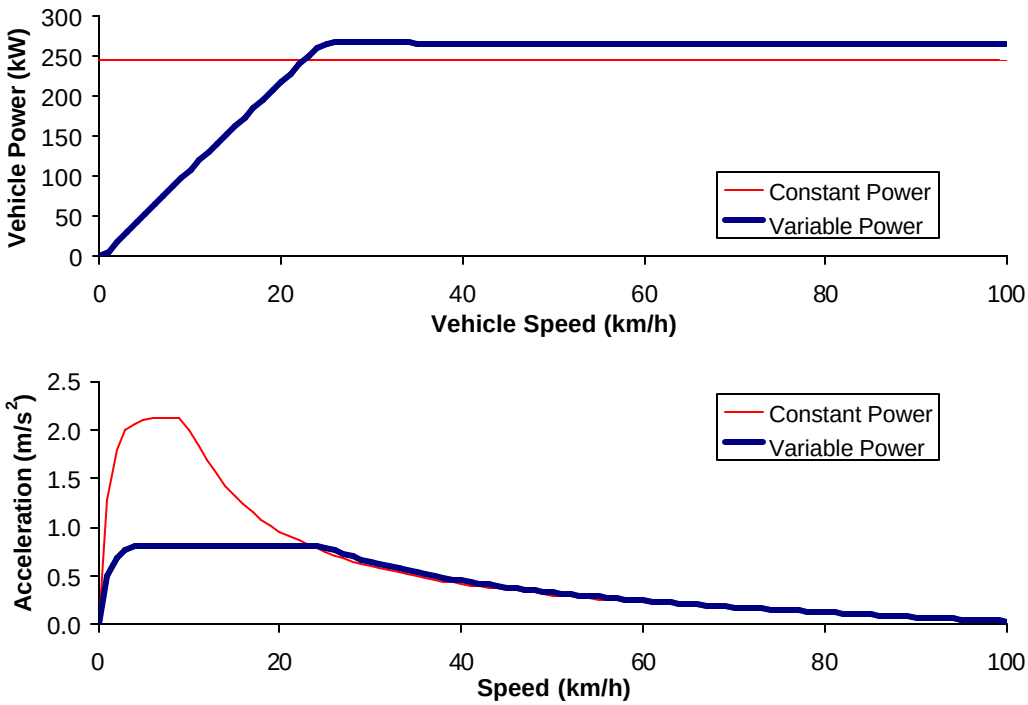

Figure 3-3: Comparison of Constant Power Model to Variable Power Model

The calibration of the variable power transmission efficiency involves determining the speed at which the vehicle power reaches its maximum (optimum speed). The optimum speed was found to vary as a function of the weight-to-power ratio. The specifics of how this relationship was derived are discussed in the literature (Rakha and Lucic, 2002); however, it is sufficient to note at this point that the relationship is a power relationship, as demonstrated by Equation 3-13. The linearly increasing power/speed relationship results in a constant acceleration as a function of vehicle speed given that force (product of the vehicle mass and acceleration) is the first derivative of power with respect to speed and that the vehicle mass is a constant.

$$b = \begin{cases} \dfrac{1}{u_0} & u < 1 \\ \dfrac{u}{u_0} & 1 \le u \le u_0 \\ 1.0 & u > u_0 \end{cases} \qquad [3\text{-}11]$$

$$F_t = 3600\, b\, \frac{P}{u} \qquad [3\text{-}12]$$

$$u_0 = 1164\, w^{-0.75} \qquad [3\text{-}13]$$

Where:

β: Variable power transmission efficiency (unitless).
u: Vehicle speed (km/h).
u_0: Speed at which vehicle attains maximum power (km/h).
w: Vehicle weight-to-power ratio (kg/kW).

3.3.8 *Calibrating the Variable Power Model*

This thesis will also examine the accuracy of the variable power model with respect to predicting the acceleration capability of the fourteen vehicles utilized in the field tests. This will require more effort, because the speed at which maximum power occurs must first be calibrated for each vehicle before the model can be applied. For trucks, this speed was related to the vehicle weight-to-power ratio, as described above. Rakha and Lucic found a better correlation between truck speeds and the speeds predicted by the variable power model in comparison to the constant power model (2002). This research attempts to determine if it is appropriate or necessary to apply the variable power model to cars. Passenger cars carry much less mass than trucks and also have fewer gears, so the gear-shifting effect may not be as substantial as it is for trucks. If the constant power model could be shown to be as effective as the variable power model for cars, it would be beneficial because the variable power model is more complex and requires additional calibration. These are the issues that this thesis attempts to address in regards to predicting maximum acceleration rates of passenger vehicles.

3.4 Predicting Typical Acceleration Behavior

The third task of this research effort involves modifying the constant power and variable power models to account for typical acceleration rates applied by drivers during their normal driving activities. It is clear that the actual acceleration rates applied by drivers will be some fraction of the maximum acceleration capability. However, it is unclear whether this is some fixed percentage throughout the acceleration of the vehicle or whether the percentage of acceleration power used varies as a function of speed or time. It is also unclear how much variability there is between different drivers or even within runs for the same driver. Therefore, the following procedure was developed for this task:

- First, a constant reduction factor will be calibrated and tried based on the results of the field data. This could be a fixed value or a range of values, depending on the dispersion of the results. The reduction factor would be multiplied by the maximum acceleration predicted by the original models to get the typical acceleration rates. The accuracy of this model will be checked against the field data.
- Second, a reduction factor that varies as a function of speed will be incorporated into the model and checked for accuracy. As was discussed in the previous chapter, constant reduction factors tended to underestimate maximum acceleration levels when applied to the linear decreasing model. By creating a reduction factor that varies with speed, we hope to create a better fit to field data.

- A recommendation for future action would be to incorporate dispersion into the model in an attempt to account for the variability observed within a single driver and between drivers. Results from the first field tests performed seemed to indicate that the variability was minimal at low speeds and then increased as speeds increased. See Figure 3-4. A randomness factor could also be incorporated into the model that would generate a distribution of driver behavior within a traffic stream.

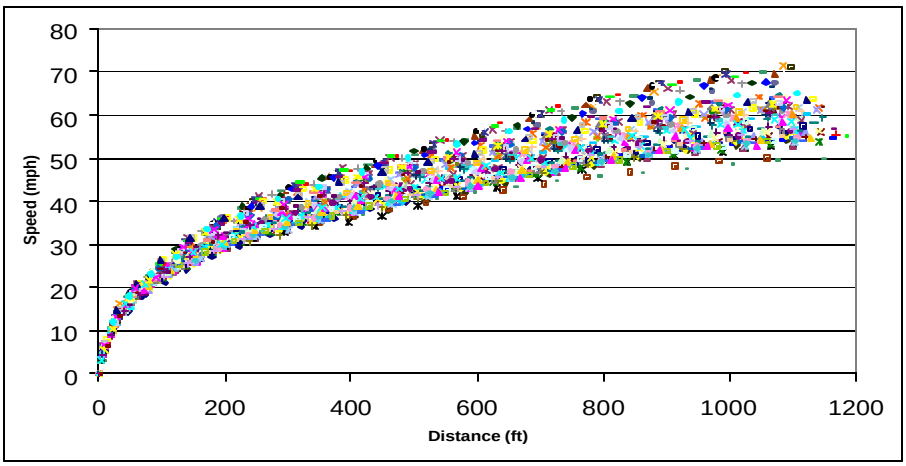

Figure 3-4: Preliminary Test Data from Various Drivers

3.5 Comparison of Models

The final task in this thesis will be to compare the models presented in this report to some of the best-performing models currently available in the literature. This will involve a statistical analysis of each of the models' performance against various data sets, including the one developed herein. We hope to show the benefit of using our models through this comparison.

3.6 Summary

This chapter described the research methodology that is being applied to the problem of developing a vehicle dynamics model to predict the maximum and typical acceleration rates of passenger vehicles. To account for some of the shortcomings of existing research efforts on the topic, four tasks have been identified to enable the development and validation of such a model. These tasks include establishing a new database, which involves performing field tests on various vehicles and drivers, applying existing maximum acceleration models developed for trucks to cars, modifying the model to account for typical driver behavior, and comparing the new models to current state-of-the-art models used in practice.

Chapter Four:
Vehicle Dynamics Model for Estimating Maximum Automobile Acceleration Levels

4.1 Introduction

Microscopic simulation software packages use car-following models to capture the interaction of a vehicle and its preceding vehicle traveling in the same lane. The process of car-following is modeled as an equation of motion under steady-state conditions plus a number of constraints that govern the behavior of vehicles while moving from one steady-state to another (decelerating and accelerating). Typically, up to two constraints are considered. The first constraint governs the vehicle acceleration behavior, which is typically a function of the vehicle dynamics. The second and final constraint ensures that vehicles have a safe position relative to the lead vehicle in order to decelerate to a complete stop without colliding with the preceding vehicle in the event that the preceding vehicle decelerates to a complete stop. In addition, vehicle acceleration behavior is critical to the accurate modeling of vehicle fuel consumption and emissions, as was demonstrated in previous research (Rakha and Ahn, 2002).

This chapter extends the research of Rakha and Crowther (2002), which examined steady-state car-following behavior by characterizing and modeling maximum vehicle acceleration behavior when a vehicle is not constrained by other surrounding traffic. A forthcoming chapter will characterize typical vehicle acceleration behavior for a single and platoon of vehicles.

The paper initially presents state-of-practice vehicle acceleration models and state-of-practice data sets for the modeling of vehicle acceleration behavior. Subsequently, the experimental design and the procedures for collecting new vehicle acceleration data are presented. The state-of-practice vehicle acceleration models are then applied to the data and the validity of the various models are characterized. Finally, the conclusions of the paper and recommendations for further research are presented.

4.2 Background

4.2.1 *State-of-Practice Vehicle Acceleration Models*

Several researchers have developed models that predict vehicle speed and acceleration profiles for inclusion in traffic simulation models. Essentially, these models can be broken down into two categories, namely models that predict acceleration behavior based on kinematics of motion and models that consider vehicle forces in estimating vehicle acceleration (i.e. vehicle dynamics models).

4.2.1.1 *Vehicle Kinematics Models*

Vehicle kinematics models take into account the mathematical relationship between acceleration, speed, and distance traveled for any moving object. They generally start with an empirical mathematical relationship between acceleration and speed or acceleration and time. The values of speed are calculated by integrating acceleration with respect to time while distance traveled is computed by integrating speed with respect to time.

Although similar in principle, kinematics models can range from very simple to very complex. The most basic of these models is the constant acceleration model. As the name suggests, this model uses a constant acceleration value for the vehicle throughout its acceleration maneuver. Because of its simplicity, this model is used in several traffic simulation packages. However, research has shown that the assumption of constant acceleration is erroneous. Specifically, vehicles tend to achieve higher acceleration rates while traveling at low speeds than they at high speeds. To account for this behavior, several models have been suggested. For example, a dual-regime model similar to the constant acceleration model was proposed (Bham, 2002). The model considers two constant acceleration rates, a high rate for low speeds and a lower rate for high speeds. Another commonly used model is the linear decay model. In this model, the acceleration rate of the vehicle starts at some maximum value at a zero speed and decreases linearly as a function of speed. Further research suggested that the maximum acceleration rate might not actually occur at time zero, but rather at some time shortly after the start of acceleration. Field data were gathered to characterize actual vehicle acceleration patterns, such as the profile shown in Figure 4-1. New models based on elaborate statistical distributions and mathematical functions were designed in an attempt to duplicate the intricate pattern of these acceleration profiles observed in field data. Examples of these models include a triangular model in which acceleration increases linearly to its maximum before decreasing linearly (Varat, 2000), a Gamma model based on the gamma statistical density function (Bham, 2002), a polynomial model (Akcelik, 1987), and several models based on the trigonometric sine function (Varat, 2000; Akcelik, 1987). More complete descriptions of all these models can be found in the literature.

Previous studies have demonstrated that the dual-regime, linear decay, and polynomial models best fit field data and were therefore chosen for analysis in this paper. These three models are described in more detail in the following sections.

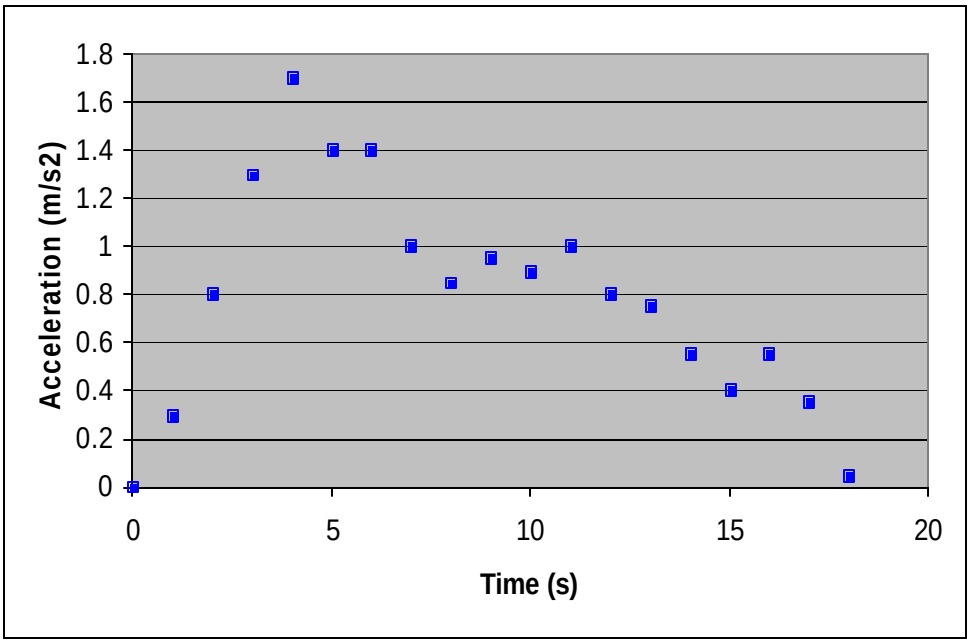

Figure 4-1: Acceleration vs. Time Data (Source: Ohio State University Study, 1968)

a. Dual-Regime Model

The dual-regime model is similar to the constant acceleration model, except that two separate acceleration rates are used, one for low speeds and one for high speeds, as shown in the following equations (Bham, 2002):

$$v_i = v_{i-1} + a_1 t, \quad 0 \le v < 13 \text{ m/s} \qquad [4\text{-}1]$$

$$v_i = v_{i-1} + a_2 t, \quad v > 13 \text{ m/s} \qquad [4\text{-}2]$$

In this formulation, a_1 and a_2 represent the acceleration rates for the first and second regimes, respectively, and can be calculated based on the results of field data. Bham and Benekohal recommended a transition point of 13 m/s for making the switch from the high acceleration rate to the lower rate when applying the model to their data. For this comparison study, a best fit was approximated for each vehicle, which did not necessarily have a transition point at 13 m/s.

b. Linear Decay Model

This linear decay acceleration model assumes that the acceleration rate varies inversely with speed (Drew, 1968). In this model, vehicles attain their maximum acceleration at a speed of zero, and the acceleration rate decreases linearly to a value of 0 at the maximum speed. The vehicle's acceleration behavior is represented by the following relationship.

$$a = a - bv \qquad [4\text{-}3]$$

In this formulation, α is a constant representing the maximum acceleration rate, and the ratio α/β represents the maximum speed that a vehicle can attain. By integrating Equation 4-3, the following relationships can be determined from the linear decay model that relate speed and distance traveled to time.

$$v = \frac{a}{b}(1 - e^{-bt}) + v_0 e^{-bt} \qquad [4\text{-}4]$$

$$x = \frac{a}{b}t - \frac{a}{b^2}(1 - e^{-bt}) + \frac{v_0}{b}(1 - e^{-bt}) \qquad [4\text{-}5]$$

c. Polynomial Model

The polynomial model was designed to satisfy the conditions of zero acceleration and zero jerk (first derivative of acceleration with respect to time) at the start and end of the acceleration maneuver. This model generates a peak in the acceleration profile near the beginning of the acceleration maneuver, which more closely matches the field results than other similar models. Acceleration at any instant *t* is computed using Equation 4-6 in conjunction with Equations 4-7 through 4-9 (Akcelik, 1987).

$$a(t) = ra_m q(1 - q^m)^2 \quad (m > -0.5) \qquad [4\text{-}6]$$

$$m = \frac{15 - 27r + (81r^2 - 138r + 73)^{0.5}}{12r - 4} \qquad [4\text{-}7]$$

$$r = \frac{v_a - v_0}{v_f - v_0} \qquad [4\text{-}8]$$

$$ra_m = \frac{2(m+1)(m+2)}{m^2} a_{avg} \qquad [4\text{-}9]$$

where:
a_m = maximum acceleration
v_a = average speed
v_o = initial speed
v_f = final speed
a_{avg} = average acceleration

By integrating Equation 4-6 the speed and distance traveled at any instant *t* can be computed using Equations 4-10 and 4-11, respectively.

$$v(t) = v_0 + t_f ra_m q^2 \left[0.5 - \frac{2q_m}{m+2} + \frac{q^{2m}}{2m+2}\right] \qquad [4\text{-}10]$$

$$x(t) = v_0 t + t_f^2 ra_m q \left[\frac{1}{6} - \frac{2q^m}{(m+2)(m+3)} + \frac{q^{2m}}{(2m+2)(2m+3)}\right] \qquad [4\text{-}11]$$

4.2.1.2 *Vehicle Dynamics Models*

The problem with the kinematics models, including the ones described above, is that by empirically developing mathematical expressions to describe the acceleration patterns of the vehicle, the actual components that go into providing the motion of the vehicle – the tractive force provided by the engine and the opposing resistance forces resisting the vehicle's motion – are not modeled explicitly. Therefore, in general the vehicle kinematics models do not provide a good fit to field data for each of the acceleration, speed, distance, and time domains. Furthermore, vehicle kinematics models do not account for different vehicle types, roadway grades, and other factors that affect the acceleration patterns of vehicles.

To better account for the actual physics of motion of an accelerating vehicle, acceleration models based on vehicle dynamics have been developed. Vehicle dynamics describes the forces acting on the vehicle that result in its motion. Tractive effort and resistance are the two primary opposing forces that determine the performance characteristics of road vehicles. The engine in the vehicle supplies the tractive-effort force, and the magnitude of this force is restricted by internal friction losses. The forces of air resistance, rolling resistance, grade resistance, and friction resistance oppose the engine tractive force and limit the acceleration capability of the vehicle.

This section describes two vehicle dynamics models, namely the Searle and Rakha models.

a. Searle Model

The Searle model is an example of a vehicle dynamics model. Searle utilized vehicle dynamics when he prepared equations for speed, time, and distance of vehicles under maximum acceleration to help with the investigation of road accidents (1999). The model does not account for the specific effects of the resistances on the vehicle, but rather predicts vehicle performance based on the ratio of engine output to the weight of the vehicle by generating a power constant, k.

$$k = \frac{7.9\, h\, P_{max}}{M} \qquad [4\text{-}12]$$

where:
k = power constant, bhp/ton (kilowatt/ton)
η = acceleration efficiency
P_{max} = maximum engine power, bhp (kilowatts)
M = mass of vehicle, tones

The acceleration efficiency term (η) accounts for losses in the transmission as well as resistances to motion, such as air resistance. The power constant, k, is then used to predict the speed of the vehicle and distance traveled, as given in the following equations.

$$v^2 = v_0^2 + 2kt \qquad [4\text{-}13]$$

$$v^3 = v_0^3 + 3kx \qquad [4\text{-}14]$$

$$x = \frac{\left[\left(v_0^2 + 2kt\right)^{1.5} - v_0^3\right]}{3k} \qquad [4\text{-}15]$$

The Searle model provides a reasonable approximation of speeds that can be obtained by vehicles within a specific time frame or over a certain distance. This is useful when trying to recreate accidents for investigations. However, the model is not as useful in describing the overall acceleration behavior of vehicles, as is required in simulation software packages. It does not accurately describe the motion of the vehicle at the beginning of acceleration from a stop or at high speeds. A complete comparison of the Searle model to other models is presented later in the paper.

b. Rakha Model

Rakha *et al*. described and applied a state-of-practice constant power vehicle dynamics model to the modeling of truck acceleration behavior (2001), while Rakha and Lucic (2002) developed a variable power vehicle dynamics model for predicting maximum truck acceleration levels. This paper seeks to apply these models to light duty vehicles and validate the models against field data. The following sections describe the vehicle dynamics models put forth by Rakha and Lucic as they can be used to predict the maximum acceleration rates of various passenger vehicles.

The model is based on the basic principle of physics that force equals mass times acceleration. If the net force on the vehicle and the vehicle mass are known, the acceleration of the vehicle can be determined by the relationship in Equation 4-16. Note that the net force on the vehicle is the difference between the force applied by the vehicle and the various resistance forces the vehicle encounters as it travels. The mass of the vehicle is constant, but the magnitude of the applied force and the resistance forces are variables. As you will see in the following sections, these values change as a function of vehicle speed and distance traveled. Therefore, given that acceleration is the second derivative of distance with respect to time, Equation 4-16 resolves to a second-order Ordinary Differential Equation (ODE) of the form indicated in Equation 4-17. It should be noted at this point that because the tractive effort includes a minimum operand, the derivative of acceleration becomes a non-continuous function.

$$a = \frac{F - R}{M} \qquad [4\text{-}16]$$

$$\ddot{x} = f(\dot{x}, x) \qquad [4\text{-}17]$$

Where:
F: residual force (N),
M: vehicle mass (kg), and
R: total resistance force (N).

i. *Tractive Force*

The first variable in the fundamental equation of the Rakha model (Equation 4-16) is the force applied by the engine in the vehicle. As Equation 4-18 indicates, the tractive force F_t is a function of the ratio between the vehicle speed v and the engine power P. The

model assumes the vehicle power to be constant and equal to the maximum potential power. The model considers two main sources of power loss that degrade the tractive effort produced by the vehicle engine. The first source of power loss is caused by engine accessories including the fan, generator, water pump, magneto, distributor, fuel pump and compressor. The second source of power loss occurs in the transmission system. Values for the engine efficiencies of the thirteen test vehicles used for data collection are provided later.

Equation 4-18 suggests that the force applied by the vehicle engine approaches infinity as the speed of the vehicle approaches zero. However, the maximum attainable tractive force is constrained by the friction between the vehicle tires on the tractive axle and the roadway pavement. Higher tractive forces would result in wheel spin. Therefore, Equation 4-19 is used to cap the force value to an attainable level. This force is a function of the mass of the vehicle on the tractive axle and the coefficient of friction between the tires and the pavement. Typical values for the percentage of mass on the tractive axle are presented later in the paper. Equation 4-20 demonstrates the overall equation for the force applied.

$$F_t = 3600\,h\,\frac{P}{v} \qquad [4\text{-}18]$$

$$F_{\max} = 9.8066\,M_{ta}\,m \qquad [4\text{-}19]$$

$$F = \min(F_t, F_{\max}) \qquad [4\text{-}20]$$

Where:

F: tractive force (N),
F_{max}: maximum tractive force (N),
F_t: tractive force (N),
M_{ta}: vehicle mass on tractive axle, $M \times perc_{ta}$ (kg),
$perc_{ta}$: percentage of vehicle mass on tractive axle (%),
M: vehicle mass (kg),
P: engine power (kW),
v: vehicle speed (km/h),
η: power transmission efficiency, and
μ: coefficient of friction between tires and pavement.

ii. *Resistance Forces*

The next variable of importance in the fundamental equation (Equation 4-16) is the resistance force. Three major types of resistance forces need to be considered, including aerodynamic, rolling, and grade resistances as suggested in the literature (Fitch, 1994; Mannering, 1990). The total resistance force is simply computed as the sum of the three resistance components, as summarized in Equation 4-21. Each of the three resistance forces is dependant on several parameters, as discussed in the following sections.

$$R = R_a + R_r + R_g \qquad [4\text{-}21]$$

Where:

R_a: aerodynamic resistance (N),
R_r: rolling resistance (N),

R_g: grade resistance (N).

The aerodynamic resistance, or air drag, is a function of the vehicle frontal area, the altitude, the drag coefficient, and the square of speed of the vehicle, as indicated in Equations 4-22 and 4-23. The constant c_1 accounts for the air density at sea level at a temperature of 15°C (59ºF). Typical values of vehicle frontal areas for different vehicle types and typical drag coefficients are provided later in the paper.

Equation 4-23 is a linear approximation that was derived from a more complex formulation (Watanada, 1987). The linear approximation was found to provide similar results to the more complex formulation for altitudes in the range of 0 to 5000 m.

$$R_a = c_1 C_d C_h A v^2 \quad [4\text{-}22]$$

$$C_h = 1 - 8.5 \times 10^{-5} H \quad [4\text{-}23]$$

Where:
A: frontal area (m^2),
C_d: air drag coefficient,
C_h: altitude coefficient,
H: altitude (m), and
c_1: constant = 0.047285.

The rolling resistance is a linear function of the vehicle speed and mass, as indicated in Equation 4-24. Typical values for rolling coefficients (C_r, c_1, *and* c_2), as a function of the road surface type, condition, and vehicle tires, are provided in the literature (Rakha *et al.*, 2001). Generally, radial tires provide a resistance that is 25 percent less than that for bias ply tires.

$$R_r = 9.8066 C_r \ (c_2 v + c_3) \frac{M}{1000} \quad [4\text{-}24]$$

Where:
M: vehicle mass (kg).
u: vehicle speed (km/h).
C_r, c_2, c_3: rolling resistance constants.

The grade resistance varies as a function of the vehicle's total mass and the percent grade that the vehicle travels along, as indicated in Equation 4-25. The grade resistance accounts for the proportion of the vehicle weight that resists the movement of the vehicle:

$$R_g = 9.8066 \ M \ i \quad [4\text{-}25]$$

Where:
M: vehicle mass (kg).
i: grade magnitude (m/100 m).

iii. *Variable Power*

It should be noted that the use of the maximum tractive force constraint that is imposed on the constant power model results in a vehicle power that increases linearly as a function of vehicle speed given that power is equal to the product of force and speed. For

example, Figure 4-2 illustrates for a sample vehicle field observed and model estimated power as a function of vehicle speed.

Rakha and Lucic (2002) demonstrated that in the case of trucks vehicle accelerations predicted by the constant power model over-estimate truck accelerations at low speeds. Rakha and Lucic demonstrated that this over-estimation of truck accelerations was attributed to the fact that the effective engine power is less during low vehicle speeds as a result of gear shift effects. Consequently, Rakha and Lucic proposed a reduction factor to account for the reduced power at low speeds in order to more capture truck acceleration behavior more accurately. This paper will investigate whether such a power reduction factor is required for light duty vehicle vehicles, as was the case for heavy duty trucks, using field observed data, as will be described later in the chapter.

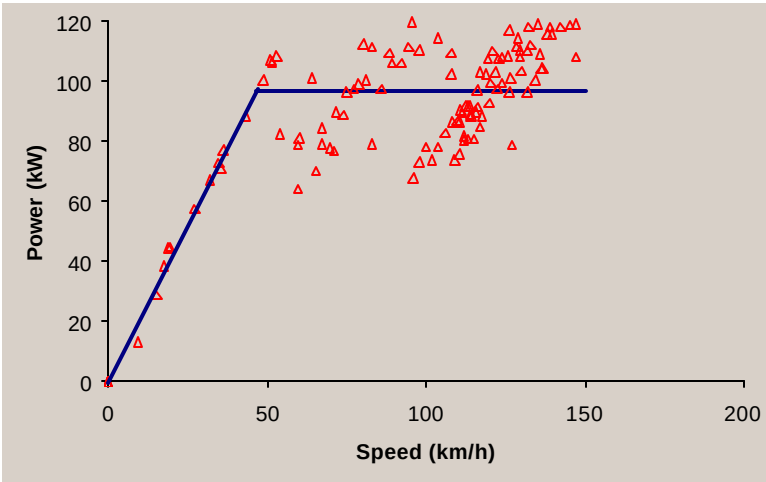

Figure 4-2: Model and Field Measured Power vs. Speed Relationship (Acura Integra)

4.2.2 *State-of-Practice Field Data Sets*

In order to create and validate the acceleration models, data sets compiled from field research are required. Unfortunately, much of the data used to verify existing models are outdated or have been extrapolated to reflect current conditions. For example, in their comparison study of existing models, Bham and Benekohal were forced to use data sets that were collected in 1968 and 1983 (2002). These data sets were used because more recent data sets were not extensive enough and did not capture the acceleration behavior of vehicles for a sufficient amount of time. Obviously, the acceleration capabilities of vehicles have changed dramatically since these data sets were collected. Bham and Benekohal tried to overcome the limitation of the old data sets by extrapolating vehicle acceleration trends from the 1968 data through the 1983 data to account for modern vehicle capabilities. However, it would be more appropriate to use current data if it were available.

Another limitation of existing data is that there is rarely information available on the vehicle types, roadway characteristics, and drivers involved in the data collection effort. Specifically, the speed and acceleration data are aggregated regardless of roadway grade, surrounding traffic, and pavement surface conditions. Furthermore, the data sets do not provide information on the type of vehicles involved in the tests, the roadway conditions, or other features that contribute to the acceleration behavior of the vehicle, such as roadway grade. Common sense suggests that the acceleration behavior of a vehicle is greatly affected by the power the vehicle can generate, the grade the vehicle is traveling on, and the resistance encountered by the vehicle. However, the existing data sets do not address these issues. Finally, the existing data sets are often collected from a traffic stream, where acceleration is limited by vehicle-to-vehicle interaction and thus might not reflect maximum vehicle acceleration behavior.

Consequently, contemporary data are required in which vehicle acceleration behavior is conducted in a controlled environment without vehicle-to-vehicle interaction. In addition, these data sets require that vehicle, driver, and roadway characteristics be documented.

4.3. Construction of Field Data Set

The field tests developed for this report were designed to create a new data set for modern vehicles and therefore eliminate the need to extrapolate results from old data. The speed and acceleration data collected for this research are complete with vehicle, pavement, and driver characteristics. The field tests performed allowed for the collection of speed data from vehicles in a controlled environment, where the acceleration is not limited by external factors other than vehicle capabilities. The data are designed to represent the maximum acceleration of a lead vehicle accelerating from a stop. The modeling of vehicle acceleration in a platoon of vehicles is an area of research that is beyond the scope of this paper and thus requires further investigation. The following sections describe the procedures applied to construct the field data set.

4.3.1 *Smart Road Test Facility*

Testing was performed during the summer of 2001 on the Smart Road test facility at the Virginia Tech Transportation Institute in Blacksburg, Virginia. Currently, the Smart Road is a 3.2-km (2-mile) experimental highway in southwest Virginia that spans varied terrain, from in-town to mountain passes. The horizontal layout of the test section is fairly straight with some minor horizontal curvature that does not impact vehicle speeds. The vertical layout of the section demonstrates a substantial upgrade that ranges from 6% at one end to 2.8% at the other end, as illustrated in Figure 4-3. Apart from a 150-m (492-ft) segment of the roadway that is a rigid pavement, the entire roadway surface is asphalt. Consequently, a rolling resistance coefficient for asphalt pavement only is utilized. The quality of the road surface was good at the time the test runs were conducted. These factors were important in identifying the road surface rolling resistance coefficients used in the Rakha model. Conducting the tests on the Smart Road allowed the vehicles to accelerate without being impeded by other traffic.

In constructing the vertical profile of the test section the elevation of 35 stations were surveyed, as indicated by the diamond symbols in Figure 4-3. The vertical profile of the test section was then generated by interpolating between station elevations using a cubic spline interpolation procedure at 1-m (3.28-ft) increments. The cubic spline interpolation ensures that the elevations, the slopes, and the rate of change of slopes are identical at the boundary conditions (in this case every meter). The grade was computed for each 1-m (3.28-ft) section and was found to vary considerably, as illustrated in Figure 4-3 (thin line). A polynomial regression relationship was fit to the grade data (R^2 of 0.951) for two reasons. First, to ensure a smooth transition in the roadway grade while maintaining the same vertical profile. Second, to facilitate the solution of the ODE because it ensures that the grade function is continuous. The modified grade and vertical elevation, which are illustrated in Figure 4-3 (thick line), demonstrate an almost identical vertical profile with much smoother grade transitions when compared to the direct interpolation. The final equation for grade as a function of distance is given as Equation 4-26.

$$i = 0.059628 + 3.32 \times 10^{-6} x - 3.79 \times 10^{-8} x^2 + 1.42 \times 10^{-11} x^3 \qquad [4\text{-}26]$$

Where:

x: distance (m).

i: grade magnitude (m/100 m).

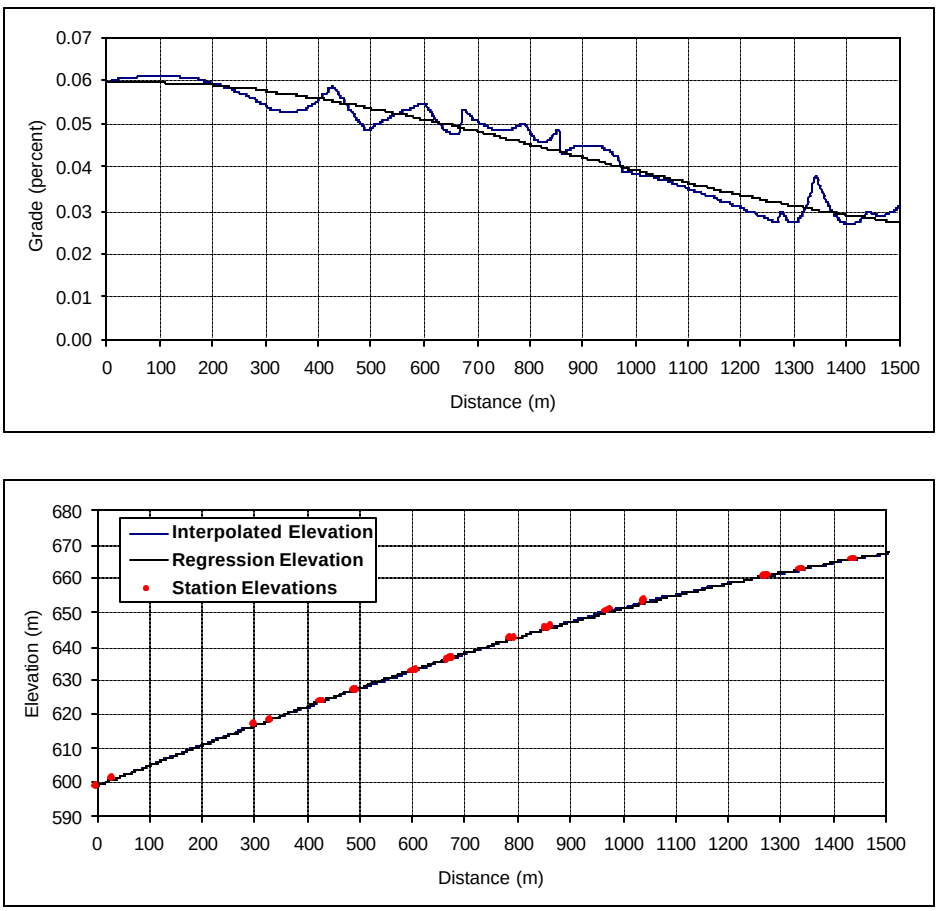

Figure 4-3: Smart Road Vertical Profile

4.3.2 *Data Collection Procedures*

Thirteen different vehicles were chosen for testing, and each was subjected to the same set of tests. The test runs involved accelerating the vehicles from a complete stop at the maximum acceleration rate for the entire 1.5-km trip. Three speed ranges were tested, namely accelerating the vehicle from 0 to 56 km/h (35 mph), 0 to 88 km/h (55 mph), and 0 km/h to the maximum attainable speed within the test section. Depending on the type of vehicle, maximum speeds attained by the end of the test section varied between 128 and 160 km/h (80 and 100 mph). In conducting the study, a minimum of five repetitions were executed for each test set in order to provide a sufficient sample size for the validation analysis. This generated a total of 15 test runs for each vehicle.

4.3.3 *Speed Measurement*

Before each run, the test vehicles were equipped with a Global Positioning System (GPS) unit that measured the vehicle speed to an accuracy of 0.1 m/s. (0.305 ft/sec). GPS is a worldwide, satellite-based radio-navigation system that can determine with certain accuracy the position and velocity of any object equipped with a GPS receiver. Typical output data from GPS receivers include latitude, longitude, altitude, speed, heading, and time. The GPS receivers used were able to update these parameters once every second. Nominal position accuracy is specified with a 25-m (82-ft) spherical error probability, while nominal velocity accuracy is specified within 0.1 m/s (0.31 ft/sec) error probability. These inaccuracies are attributed to a number of sources of error. The majority of these errors are linked to the way the distance between a satellite and a GPS receiver is measured. Within the system, distances are measured by calculating the time it takes for a signal to travel between a satellite and a receiver. Consequently, any delay in the signal transmission then results in distance over-estimation and inaccuracies in the estimated position of the object.

4.3.4 *Test Vehicle Characteristics*

The thirteen test vehicles were selected to cover a wide range of light duty vehicles, as demonstrated in Table 4-1. Specifically, the vehicles were selected to reflect the population of light duty vehicles on the roads in the year 2001. Vehicles were selected from faculty and students at the Virginia Tech Transportation Institute, and therefore constitute the various types of automobiles that were in use at the time. The vehicles represent a wide range of sizes and a variety of EPA vehicle classes including subcompact cars, compact cars, midsize cars, large cars, sport utility vehicles (SUV), pickup trucks, and minivans. Many characteristics of each vehicle were recorded including weight, length, frontal area, type of tires, engine type and power, and air drag coefficient. These parameters serve as inputs to the Rakha model, and the values used are described in the following section.

Table 4-1: Sample Vehicles Tested

Vehicle	Vehicle Class
1995 Acura Integra SE	Subcompact Car
1996 Geo Metro Hatchback	
1995 Saturn SL	Compact Car
2001 Plymouth Neon	
2001 Mazda Protégé LX 2.0	
1995 BMW 740I	Midsize Car
1998 Ford Taurus	
1998 Honda Accord	
1995 Dodge Intrepid	Large Car
1999 Ford Crown Victoria	
1998 Ford Windstar LX	Minivan
1995 Chevy S-10	Pickup Truck
1995 Chevy Blazer	Sport Utility Vehicle

4.4. Model Construction and Comparison

As mentioned earlier, this research effort involved applying the Rakha model, originally developed for trucks, to a variety of passenger vehicles. Specifically, the parameters for each vehicle was determined and input into the model equations to generate acceleration, speed, and distance values. This process is described in the following sections.

4.4.1 *Model Parameters*

The equations that go into the model were described earlier. To apply the model successfully, it is necessary to generate the values of the parameters for each vehicle and discuss how they can be obtained. The following is a list of vehicle and roadway characteristics that are required for the model. The fact that there are numerous input parameters emphasizes the complexity of vehicle acceleration behavior and demonstrates why it is difficult to model acceleration patterns. However, while there are numerous input parameters, these parameters are fairly easy to obtain either from vehicle manuals or from the World Wide Web. The values of all the parameters used for the thirteen vehicles in our tests are summarized in Table 4-2.

Table 4-2: Model Input Parameters

Vehicle	1995 Accura Integra	1995 Chevy Blazer	1995 Chevy S10	1995 Dodge Intrepid	1996 Geo Metro	1998 Ford Taurus	1998 Ford Windstar	1998 Honda Accord	1999 Ford Crown Vic	2001 Mazda Protégé	2001 Plymouth Neon	1995 BMW 740I	1995 Saturn SL
Power (hp)	142	195	155	161	55	145	200	150	200	130	132	282	124
% Mass Tractive Axle	0.515	0.560	0.605	0.535	0.380	0.575	0.550	0.610	0.590	0.525	0.495	0.515	0.560
Altitude (m)	599	599	599	599	599	599	599	599	599	599	599	599	599
Grade	Variable	Variable	Variable	Variable	Variable	Variable	Variable	Variable	Variable	Variable	Variable	Variable	Variable
Engine Efficiency	0.68	0.65	0.72	0.68	0.65	0.8	0.65	0.75	0.7	0.7	0.75	0.7	0.72
Coefficient Friction	0.6	0.6	0.6	0.6	0.6	0.6	0.6	0.6	0.6	0.6	0.6	0.6	0.6
Cd	0.32	0.45	0.45	0.31	0.34	0.3	0.4	0.34	0.34	0.34	0.36	0.32	0.33
Ch	0.95	0.95	0.95	0.95	0.95	0.95	0.95	0.95	0.95	0.95	0.95	0.95	0.95
C1	0.047285	0.047285	0.047285	0.047285	0.047285	0.047285	0.047285	0.047285	0.047285	0.047285	0.047285	0.047285	0.047285
C2	0.0328	0.0328	0.0328	0.0328	0.0328	0.0328	0.0328	0.0328	0.0328	0.0328	0.0328	0.0328	0.0328
C3	4.575	4.575	4.575	4.575	4.575	4.575	4.575	4.575	4.575	4.575	4.575	4.575	4.575
Cr	1.25	1.25	1.25	1.25	1.25	1.25	1.25	1.25	1.25	1.25	1.25	1.25	1.25
Frontal Area (m^2)	1.94	2.49	2.31	2.3	1.88	2.26	2.73	2.12	2.44	2.04	2.07	2.27	1.95
Power (kW)	105.932	145.47	115.63	120.106	41.03	108.17	149.2	111.9	149.2	96.98	98.472	210.372	92.504
Mass (kg)	1670	2310	1930	2040	1130	1970	2270	1770	2300	1610	1650	2370	1240

1. Vehicle Engine Power: The engine power can easily be obtained from the vehicle specifications and is usually given in the units of horsepower. To convert from horsepower to kilowatts, multiply the value by 0.746.

2. Engine Efficiency: Power losses in the engine due to internal friction and other factors generally account for between 20-35% losses of the engine losses for light duty vehicles. Therefore, typical efficiency values range between 0.65-0.80.

3. Vehicle Mass: The vehicle mass is an important parameter in the model. The curb weight is available within the vehicle specifications. Note that you should include the weight of passengers in the vehicle.

4. Percentage of Vehicle Mass on the Tractive Axle: For a four-wheel drive vehicle, this value is 100%. However, most light duty vehicles are two-wheel drive. Typical values for two-wheel drive vehicles are in the range of 50-65%, because most vehicles are front-wheel drive. Conversely, rear-wheel drive vehicles have a tractive axle mass of 35-50% the total mass. As part of the testing, the axles were weighed separately to obtain this value.

5. Pavement: The pavement type and condition are required to determine several constants.

6. Coefficient of Friction: The value of the coefficient of friction is dependent on the pavement type and condition. For concrete pavements, the coefficient of friction varies from 0.8 to 0.7 to 0.6 depending for an excellent, good, or poor condition, respectively. For asphalt pavements, the values are 0.6, 0.5, and 0.4 for good, fair, and poor conditions, respectively. The Smart Road test facility was a good asphalt surface at the time of testing.

7. Altitude: This is the altitude above sea level for the testing location, in meters. In the case of the Smart Road the altitude was 600m.

8. Air Drag Coefficient: The air drag coefficient is given in the vehicle specifications. Typical values for light duty vehicles range from 0.30 to 0.35, depending on the aerodynamic features incorporated into the body of the vehicle.

9. Frontal Area: The frontal area of the vehicle can be approximated as 85% of the height times the width of the vehicle if it is not given directly in the vehicle specifications.

10. Rolling Resistance Constants: Three rolling resistance constants are used in the model. The constant C_r is a function of the pavement type and condition. For concrete pavements, the coefficient varies from 1.0 to 1.5 to 2.0 depending for excellent, good, or poor pavements, respectively. For asphalt pavements, the values are 1.25, 1.75, and 2.25 for good, fair, and poor pavements, respectively. The constants C_2 and C_3 depend on tire

type. Most light duty vehicles use radial tires. The constants for radial tires are 0.0328 and 4.575, respectively. If bias ply tires are used, the constants are 0.0438 and 6.100.

11. Grade: The grade of the roadway is given as a decimal (m/100 m). The grade is often considered a constant for a given section of roadway. However, the grade of the Smart Road test facility was computed using Equation 4-26.

4.4.2 *Model Application*

The previous section described the input parameters to the various vehicle acceleration models. This section describes how to solve the equations of motion and apply the model to predict the speed and acceleration rates for different cars.

The second order ordinary differential equation (ODE) shown in Equation 4-17 can be recast as two first order ODE's and a numerical solution can be reached using an Euler approximation as shown below in Equations 4-27, 4-28, 4-29, and 4-30:

$$a(t_i) = \frac{F(t_i) - R(t_i)}{M} \qquad [4\text{-}27]$$

$$\begin{Bmatrix} \dot{v}(t_i) \\ \dot{x}(t_i) \end{Bmatrix} = \begin{Bmatrix} a(t_i) \\ v(t_i) \end{Bmatrix} \qquad [4\text{-}28]$$

$$v(t_i) = v(t_{i-1}) + a(t_{i-1})\Delta t \qquad [4\text{-}29]$$

$$x(t_i) = x(t_{i-1}) + v(t_{i-1})\Delta t \qquad [4\text{-}30]$$

Where:
a = acceleration (m/s2)
v = velocity (m/s)
x = distance traveled (m)
$t_i = t_0 + i\Delta t$ for i = 1,2,….,n

The smaller the value of Δt used, the more accurate the model will be. For our formulations, a Δt of 0.1 seconds was used. By inserting these equations into a spreadsheet, as well as equations for the forces and resistances and the parameters for the vehicle and roadway, the values for distance, speed, and acceleration are generated for a vehicle at any given time. See Table 4-3 for a sample spreadsheet.

Table 4-3: Sample Model Spreadsheet (Saturn SL)

Time (s)	Dist (m)	Spd (km/h)	Acc (m/s^2)	F	Grade	Ra	Rr	Rg	R
0.0	0.00	0.00	0.00	4086	0.05963	0.0	69.5	725.1	794.6
0.1	0.00	0.00	2.65	4086	0.05963	0.0	69.5	725.1	794.6
0.2	0.00	0.96	2.65	4086	0.05963	0.0	70.0	725.1	795.1
0.3	0.03	1.91	2.65	4086	0.05963	0.1	70.5	725.1	795.7
0.4	0.08	2.87	2.65	4086	0.05963	0.2	71.0	725.1	796.3
0.5	0.16	3.82	2.65	4086	0.05963	0.4	71.4	725.1	797.0
5.9	43.57	54.71	2.56	4086	0.05970	86.4	96.8	726.0	909.2
6.0	45.09	55.63	2.56	4086	0.05970	89.4	97.3	726.0	912.6
6.1	46.63	56.55	2.56	4086	0.05970	92.4	97.7	726.0	916.1
6.2	48.20	57.47	2.55	4086	0.05970	95.4	98.2	726.0	919.6
6.3	49.80	58.39	2.55	4086	0.05970	98.5	98.7	726.0	923.1
6.4	51.42	59.31	2.51	4043	0.05970	101.6	99.1	726.0	926.7
6.5	53.07	60.21	2.46	3982	0.05970	104.7	99.6	726.0	930.2
6.6	54.74	61.10	2.41	3924	0.05970	107.8	100.0	725.9	933.8
6.7	56.44	61.97	2.36	3869	0.05970	110.9	100.4	725.9	937.3
6.8	58.16	62.82	2.32	3817	0.05970	114.0	100.9	725.9	940.7
6.9	59.91	63.65	2.28	3767	0.05969	117.0	101.3	725.9	944.2
7.0	61.67	64.47	2.23	3719	0.05969	120.0	101.7	725.9	947.6
7.1	63.46	65.28	2.20	3673	0.05969	123.1	102.1	725.8	951.0
7.2	65.28	66.07	2.16	3629	0.05969	126.1	102.5	725.8	954.3
7.3	67.11	66.85	2.12	3587	0.05968	129.0	102.9	725.8	957.7
7.4	68.97	67.61	2.09	3546	0.05968	132.0	103.2	725.7	961.0
7.5	70.85	68.36	2.05	3507	0.05968	135.0	103.6	725.7	964.3
7.6	72.75	69.10	2.02	3470	0.05967	137.9	104.0	725.7	967.5
7.7	74.67	69.82	1.99	3434	0.05967	140.8	104.4	725.6	970.8
7.8	76.61	70.54	1.96	3399	0.05967	143.7	104.7	725.6	974.0
7.9	78.57	71.24	1.93	3366	0.05966	146.6	105.1	725.5	977.1
8.0	80.54	71.94	1.90	3333	0.05966	149.4	105.4	725.4	980.3

4.4.3 *Constant Power Assumption*

As was mentioned earlier Rakha and Lucic had observed a reduction in vehicle power at low speeds to account for the build-up of power that occurs as the trucks accelerate through the gears (2002). However, it was unclear whether this behavior would occur for light duty vehicles, because these vehicles have fewer gears, carry less mass, and generally use automatic transmissions.

To test the validity of the constant power model, power was plotted versus speed using the data obtained from the field tests for each of the thirteen test vehicles. The results indicated a strong linear relationship between power and speed, as was demonstrated in the plot for the Acura Integra in Figure 4-2. An R^2 value of 0.9945 was obtained for this linear regression. The plots for ten of the test vehicles had an R^2 value above 0.93. The Neon and BMW also exhibited reasonable correlation with R^2 values of 0.86 and 0.88, respectively. The Geo Metro had the lowest correlation, 0.74, which can be partly attributed to the fact that it is a manual transmission vehicle.

In addition to checking the validity of a constant power assumption, the power versus speed plot was also used to improve the calculation of the percentage of mass on the tractive axle. The slope of the power versus speed plot was used to determine the actual

maximum force applied by the engine. Recall that Equation 4-19 gives the theoretical value of this maximum force. Slight adjustments to the percentage of mass on the tractive axle values were made (less than 10 percent) so that the model would fit to the field data more closely.

4.4.4 *Vehicle Dynamics Model Predictions*

The vehicle dynamics model (Rakha *et al*., 2002) demonstrated a strong correlation to the thirteen vehicle field data. Specifically, the model demonstrated a good fit in the acceleration versus speed, acceleration versus time, acceleration versus distance, speed versus time, and speed versus distance domains, as demonstrated in Figure 4-4 through Figure 4-16. In addition, the model was able to predict vehicle speed and acceleration profiles accurately for vehicles ranging from subcompact cars to large cars to SUV's and pick-up trucks. Consequently, the results clearly demonstrate the flexibility and validity of the model in predicting maximum vehicle acceleration levels.

While the vehicle dynamics model did offer accurate modeling of vehicle acceleration behavior, the model did tend to over-estimate vehicle speeds for two test vehicles. Specifically, the field speed profiles for the Neon (Figure 4-5) and Blazer (Figure 4-14) vehicles seem to demonstrate a slight drop in vehicle acceleration towards the end of the test run, which is not captured by the vehicle dynamics model. However, these drops in vehicle acceleration may be attributed to the test vehicle not properly shifting into the final gear. Also, the model seems to underestimate acceleration rates at low speeds for some of the vehicles. It is unclear whether these higher acceleration rates are a result of a build-up of power within the vehicle, or if there is just high variability in vehicle acceleration capabilities at low speeds. It should be noted that the data from the test vehicles in Figure 4-4 through Figure 4-16 represent a series of 5 runs.

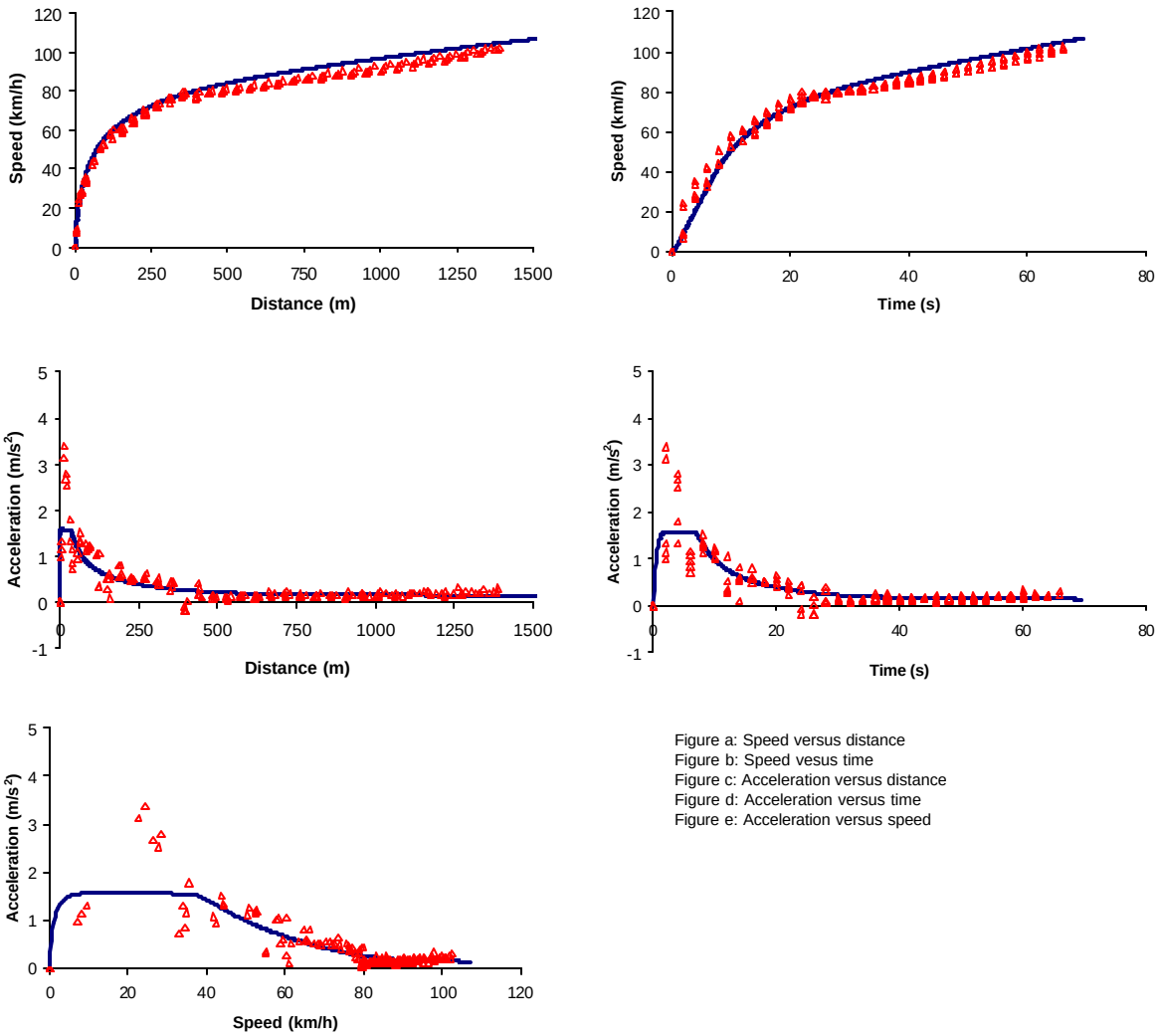

Figure a: Speed versus distance
Figure b: Speed vesus time
Figure c: Acceleration versus distance
Figure d: Acceleration versus time
Figure e: Acceleration versus speed

Figure 4-4: Model Predictions versus Field Data (Geo Metro)

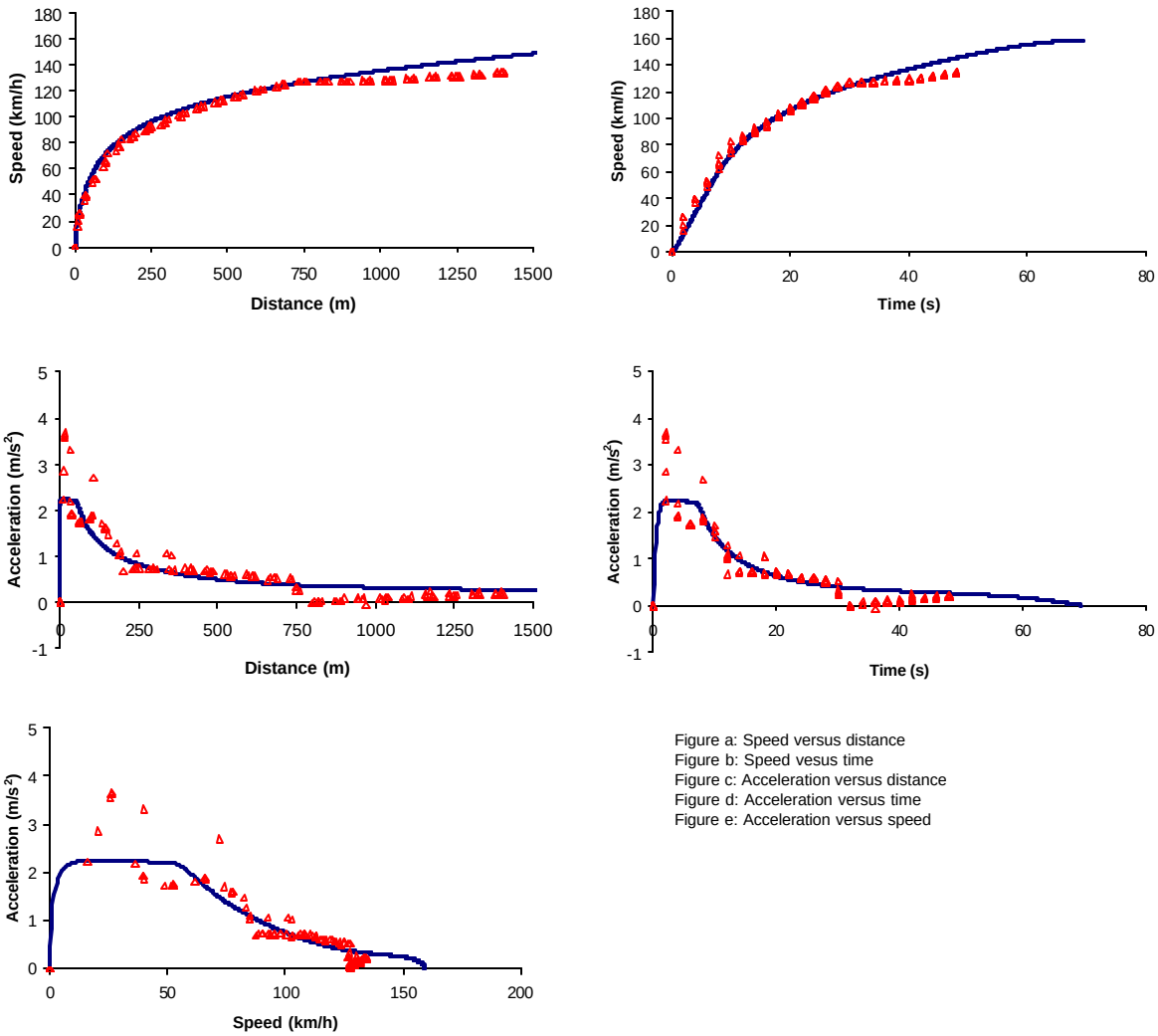

Figure a: Speed versus distance
Figure b: Speed vesus time
Figure c: Acceleration versus distance
Figure d: Acceleration versus time
Figure e: Acceleration versus speed

Figure 4-5: Model Predictions versus Field Data (Plymouth Neon)

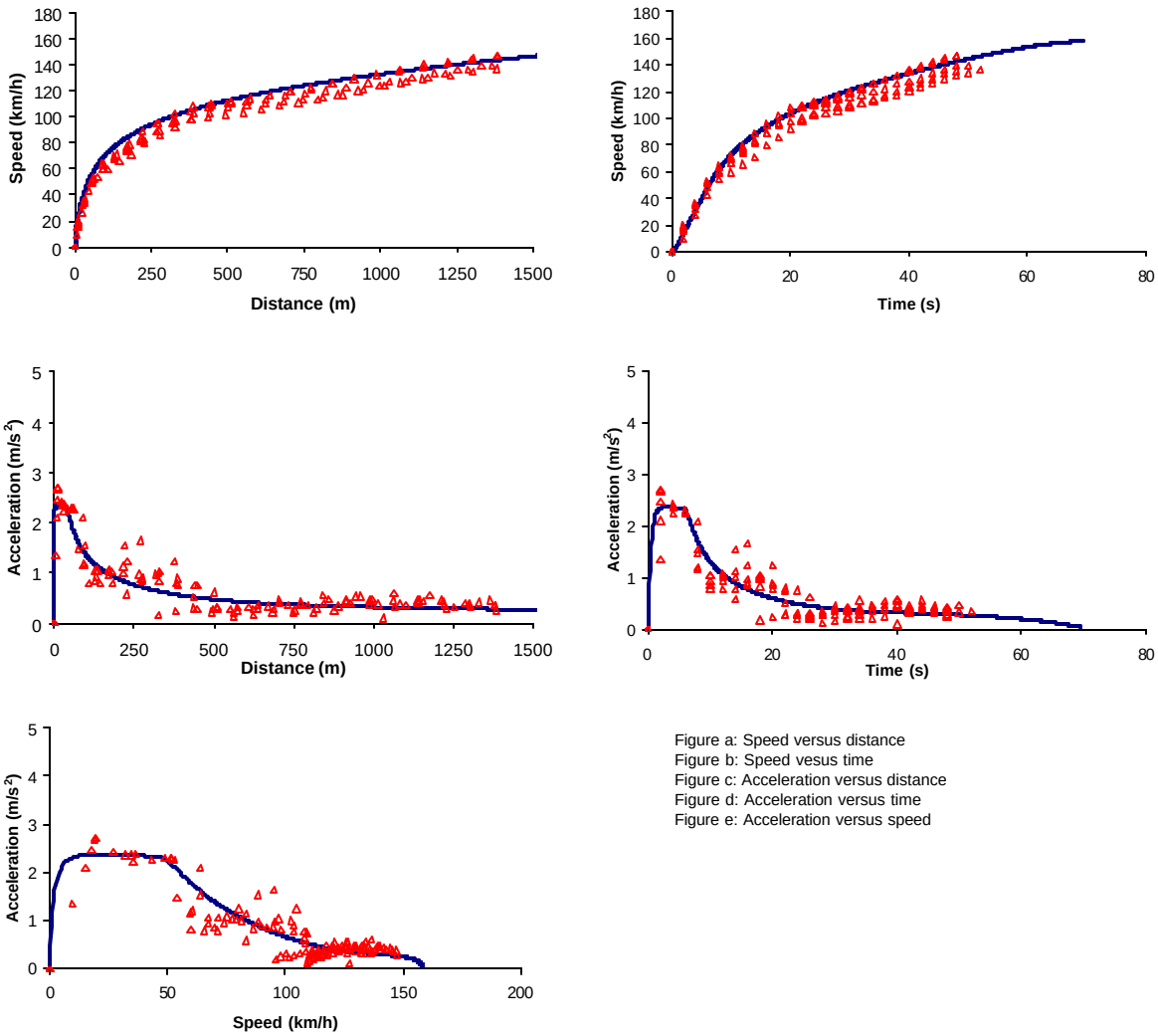

Figure a: Speed versus distance
Figure b: Speed vesus time
Figure c: Acceleration versus distance
Figure d: Acceleration versus time
Figure e: Acceleration versus speed

Figure 4-6: Model Predictions versus Field Data (Acura Integra)

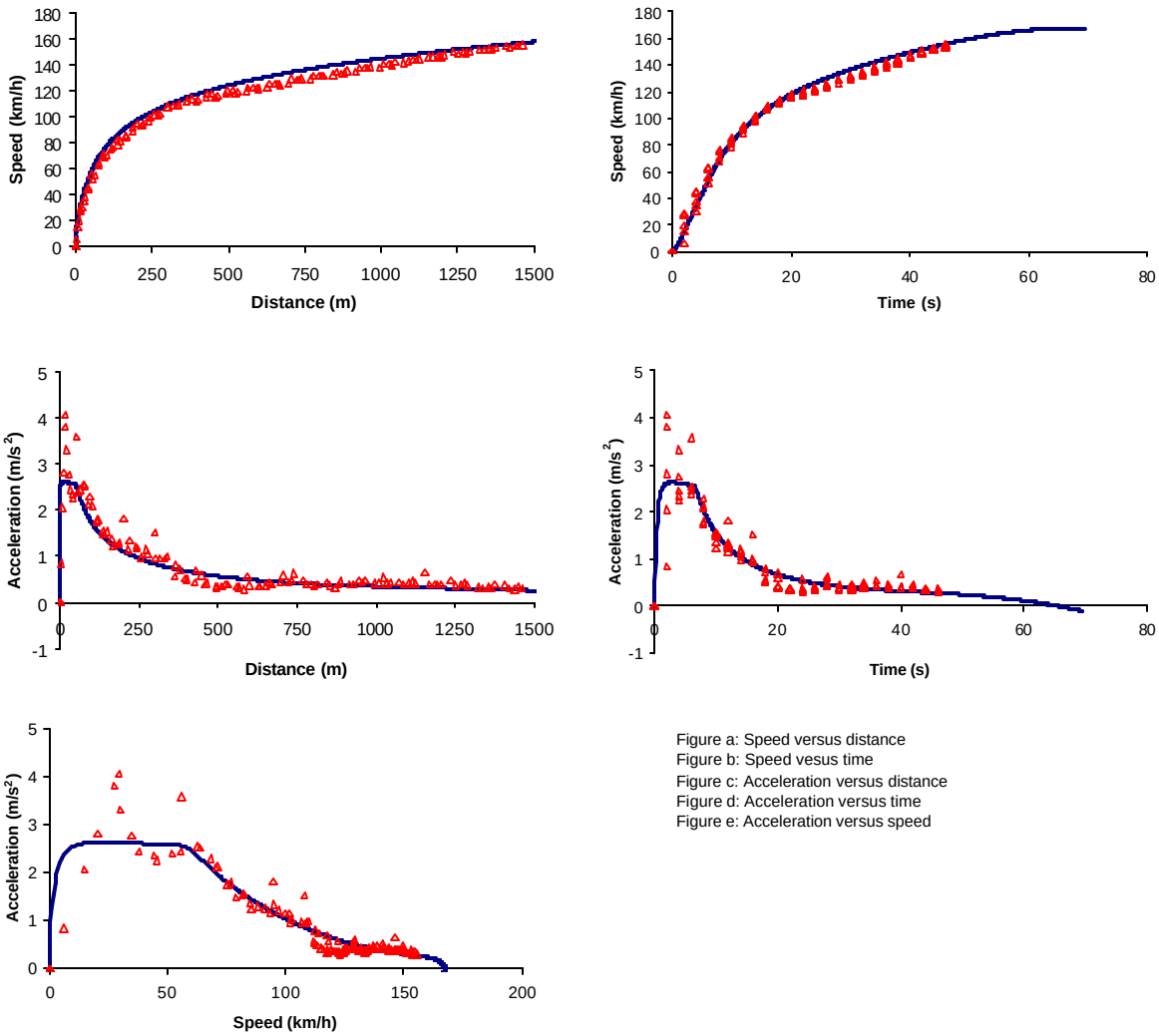

Figure a: Speed versus distance
Figure b: Speed vesus time
Figure c: Acceleration versus distance
Figure d: Acceleration versus time
Figure e: Acceleration versus speed

Figure 4-7: Model Predictions versus Field Data (Saturn SL)

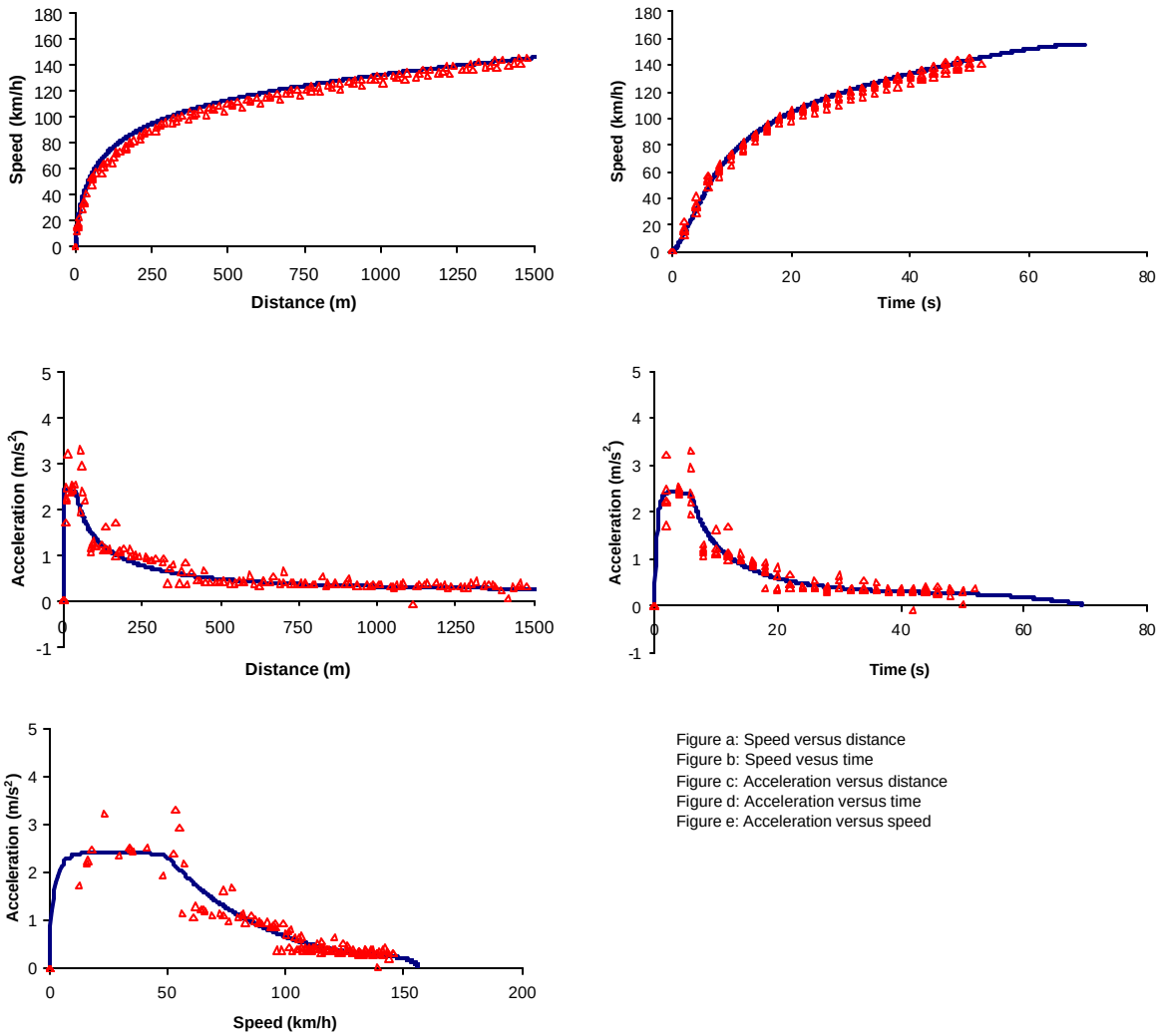

Figure a: Speed versus distance
Figure b: Speed vesus time
Figure c: Acceleration versus distance
Figure d: Acceleration versus time
Figure e: Acceleration versus speed

Figure 4-8: Model Predictions versus Field Data (Mazda Protégé)

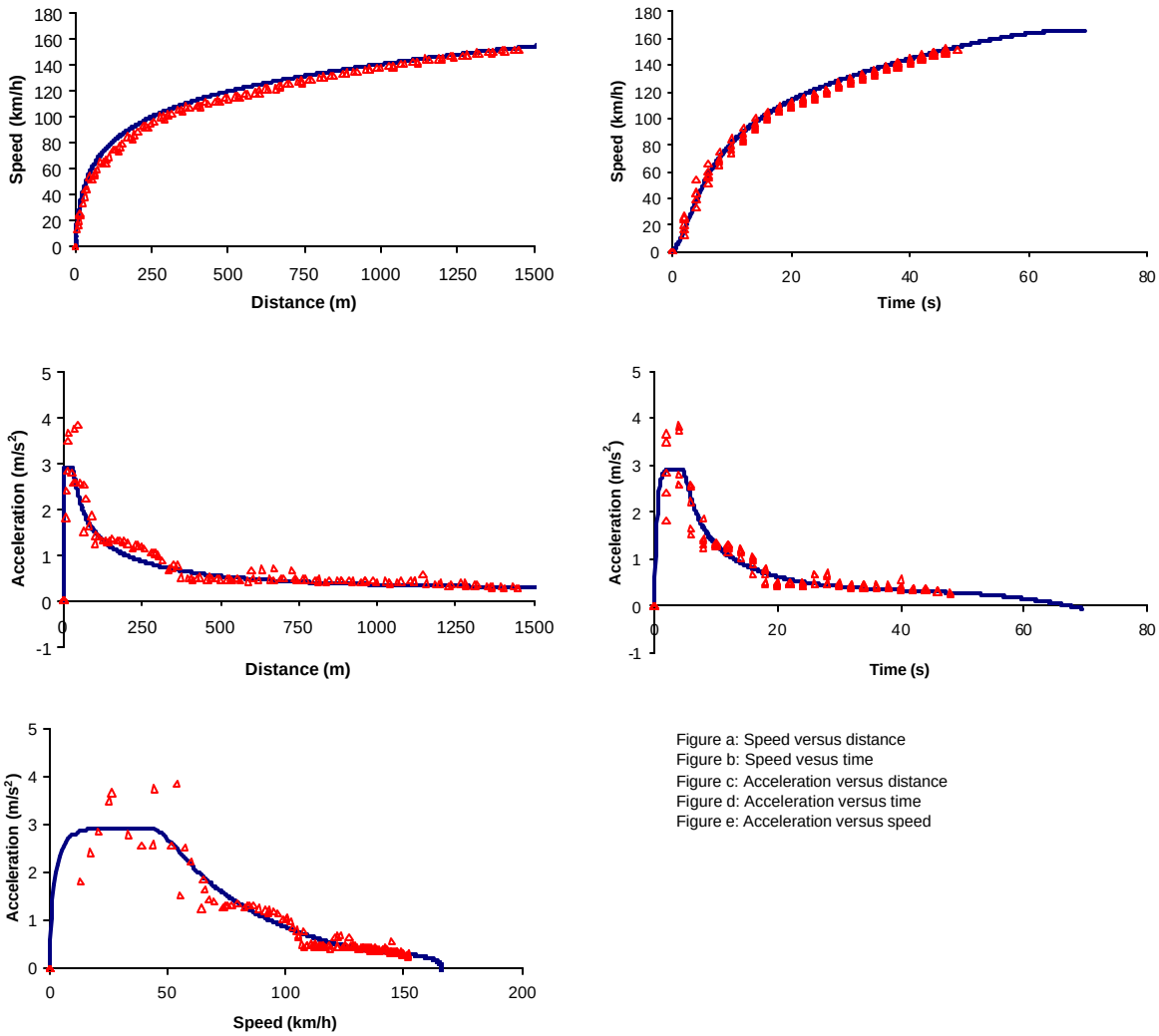

Figure a: Speed versus distance
Figure b: Speed vesus time
Figure c: Acceleration versus distance
Figure d: Acceleration versus time
Figure e: Acceleration versus speed

Figure 4-9: Model Predictions versus Field Data (Honda Accord)

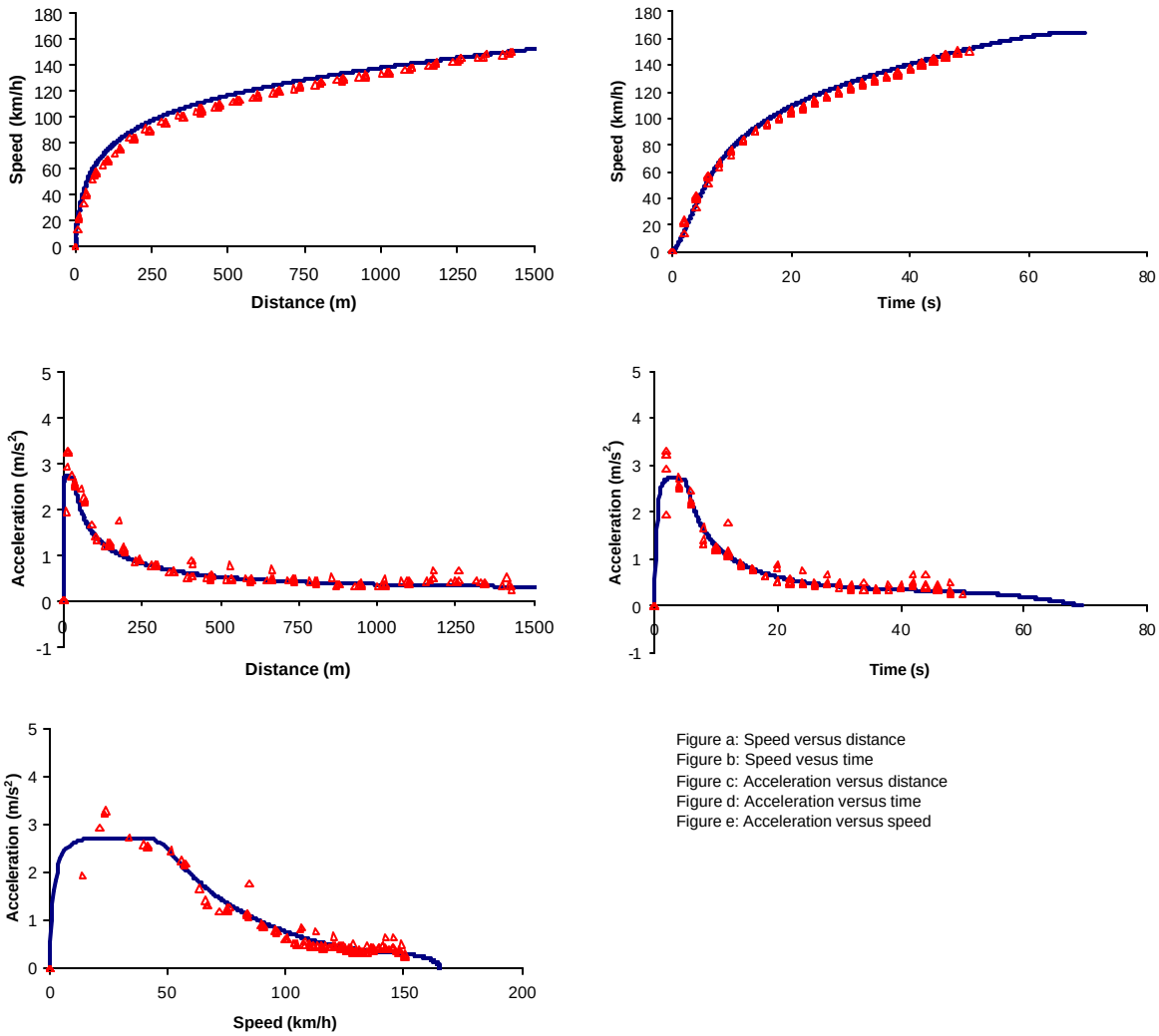

Figure a: Speed versus distance
Figure b: Speed vesus time
Figure c: Acceleration versus distance
Figure d: Acceleration versus time
Figure e: Acceleration versus speed

Figure 4-10: Model Predictions versus Field Data (Ford Taurus)

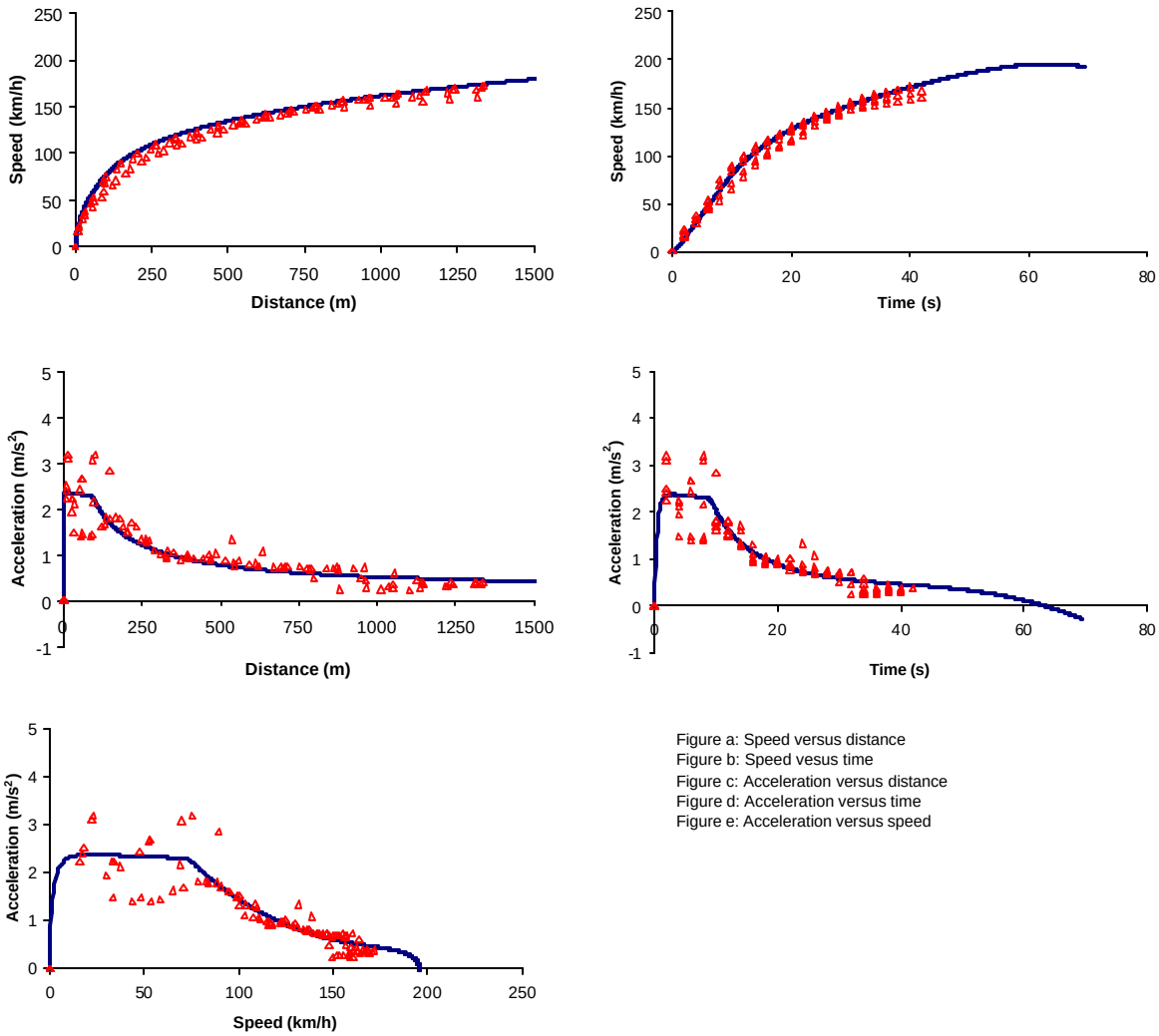

Figure a: Speed versus distance
Figure b: Speed vesus time
Figure c: Acceleration versus distance
Figure d: Acceleration versus time
Figure e: Acceleration versus speed

Figure 4-11: Model Predictions versus Field Data (BMW)

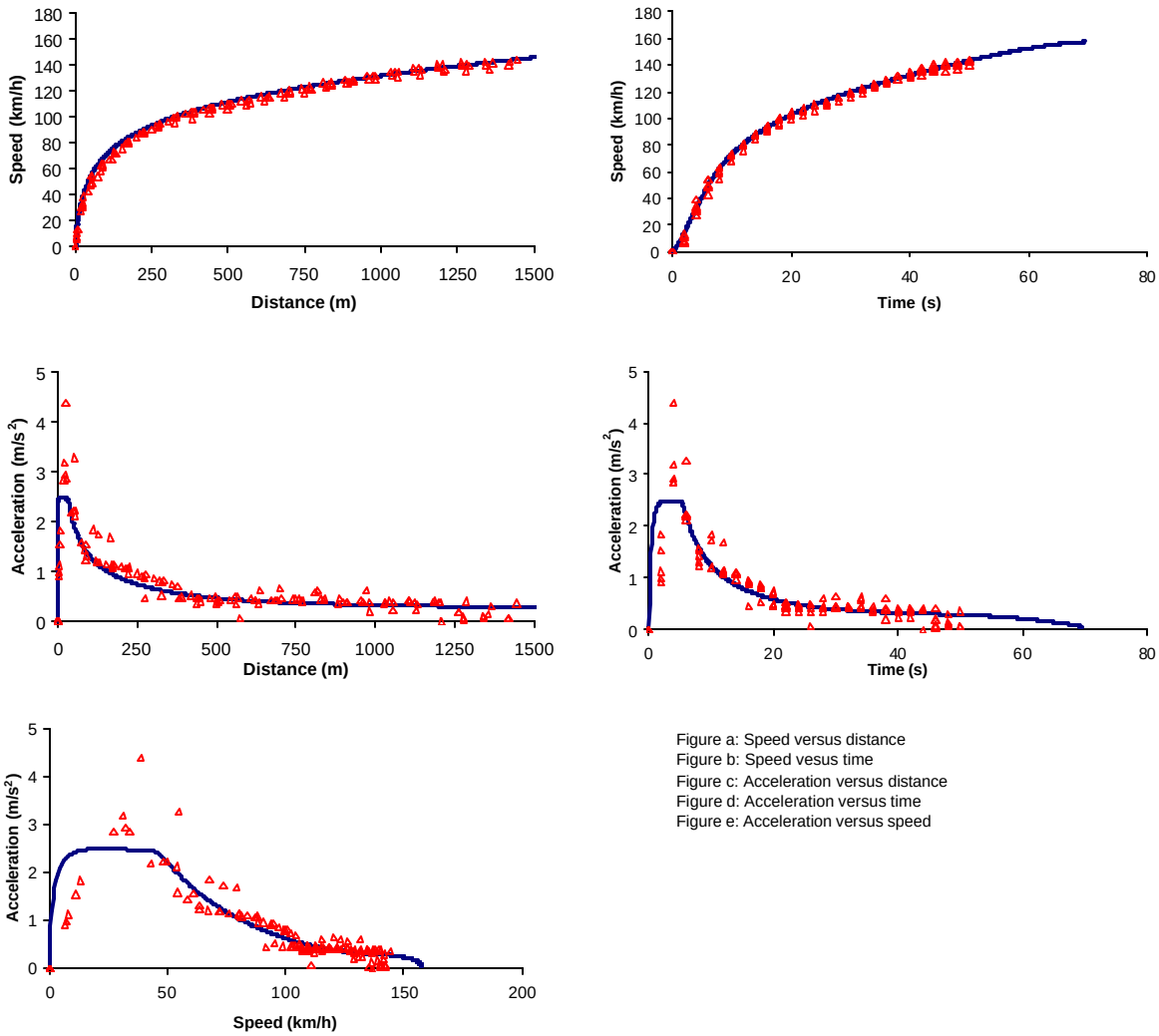

Figure a: Speed versus distance
Figure b: Speed vesus time
Figure c: Acceleration versus distance
Figure d: Acceleration versus time
Figure e: Acceleration versus speed

Figure 4-12: Model Predictions versus Field Data (Dodge Intrepid)

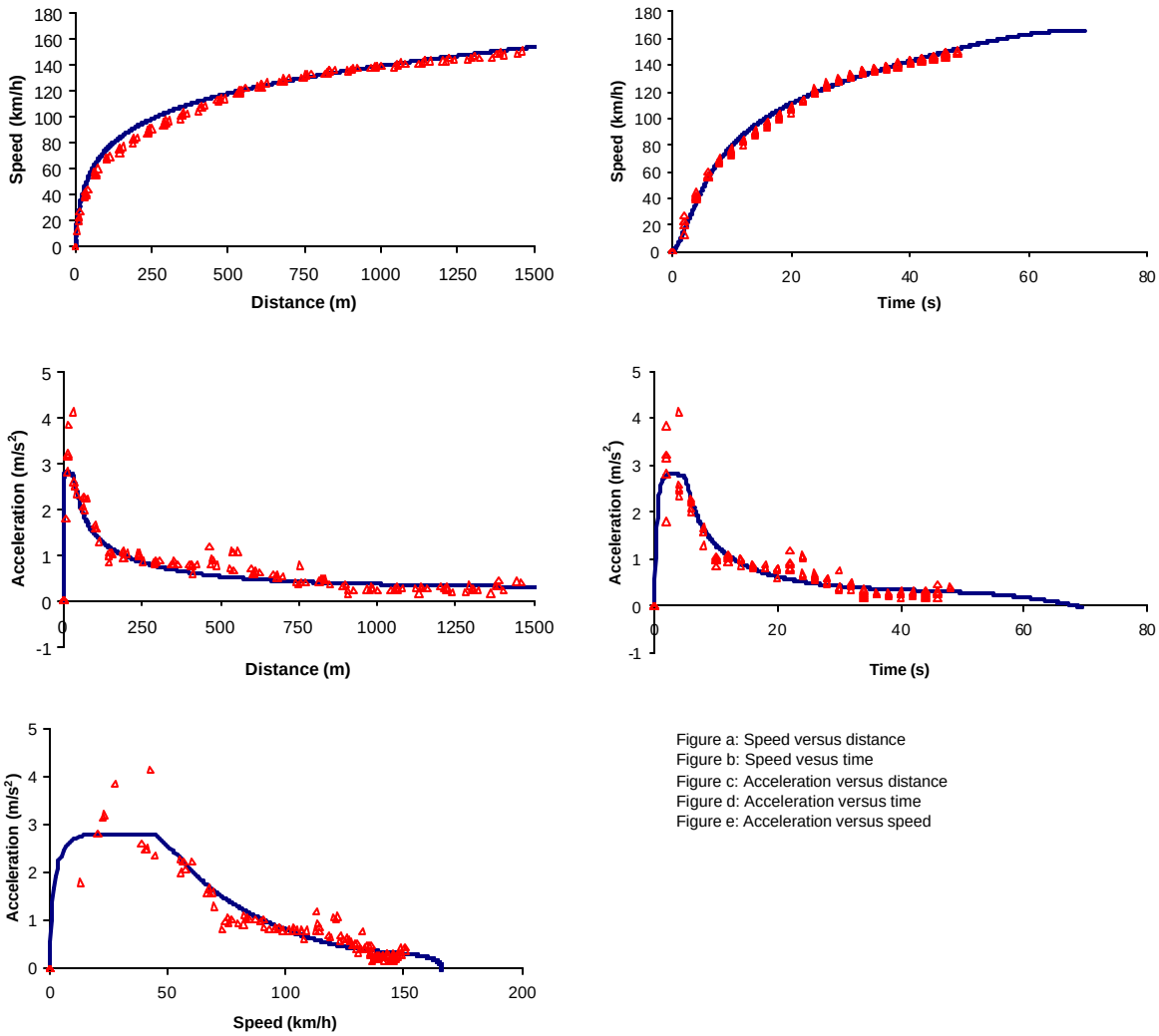

Figure a: Speed versus distance
Figure b: Speed vesus time
Figure c: Acceleration versus distance
Figure d: Acceleration versus time
Figure e: Acceleration versus speed

Figure 4-13: Model Predictions versus Field Data (Crown Victoria)

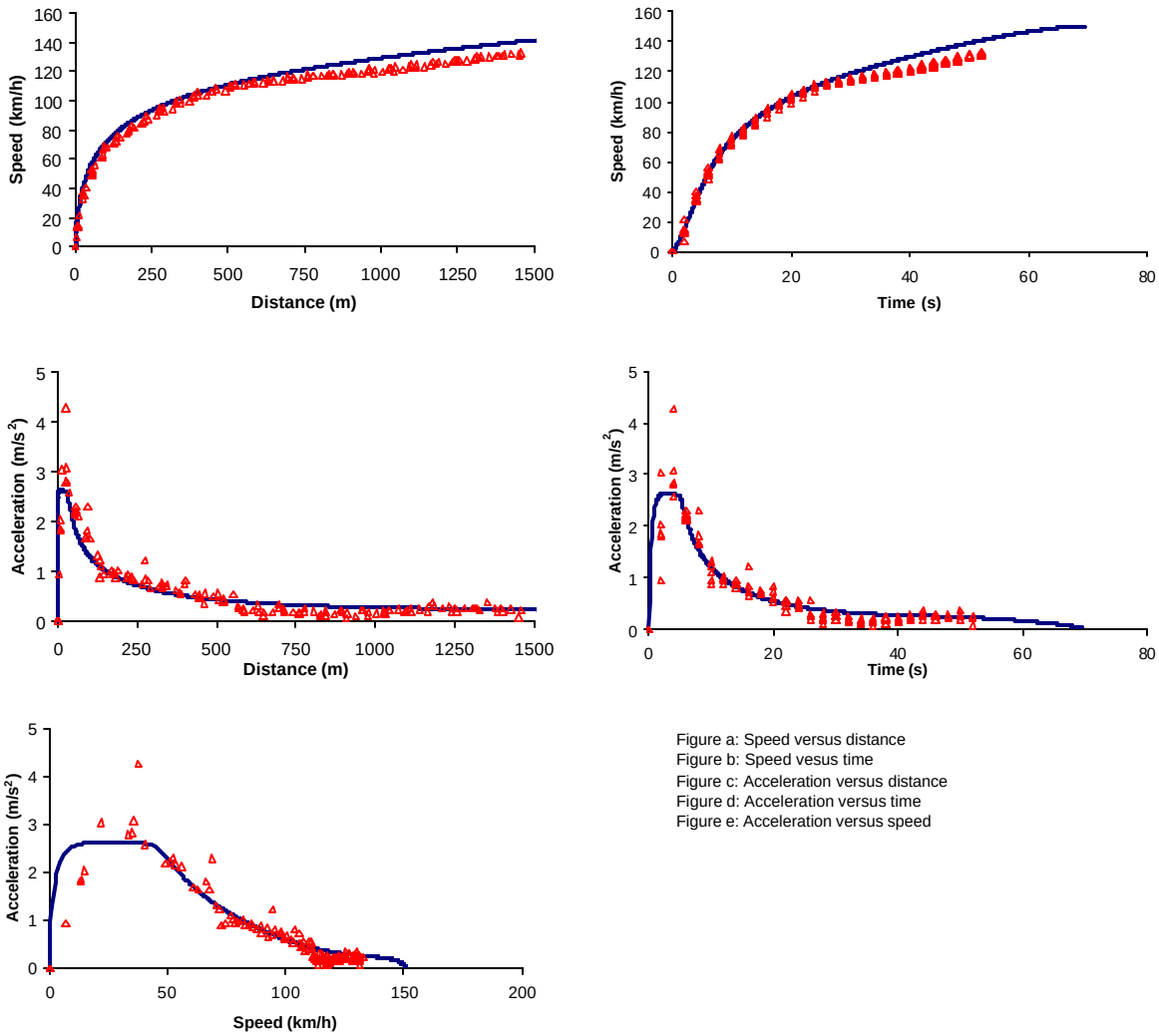

Figure a: Speed versus distance
Figure b: Speed vesus time
Figure c: Acceleration versus distance
Figure d: Acceleration versus time
Figure e: Acceleration versus speed

Figure 4-14: Model Predictions versus Field Data (Chevy Blazer)

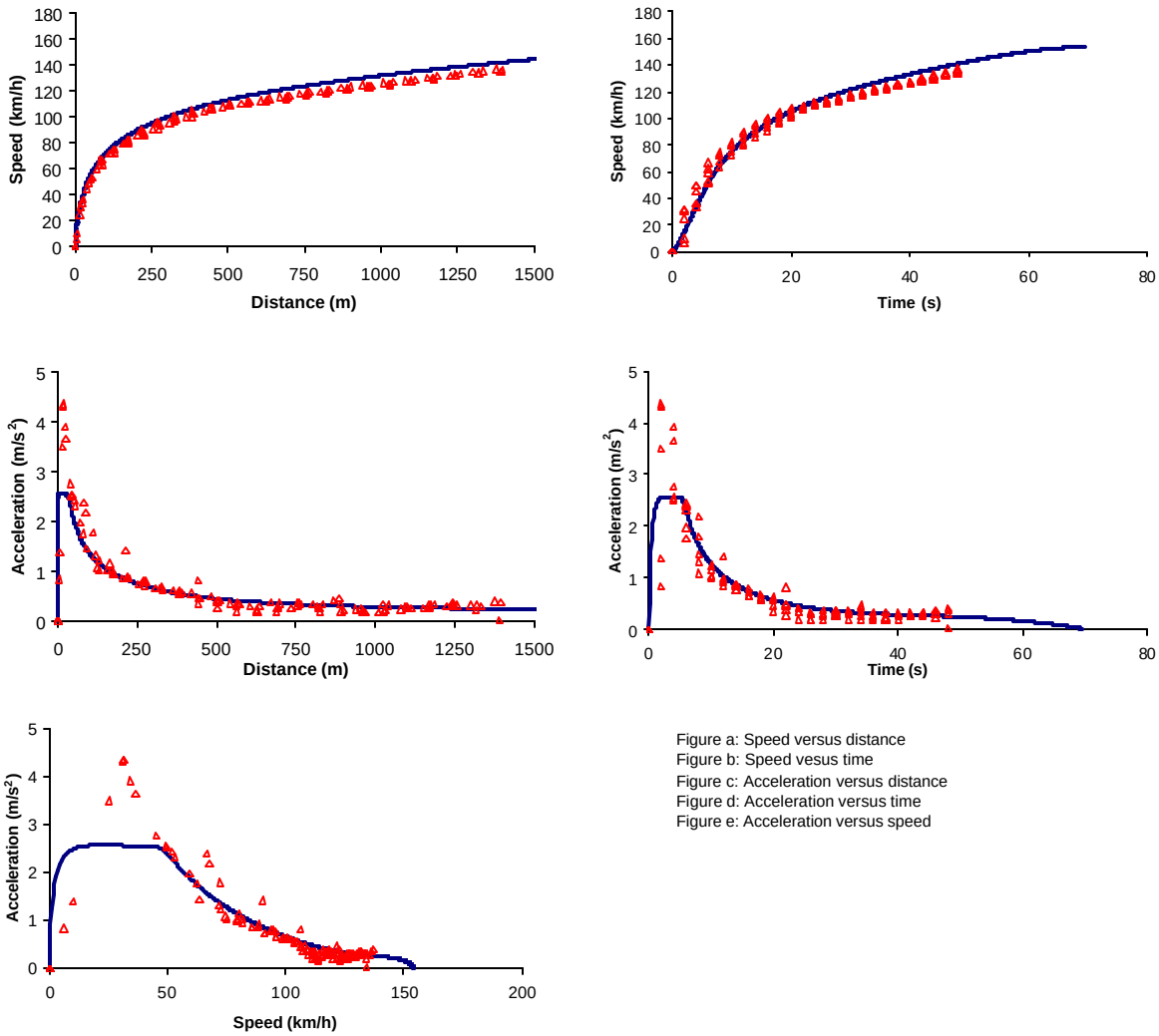

Figure a: Speed versus distance
Figure b: Speed vesus time
Figure c: Acceleration versus distance
Figure d: Acceleration versus time
Figure e: Acceleration versus speed

Figure 4-15: Model Predictions versus Field Data (Ford Windstar)

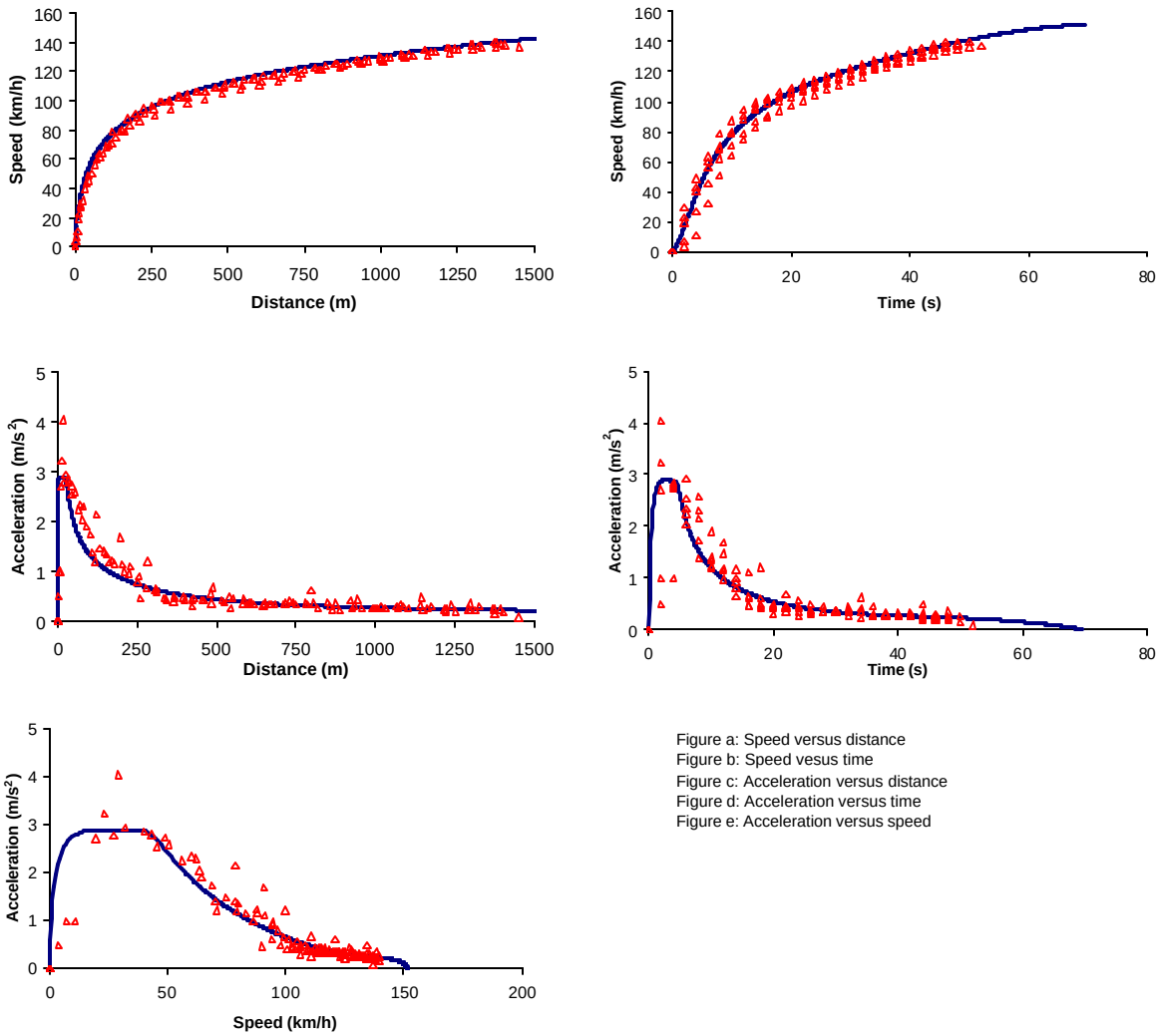

Figure a: Speed versus distance
Figure b: Speed vesus time
Figure c: Acceleration versus distance
Figure d: Acceleration versus time
Figure e: Acceleration versus speed

Figure 4-16: Model Predictions versus Field Data (Chevy S-10)

4.4.5 *Comparison of State-of-Practice Models*

A comparison study was performed involving the Rakha model and state-of-the-art acceleration models. The four existing models chosen for comparison include the Dual-Regime model, the Linear Decay model, the Polynomial model, and the Searle model. The dual-regime model was chosen because it was recommended by Bham and Benekohal in a comprehensive comparison study they performed involving fourteen models (2002). The Linear decay model is recommended for use in a paper by Long (2000) and also appears in several textbooks, including one by Drew (1968). In addition, the Polynomial model was recommended in a comparison study performed by Akçelik (1987). Finally, the Searle model was chosen for comparison because it represents another example of a vehicle dynamics model (1999).

4.4.5.1 *Comparison Results*

Data from five of the thirteen test vehicles were selected for comparison purposes. The five vehicles chosen were the Mazda Protégé, Dodge Intrepid, Chevy Blazer, Ford Windstar, and Chevy S-10. These vehicles were chosen because they represent a variety of vehicle types, including small, large, SUV, minivan, and pick-up truck vehicles, respectively. The parameters for each of the models were chosen in an attempt to create a best fit between model estimates and field data.

Figures 4-17 through Figure 4-21 illustrate the dual-regime model predictions superimposed on the field measurements for each of the five test vehicles. The calibrated input parameters for the dual-regime model included the final speed at the end of acceleration, the total acceleration time, the speed breakpoint between the two regimes, and time to reach the second regime. These parameters were calibrated to provide a best fit in the speed versus time regime for each vehicle.

The dual-regime model appears to provide a reasonable fit to the speed profiles of the vehicles with respect to distance and time. The model does tend to overestimate speeds in the middle of the distance profile, towards the end of the first regime. Furthermore, the model tends to underestimate vehicle speeds at the beginning of the time profiles for the Blazer and Windstar test vehicles. The acceleration plots, however, do not provide a reasonable fit to field data. The major disadvantage of the model is the discontinuity in the acceleration profile. Specifically, the instantaneous drop in the vehicle acceleration rate appears to be unrealistic. However, the simplicity of the model and its ability to generate reasonable speed profiles makes the model useful in certain applications.

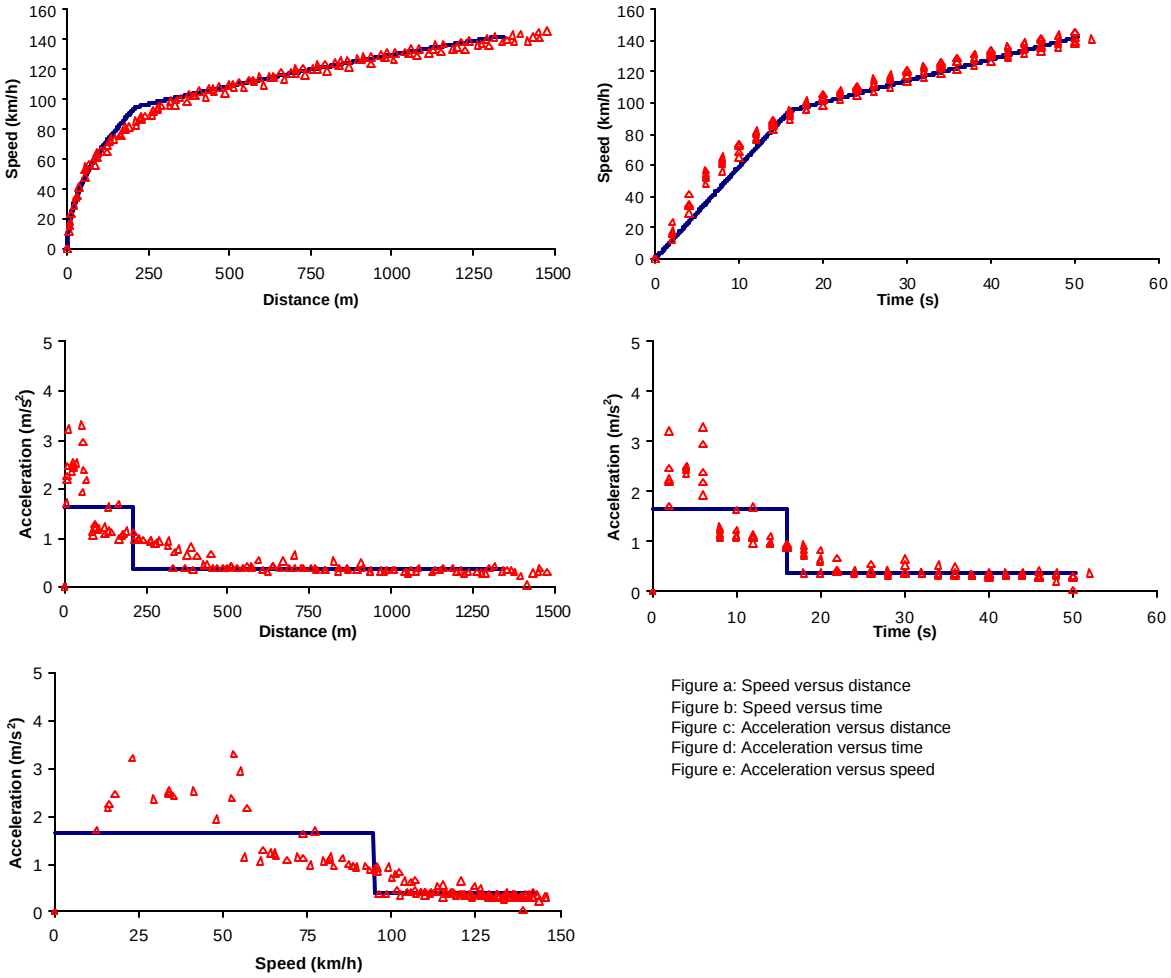

Figure 4-17: Dual-Regime Model Fit to Field Data (Mazda Protégé)

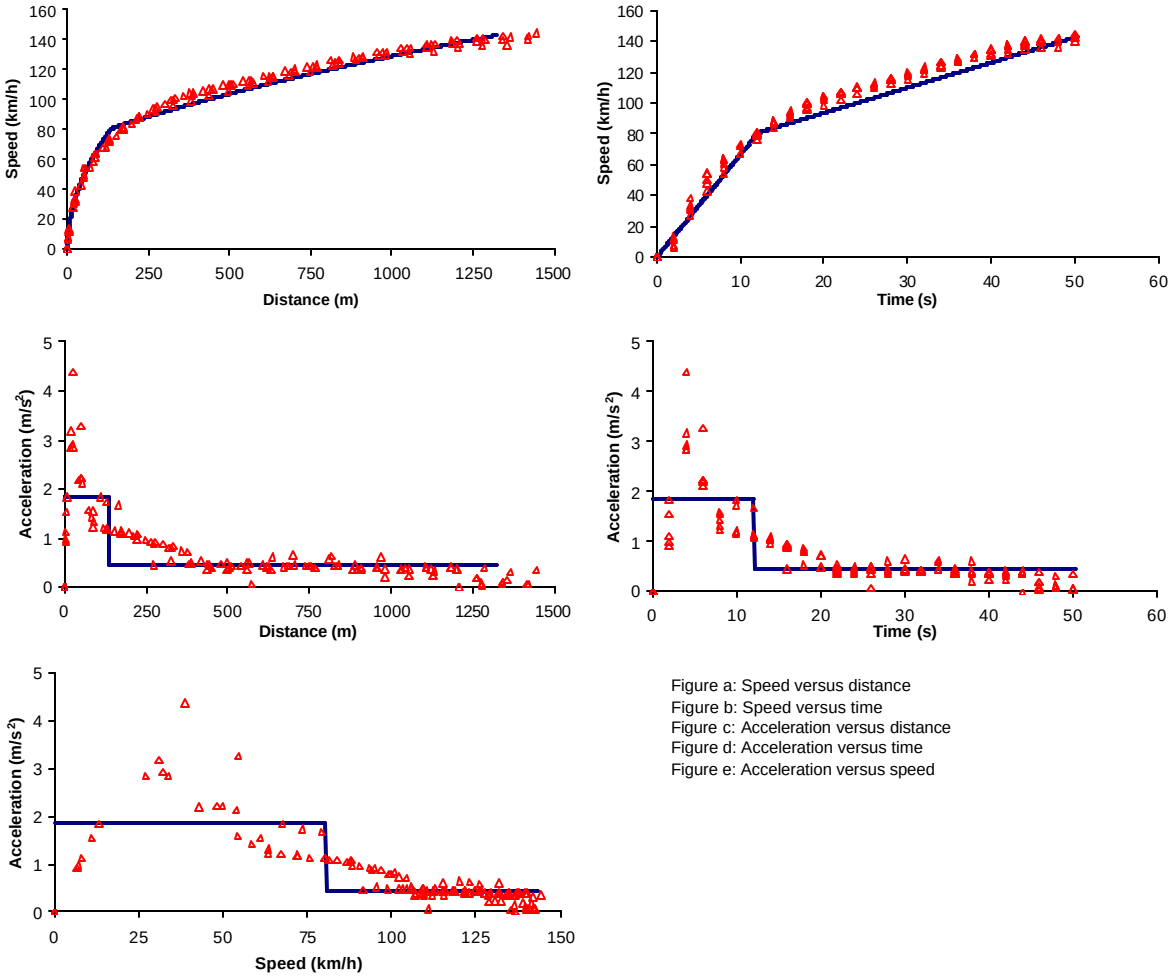

Figure 4-18: Dual-Regime Model Fit to Field Data (Dodge Intrepid)

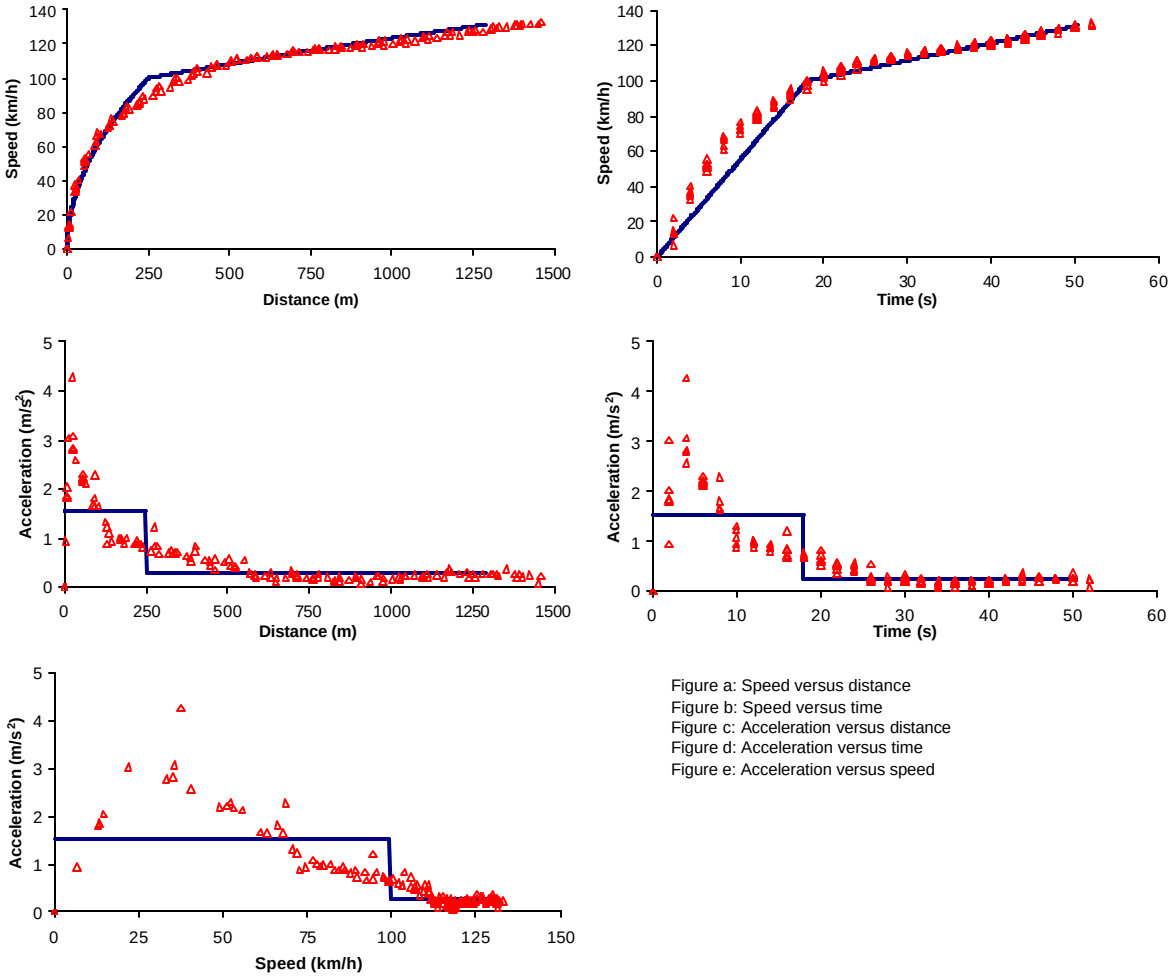

Figure a: Speed versus distance
Figure b: Speed versus time
Figure c: Acceleration versus distance
Figure d: Acceleration versus time
Figure e: Acceleration versus speed

Figure 4-19: Dual-Regime Model Fit to Field Data (Chevy Blazer)

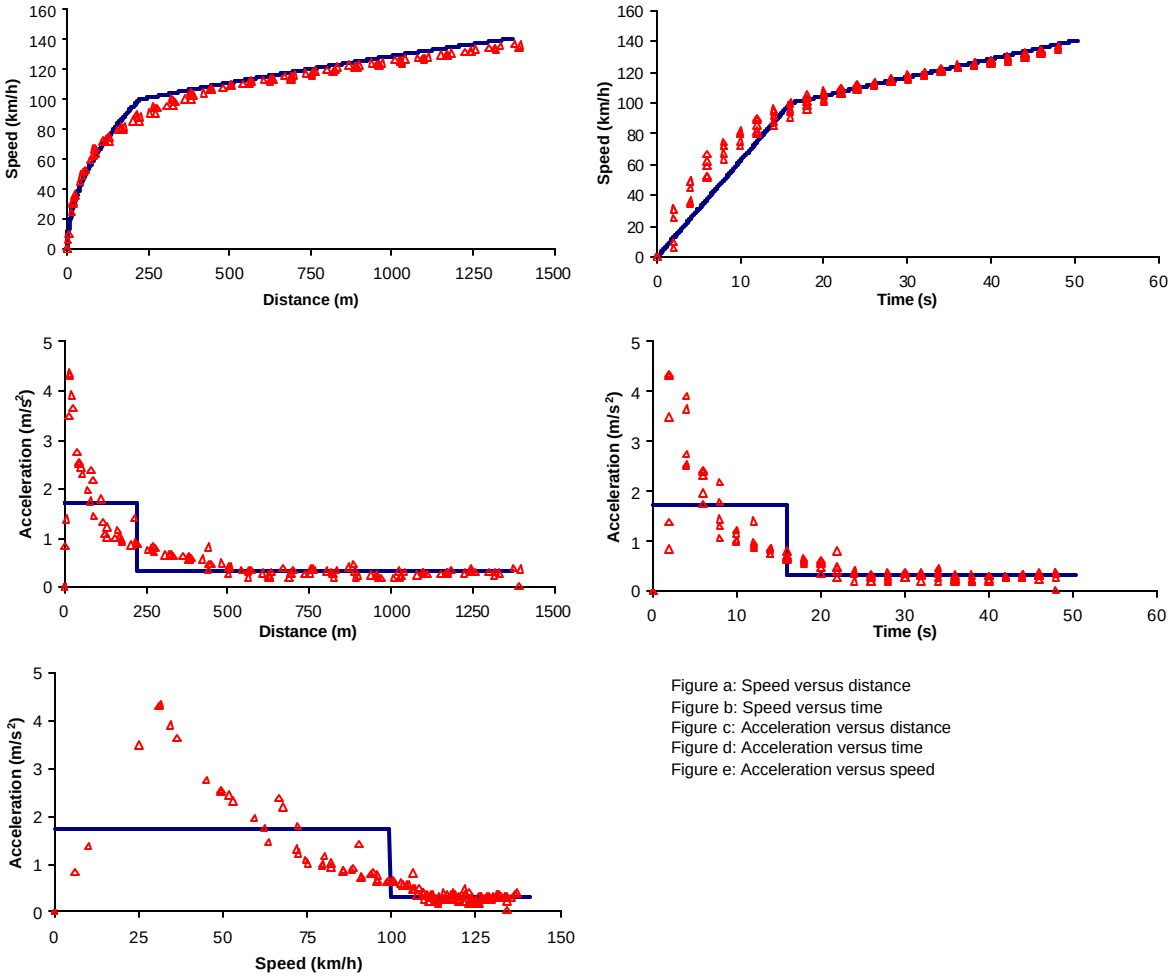

Figure a: Speed versus distance
Figure b: Speed versus time
Figure c: Acceleration versus distance
Figure d: Acceleration versus time
Figure e: Acceleration versus speed

Figure 4-20: Dual-Regime Model Fit to Field Data (Ford Windstar)

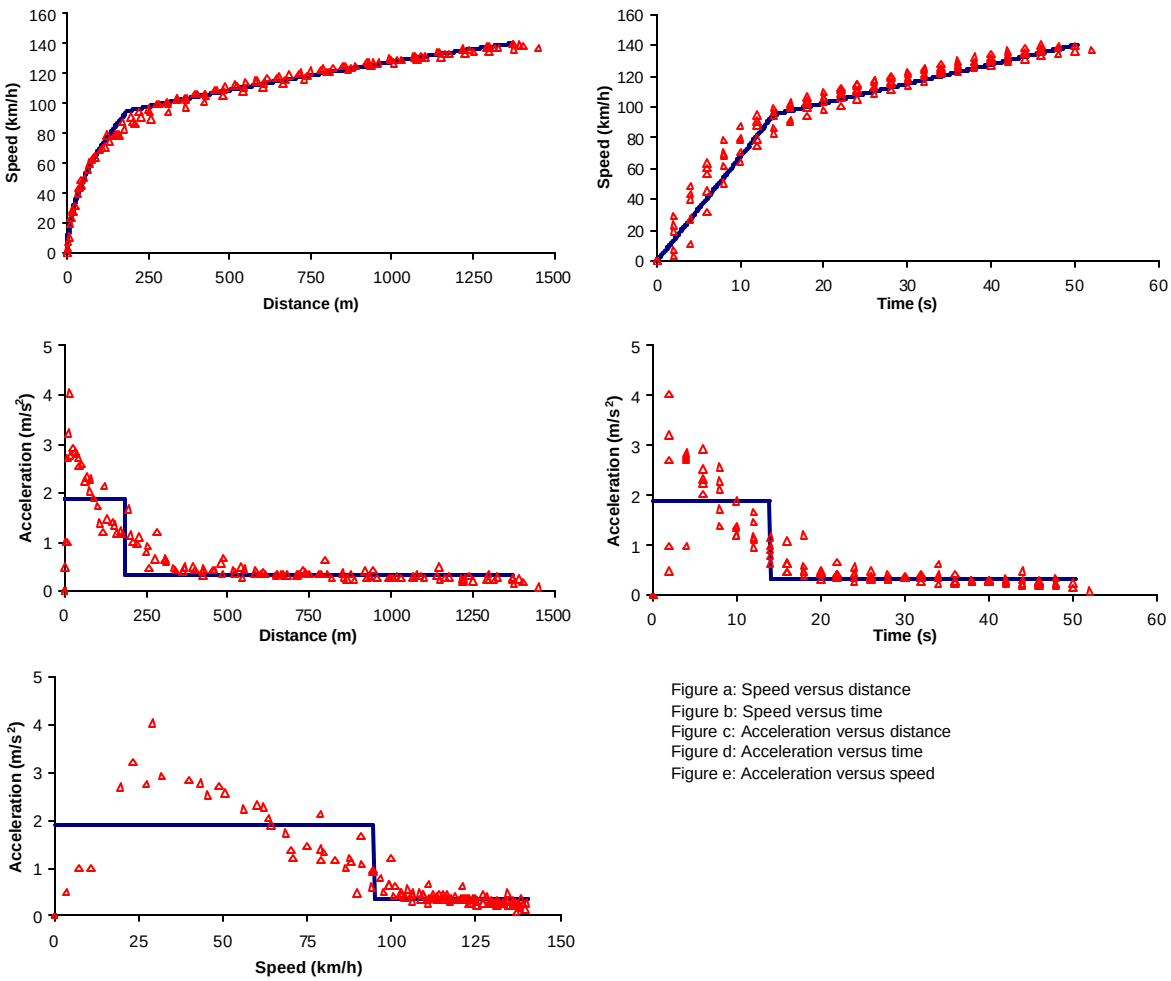

Figure 4-21: Dual-Regime Model Fit to Field Data (Chevy S-10)

For the linear decay model, the parameters of maximum acceleration and maximum speed were calibrated to obtain an optimum fit between model estimates and field data in the acceleration-speed regime. The linear decay model shows a good fit for both the speed profiles, as indicated by Figure 4-22 through Figure 4-26. The linear decay model also improves on the dual-regime model by providing a continuous acceleration function that more closely resembles field data. The linear decay model also accounts for the apparent curvature in the data for the plots of acceleration versus time and distance. However, the data in the acceleration versus speed plot also seems to exhibit some curvature, while the model predicts a linear function. Therefore, the model tends to underestimate the acceleration rate of the vehicle when the vehicle is traveling at low speeds. This model appears to be the best kinematics model, but it requires accurate field data before it can be applied.

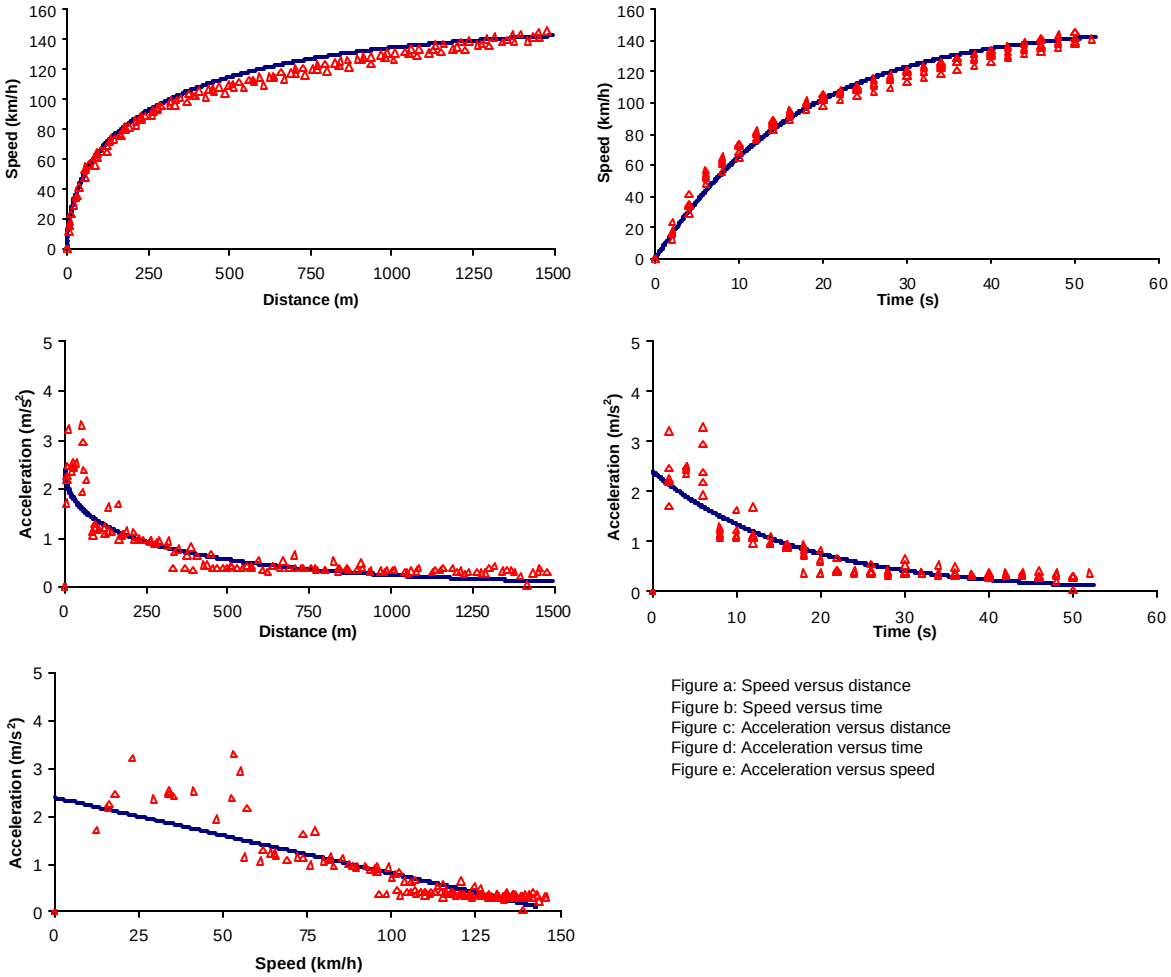

Figure 4-22: Linear Decay Model Fit to Field Data (Mazda Protégé)

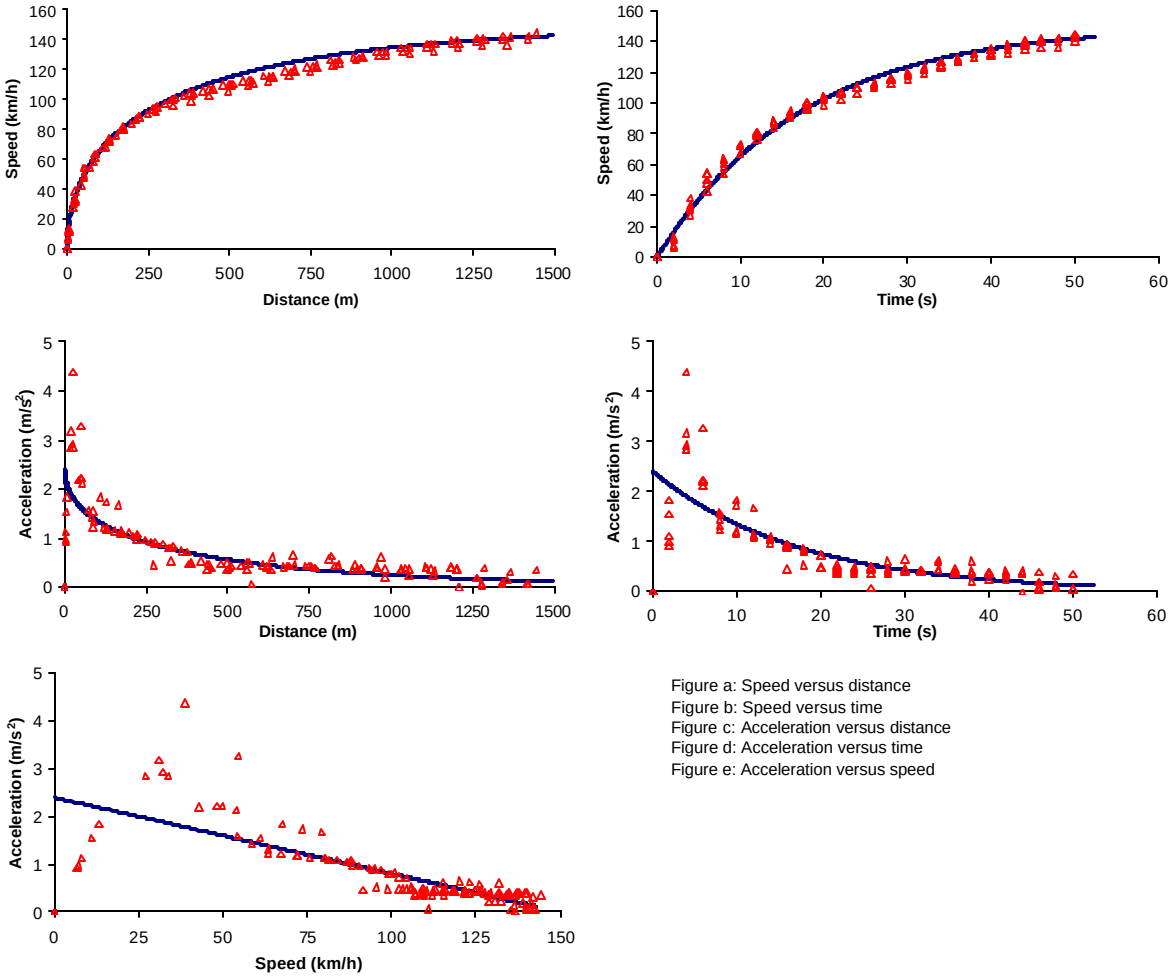

Figure 4-23: Linear Decay Model Fit to Field Data (Dodge Intrepid)

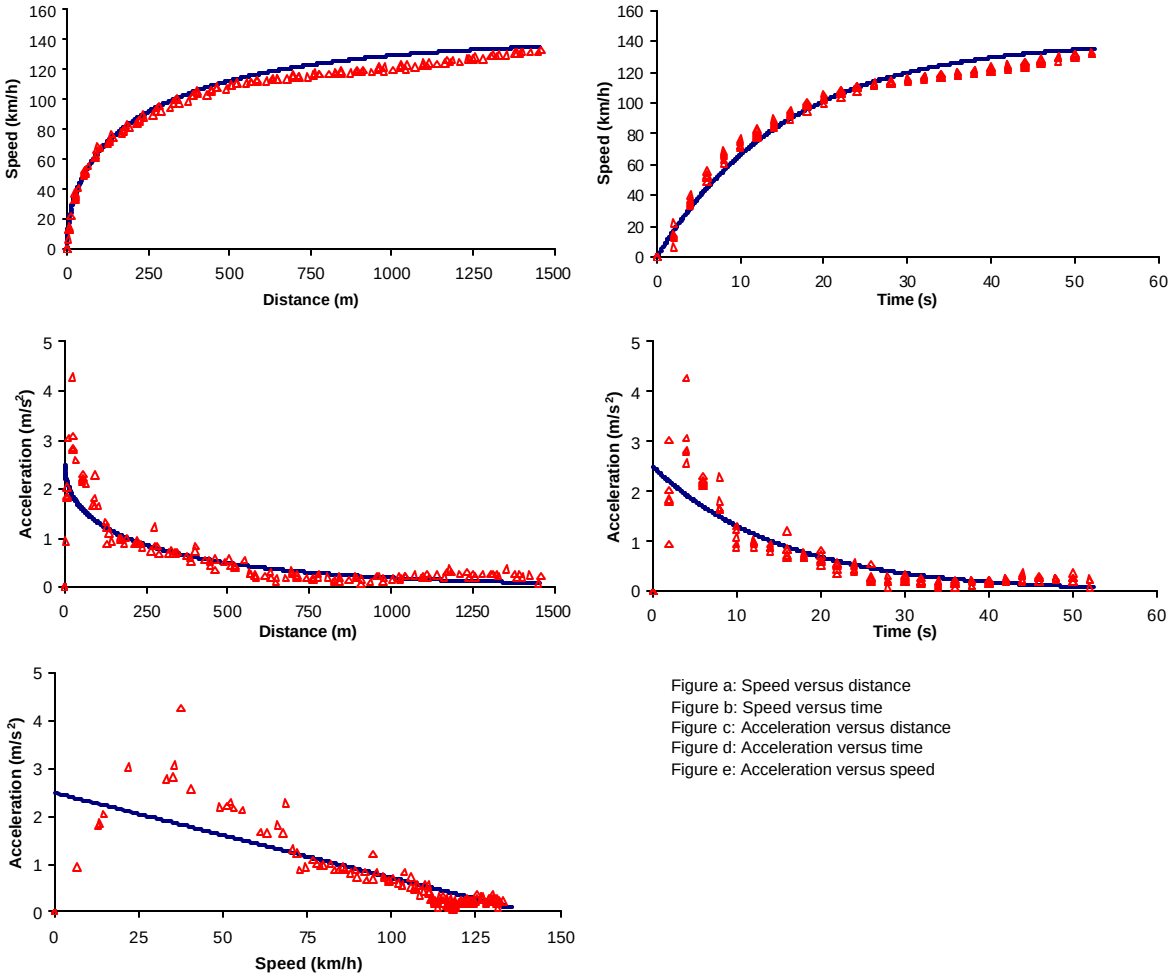

Figure a: Speed versus distance
Figure b: Speed versus time
Figure c: Acceleration versus distance
Figure d: Acceleration versus time
Figure e: Acceleration versus speed

Figure 4-24: Linear Decay Model Fit to Field Data (Chevy Blazer)

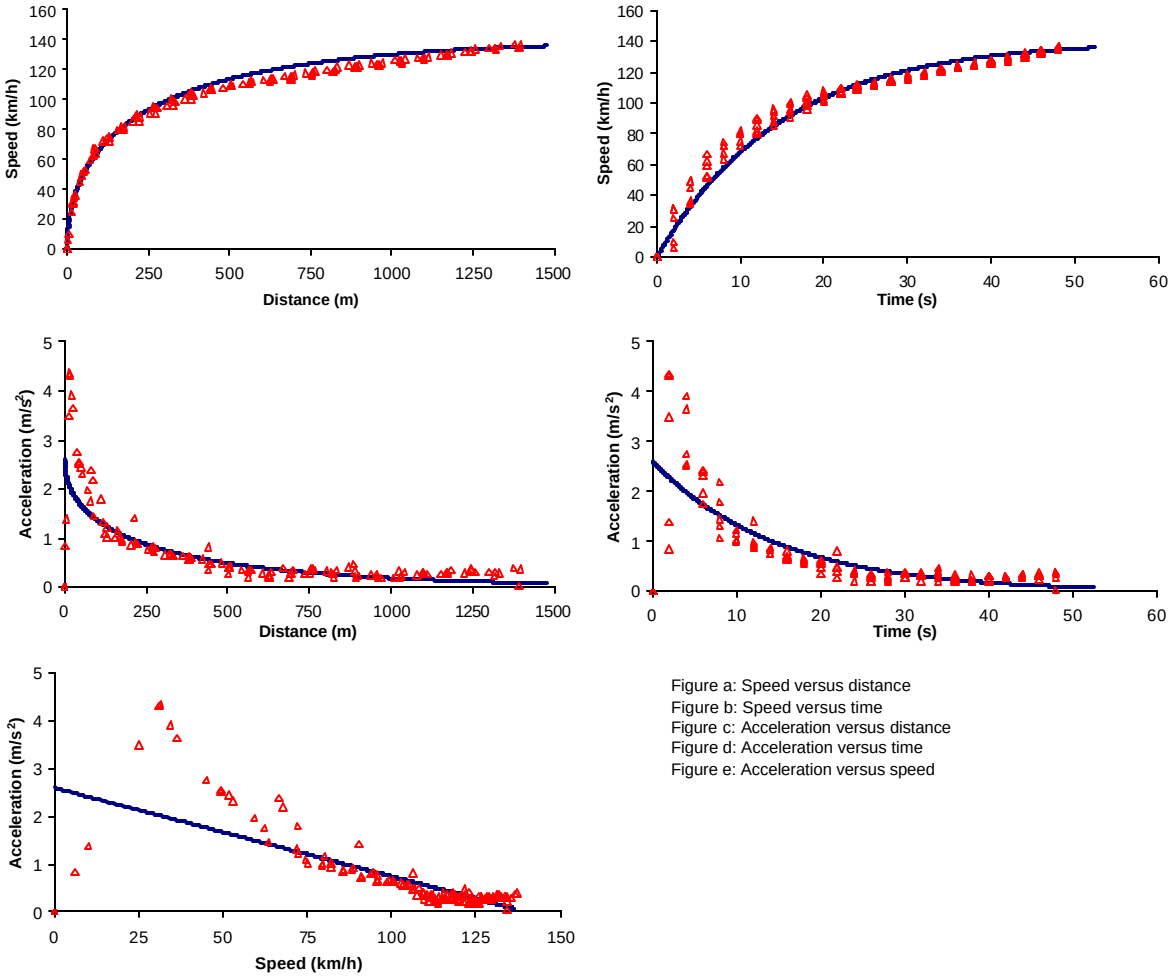

Figure a: Speed versus distance
Figure b: Speed versus time
Figure c: Acceleration versus distance
Figure d: Acceleration versus time
Figure e: Acceleration versus speed

Figure 4-25: Linear Decay Model Fit to Field Data (Ford Windstar)

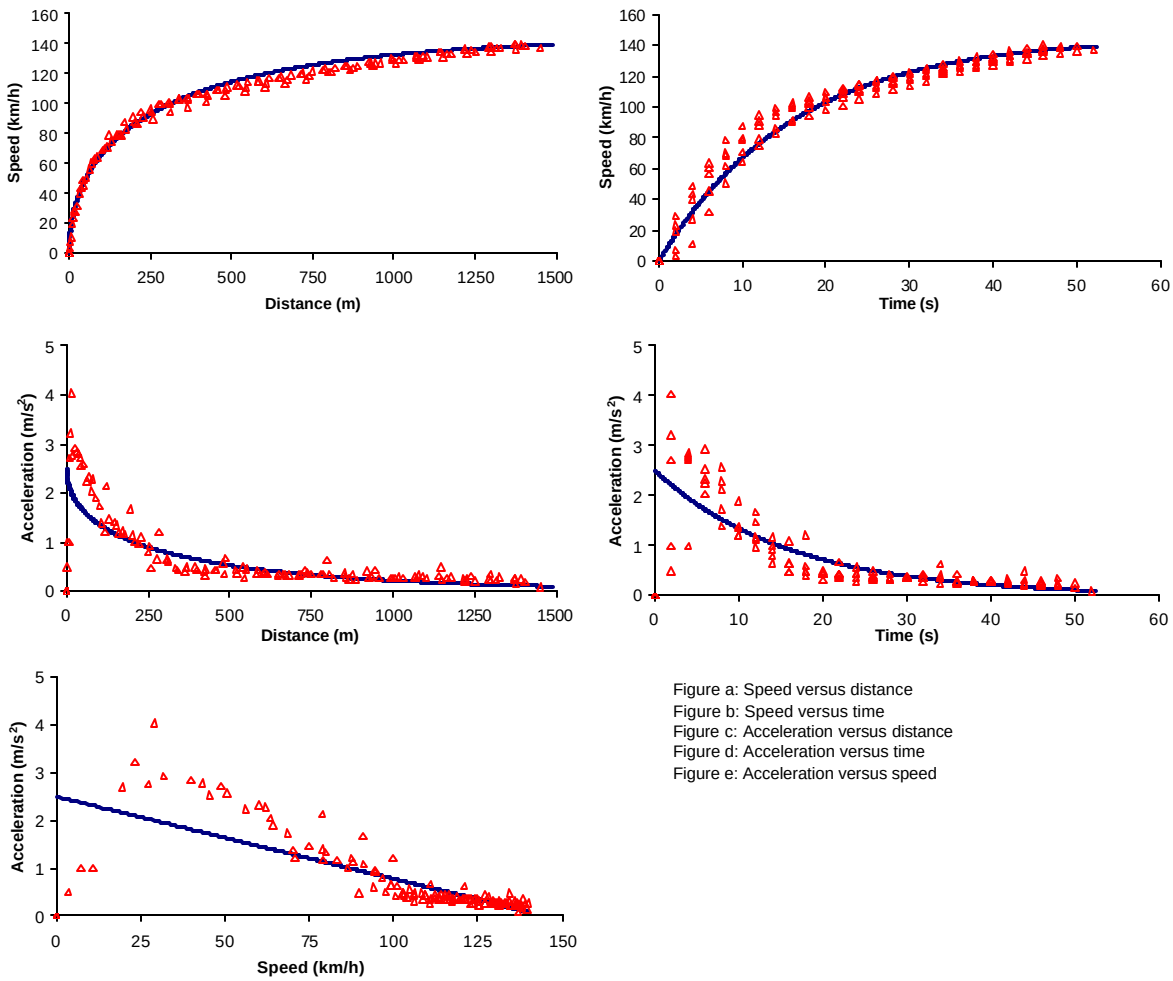

Figure 4-26: Linear Decay Model Fit to Field Data (Chevy S-10)

Four parameters were required for the calibration of the polynomial model, including initial and final speeds, acceleration time, and acceleration distance. The final speed, time, and distance in the model relates to the maximum possible speed the vehicle can attain. Since the vehicles in the data set did not necessarily reach their maximum speed over the 1.5-km test section, this parameter was more difficult to calibrate. Figure 4-27 through Figure 4-31 indicate that the polynomial model provides a fairly reasonable fit to the speed profiles of the vehicles, although it does tend to overestimate speeds towards the end of the runs. The model was designed to follow the shape of the acceleration versus time plot, and therefore generally shows the proper trend in this domain. However, the model seems to invert the trend in the acceleration versus speed domain. Specifically, while the field data suggest a curve approaching a slope of zero for high speeds, the polynomial model suggests a curve whose slope approaches infinity as speed increases. This model was shown to accurately predict distance traveled and fuel consumption by Akçelik (1987), however, this study demonstrates that the model does not reflect field data accurately.

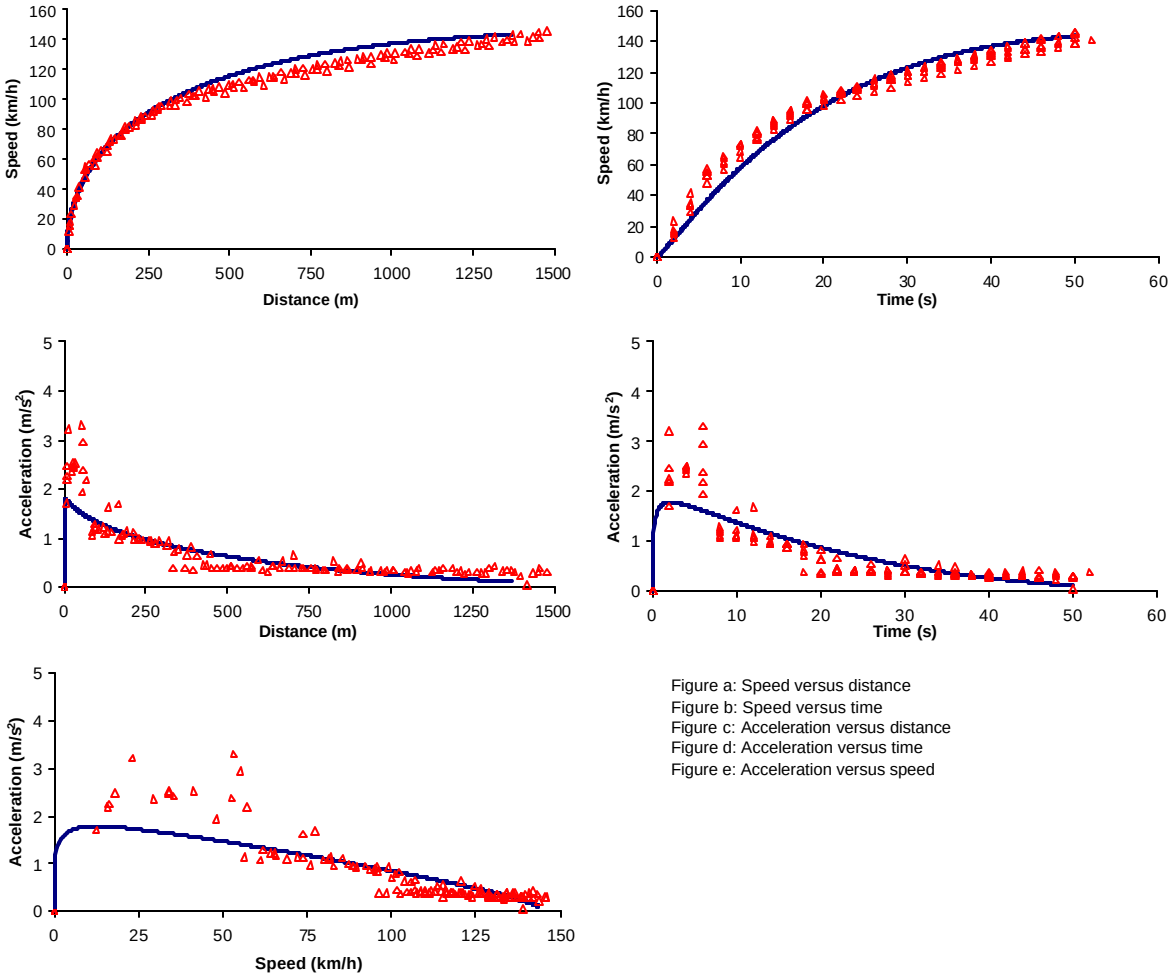

Figure 4-27: Polynomial Model Fit to Field Data (Mazda Protégé)

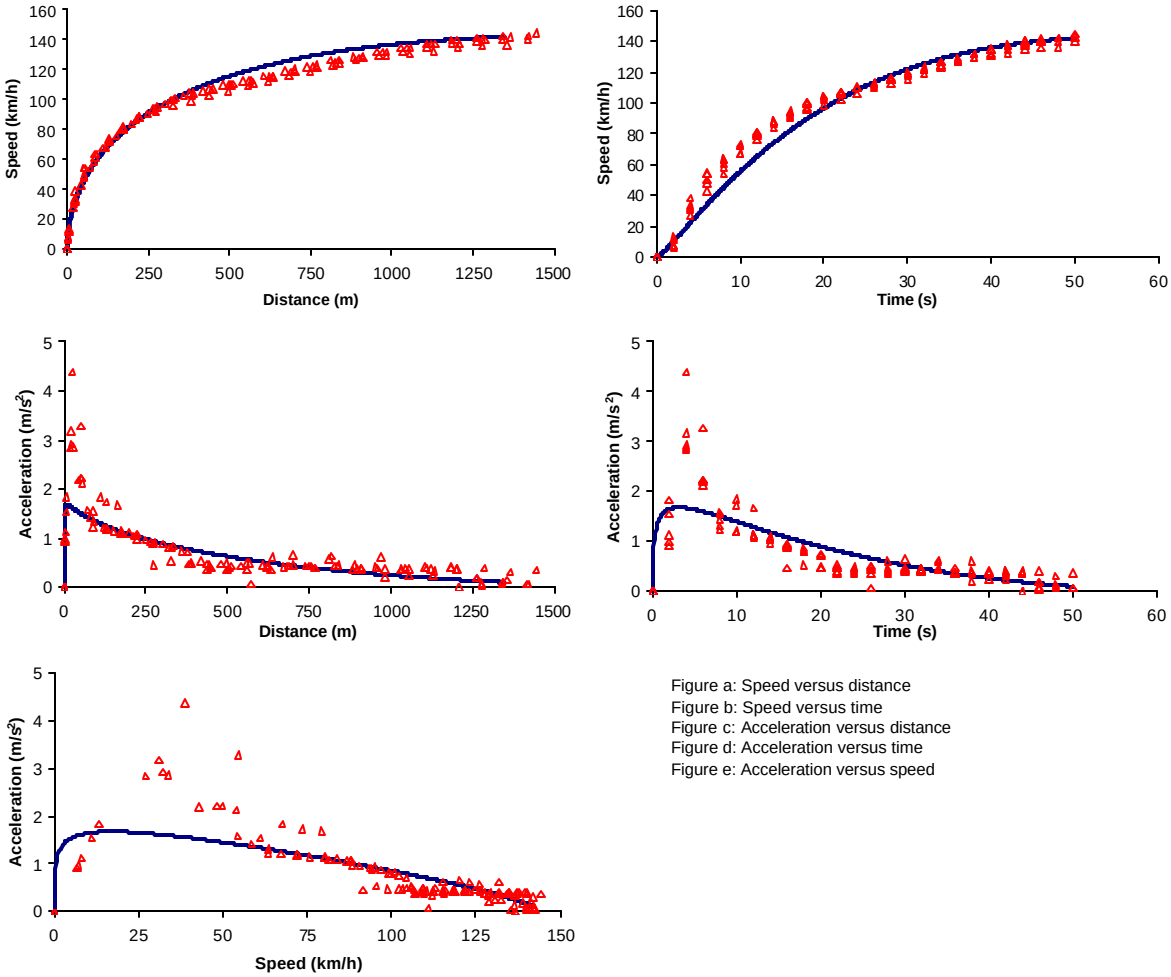

Figure 4-28: Polynomial Model Fit to Field Data (Dodge Intrepid)

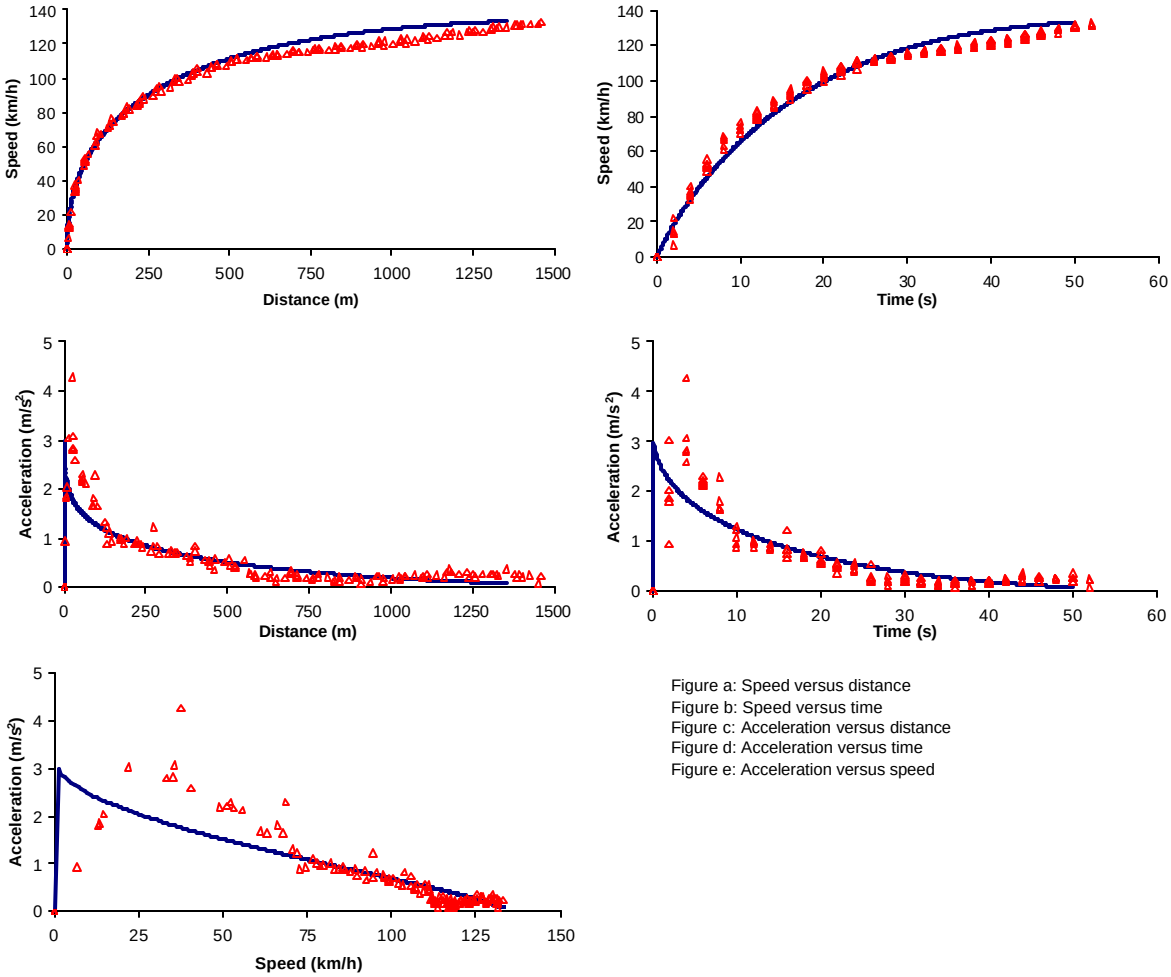

Figure 4-29: Polynomial Model Fit to Field Data (Chevy Blazer)

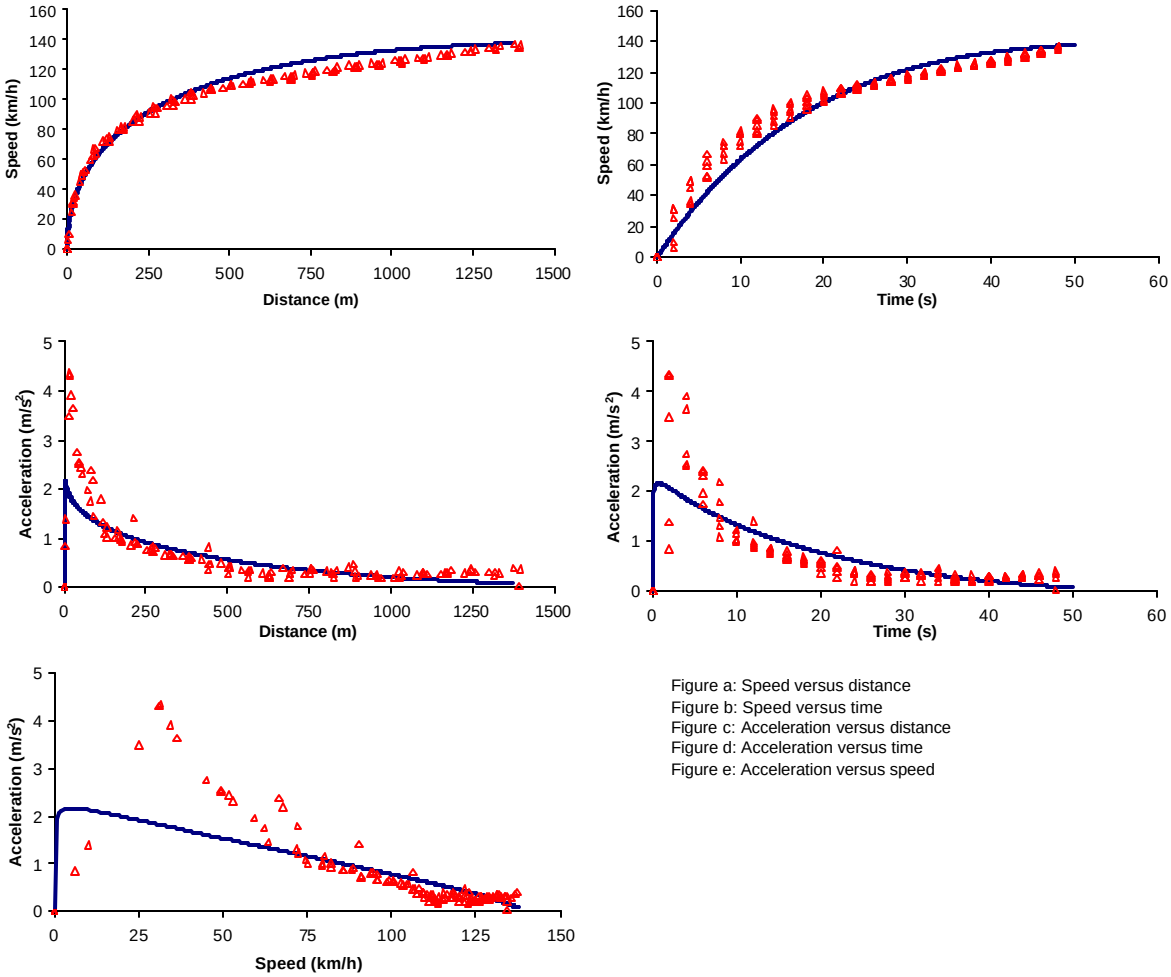

Figure a: Speed versus distance
Figure b: Speed versus time
Figure c: Acceleration versus distance
Figure d: Acceleration versus time
Figure e: Acceleration versus speed

Figure 4-30: Polynomial Model Fit to Field Data (Ford Windstar)

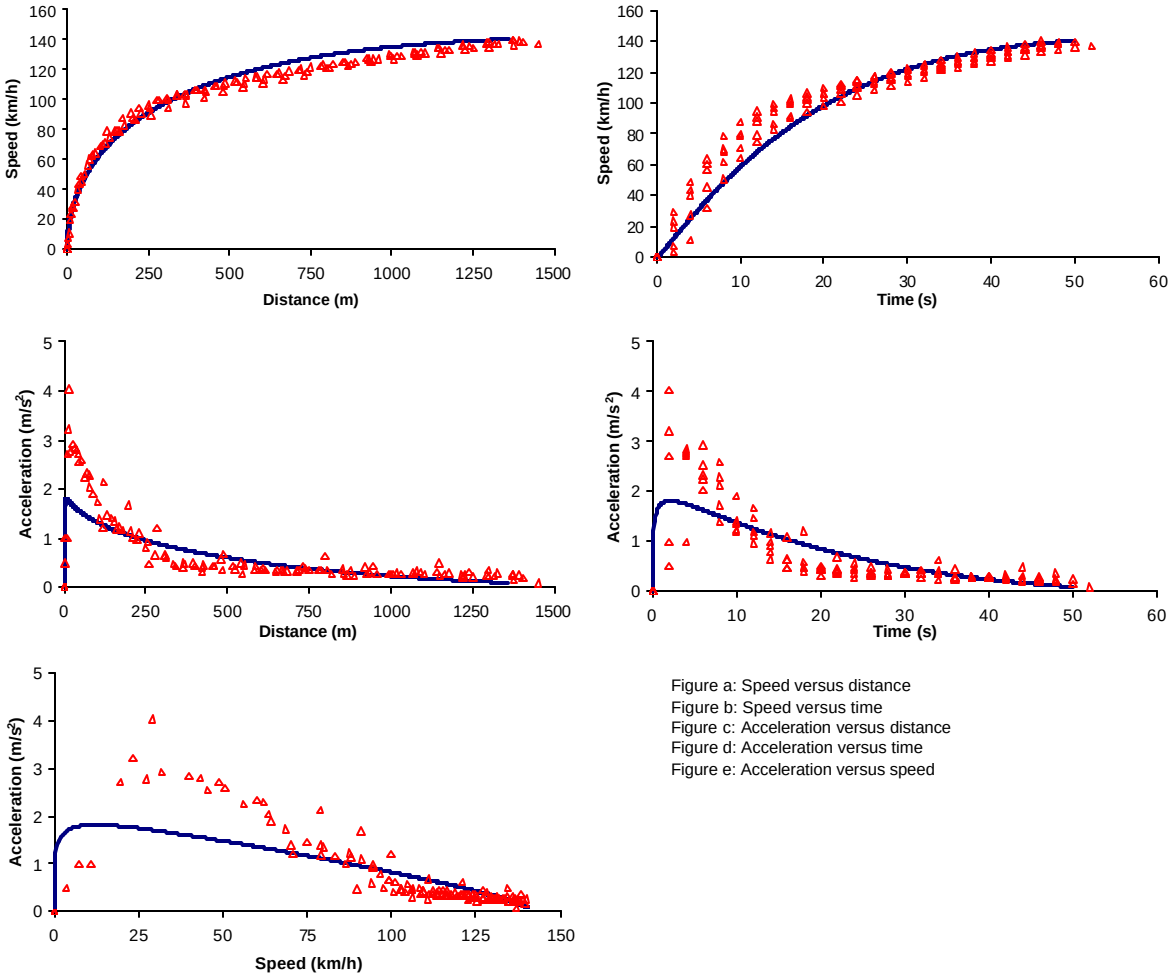

Figure 4-31: Polynomial Model Fit to Field Data (Chevy S-10)

The power constant, k, used in the Searle model was determined for each of the vehicles in the study. The Searle model appears to break down at very low speeds and speeds outside the normal driving range, as indicated by Figure 4-32 through Figure 4-36. The model predicts acceleration rates approaching infinity for low speeds, because it does not account for the potential of wheel spinning at low speeds. The vehicle dynamics model presented by Rakha et al. (2001) introduces a maximum force value that is dependent on friction between the vehicle tires and pavement surface, as indicated by Equation 4-19. The Searle model also greatly overestimates speeds beyond speeds of 120 km/h (75 mph). Because of these limitations, the Searle model is only useful in limited applications.

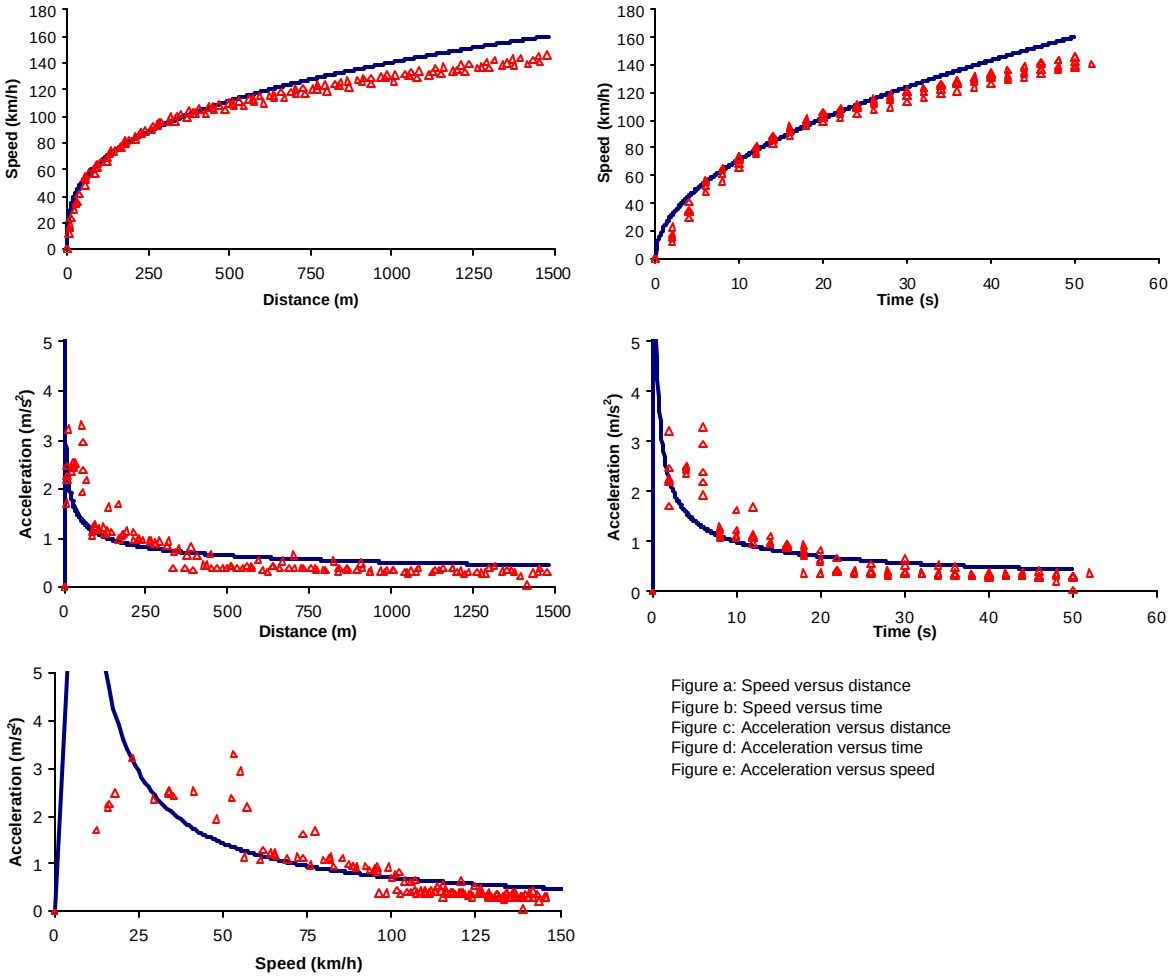

Figure a: Speed versus distance
Figure b: Speed versus time
Figure c: Acceleration versus distance
Figure d: Acceleration versus time
Figure e: Acceleration versus speed

Figure 4-32: Searle Model Fit to Field Data (Mazda Protégé)

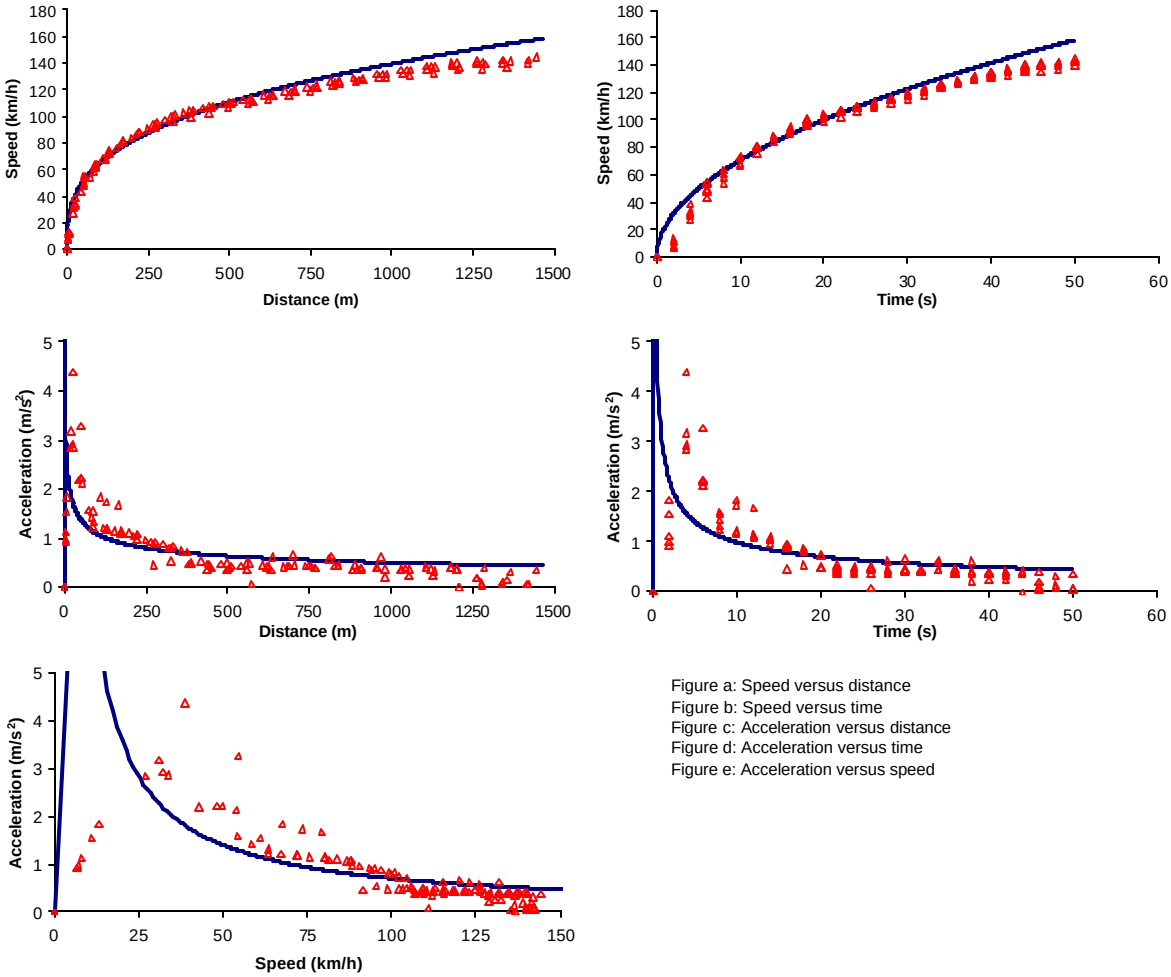

Figure a: Speed versus distance
Figure b: Speed versus time
Figure c: Acceleration versus distance
Figure d: Acceleration versus time
Figure e: Acceleration versus speed

Figure 4-33: Searle Model Fit to Field Data (Dodge Intrepid)

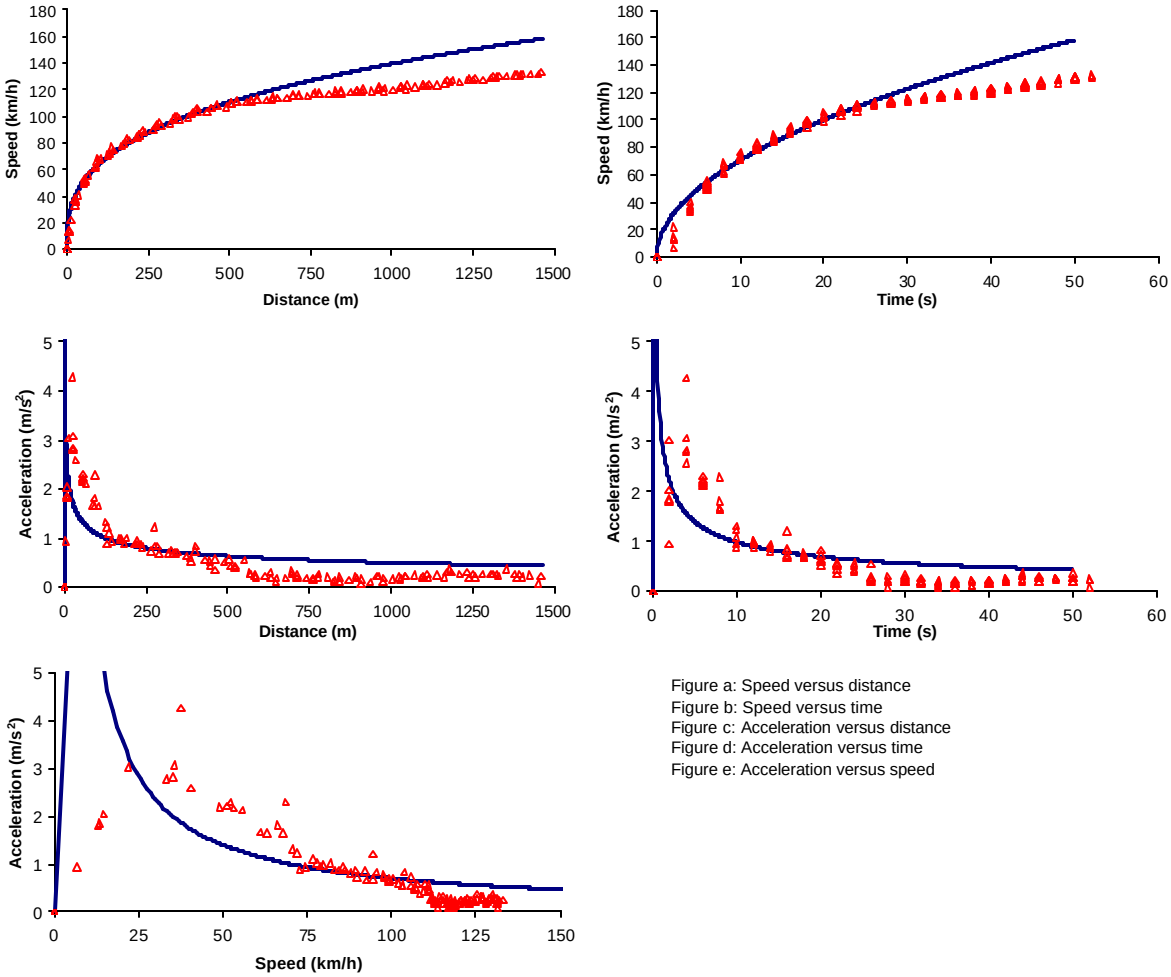

Figure a: Speed versus distance
Figure b: Speed versus time
Figure c: Acceleration versus distance
Figure d: Acceleration versus time
Figure e: Acceleration versus speed

Figure 4-34: Searle Model Fit to Field Data (Chevy Blazer)

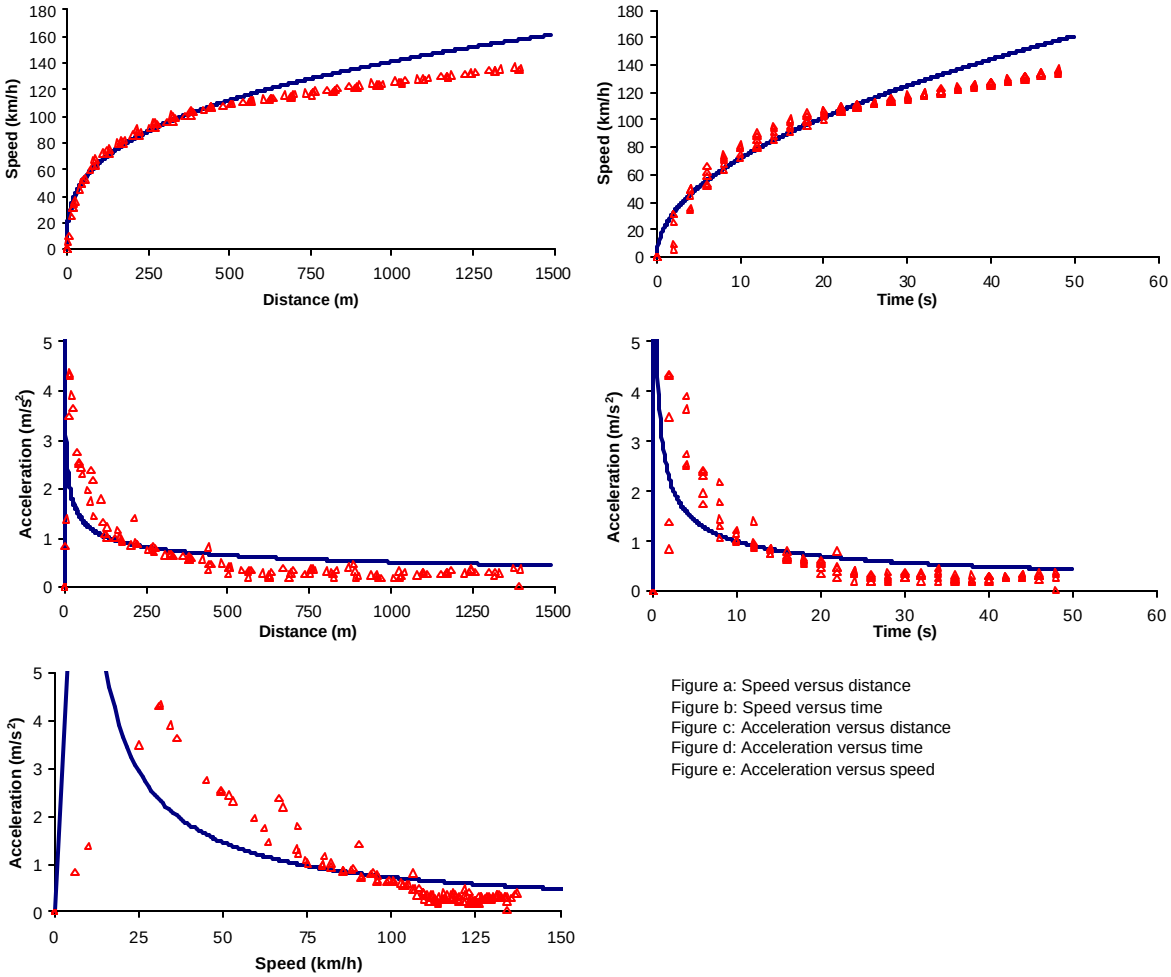

Figure a: Speed versus distance
Figure b: Speed versus time
Figure c: Acceleration versus distance
Figure d: Acceleration versus time
Figure e: Acceleration versus speed

Figure 4-35: Searle Model Fit to Field Data (Ford Windstar)

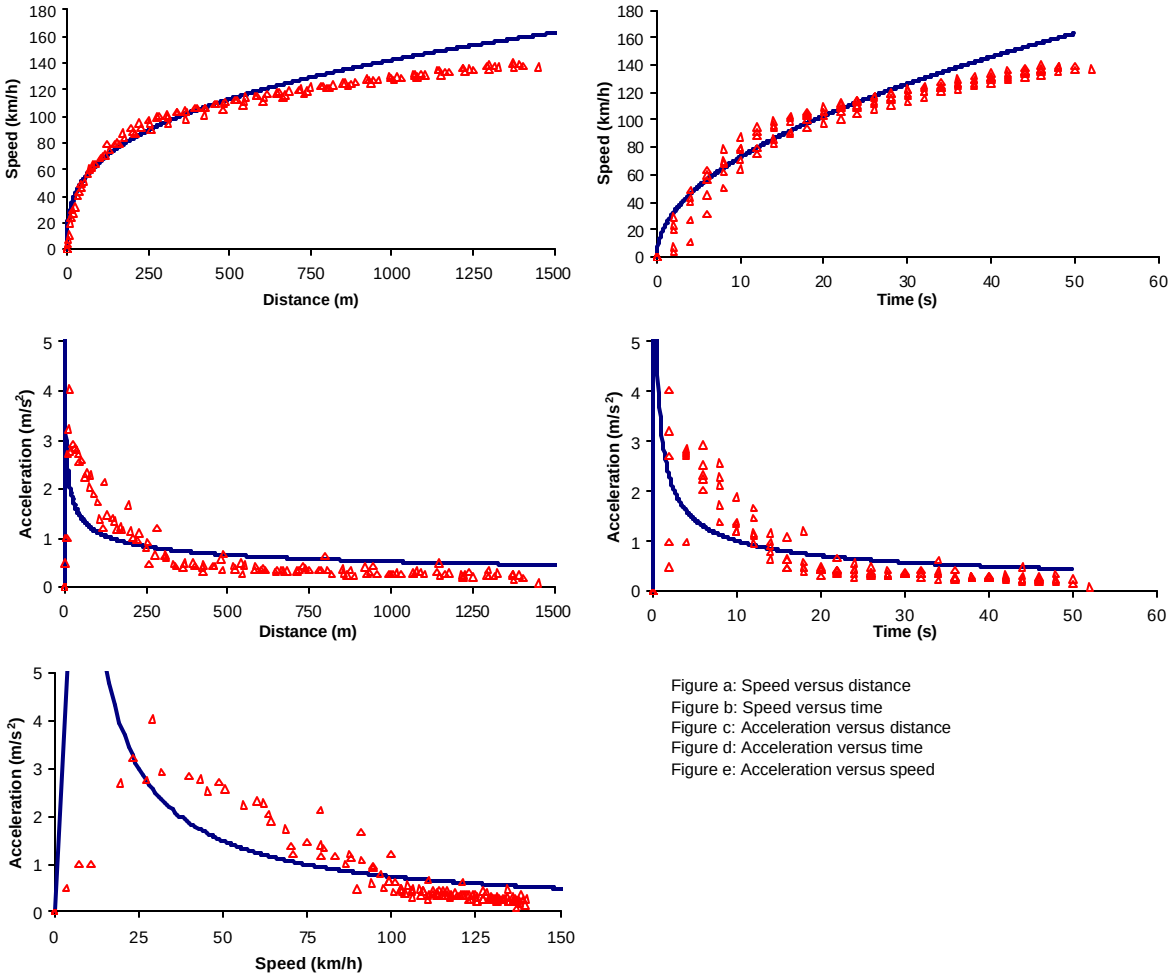

Figure a: Speed versus distance
Figure b: Speed versus time
Figure c: Acceleration versus distance
Figure d: Acceleration versus time
Figure e: Acceleration versus speed

Figure 4-36: Searle Model Fit to Field Data (Chevy S-10)

4.4.6 *Advantages of Vehicle Dynamics Model*

Based on this comparison study, three primary advantages of the Rakha dynamics model can be observed:

1. Good Fit in all Domains: The vehicle dynamics model offers a good fit to field data in each of the domains, namely speed versus distance, speed versus time, acceleration versus speed, acceleration versus time, and acceleration versus distance. Alternatively, the other models, especially the empirical models, are designed to fit a single domain, and therefore do not fit well over all domains.

2. Model Flexibility: The vehicle dynamics model is able to adapt to different vehicle types, different pavement conditions, and travel over different terrain.

3. Simple Calibration: Another advantage of the vehicle dynamics model is that it does not require field data sets to calibrate input parameters. Specifically, input parameters can be obtained from vehicle manuals, car magazines, and/or the World Wide Web. Alternatively, the other models require field data for the calibration of input parameters.

4.5. Conclusions and Recommendations for Further Research

The paper constructs a database of unconstrained vehicle acceleration data for thirteen light duty vehicles and trucks. In addition, the paper validates a vehicle dynamics model for predicting maximum light duty vehicle acceleration rates. The model is compared to four of state-of-art acceleration models using the developed data set. Advantages of the vehicle dynamics model are presented, including its ability to accurately predict vehicle behavior with readily available input parameters and its flexibility in estimating acceleration rates of both large and small vehicles on varied terrain.

It is recommended that further research be conducted in a number of areas. First, there is a need to collect field data on typical lead vehicle acceleration (not interacting with other preceding vehicles). Second, data are required on vehicle acceleration behavior within a platoon (interacting with other vehicles). Third, data are required on typical vehicle acceleration during critical events, including merging with freeway traffic at an on-ramp and accelerating to overtake a vehicle. For all these scenarios vehicle acceleration models should be developed to capture driver behavior in the non-steady state car-following mode of operation. The next chapter serves to address some of these issues.

Chapter Five:
Modeling Typical Acceleration Behavior

5.1 Introduction

Our roadways are filled with a broad range of vehicles driven by a wide variety of drivers. The drivers vary from old to young, male to female, aggressive to passive. The acceleration behavior of these drivers varies greatly. The aggressiveness of the drivers can be influenced by a large number of factors, including the other cars on the road or even the mood of the driver on a given day. Consequently, it's difficult to accurately predict actual driver behavior and be able to model conditions that are actually present on our roadway infrastructure. However, simulation models, fuel consumption models, and emissions models, among others, are essential tools for engineers trying to solve real-world problems. These tools require accurate representations of actual situations in order to be effective. Therefore, a model that accounts for different driver types and vehicle behavior is essential.

However, limited effort has been made to try to categorize the typical acceleration behavior of drivers. Only a few generalizations about typical driver behavior have been proposed in the literature as it relates to the maximum performance of the vehicle. In a 1937 study by the Bureau of Public Roads, Loutzenheiser suggested that drivers accelerate at a rate approximately two-thirds of the vehicle capability (1938). In 1954, the Blue Book recommended using a value of 60% when comparing typical acceleration to maximum acceleration for an average driver (AASHTO). However, a study by Long showed that applying the value of 60% to the popular linear decay acceleration model produced erroneous results when compared to field data (2000). Using the linear decay model, Long recommends using an alpha value of 2 m/s^2 and a beta value of 0.12 to depict average accelerations of passenger cars. Other values for various vehicles are recommended by Long in the literature (2000).

Many other models have been developed to predict vehicle acceleration patterns based on empirical relationships generated from field data. However, these models must been updated often as the capabilities of vehicles change, speed limits on our highways change, and the demographics of drivers on the road change. The goal of this paper is to develop a distribution of factors to represent the acceleration patterns of the driving public and therefore create an acceleration model that more accurately represents actual conditions.

5.2 Maximum Model

Before creating a model for typical acceleration, we must start with a model for maximum acceleration. The Rakha model is a vehicle dynamics model that has been used to predict the maximum speed and acceleration profiles of a variety of passenger vehicles and trucks based on the forces acting on the vehicle. Using readily available input parameters about the vehicle and roadway, the Rakha model has been shown to

replicate data collected from field research in the domains of speed versus time, speed versus distance, acceleration versus time, acceleration versus distance, and acceleration versus speed. A thorough description of the Rakha model can be found in Chapter 4. The goal of this chapter is to develop an appropriate modification to the Rakha model that will enable it to predict typical driver behavior for a variety of driver types.

5.3 Field Tests

The first step in the research effort was the collection of a new set of field data. Existing data sets did not contain information about the individual drivers and vehicles that was necessary for the model. Therefore, field tests were performed as described in the following section.

5.3.1 *Test Procedure*

Testing was performed in the spring and summer of 2002 at the Smart Road research facility in Blacksburg, Virginia. The test involved accelerating a vehicle from a stop over a distance of approximately 1100 feet (335 m) at a driver's normal acceleration rate. The test was performed on a relatively flat and straight stretch of roadway controlled by a stop sign and subject to very light traffic volumes that would not interfere with each run. The goal was to simulate the typical acceleration profile of a lead vehicle at a stop line. Twenty different drivers volunteered for the test, and they are described in the following section. The test vehicle used in the test was a 1999 Ford Crown Victoria, which had been equipped with a GPS unit that collected speed data for the vehicle every second. The same vehicle was used for each driver, in order to serve as the control for the experiment. The drivers were each allowed to drive the vehicle for a while to get familiar with the car before starting the testing. The drivers were aware that they were being tested, and were told to accelerate at their normal rate until the end of the test section. To account for variability within the driver, up to twenty-five runs were conducted. From these runs, speed, time, and distance measurements were recorded. The results are presented later in this report.

5.3.2 *Test Drivers*

The test drivers were random volunteers chosen to reflect the driving population on the road today. Twenty drivers overall were chosen, including eleven men and nine women. The drivers ranged in age from 21 to 45. Table 5-1 shows a breakdown of licensed drivers on the road for the year 1999, listed by age and gender, according to federal highway administration statistics. Note that the age group studied in this research project reflects over half of the driver population on the road. Further research needs to be done on teenage drivers and elderly drivers, which was beyond the scope of this paper. Over fifty percent of drivers nationally are male, and therefore 55% of drivers studied for this research were male. Table 5-2 shows a breakdown of the drivers used in the study.

Table 5-1: National Driver Statistics, Source FHWA

DISTRIBUTION OF LICENSED DRIVERS

1999

BY SEX AND PERCENTAGE IN EACH AGE GROUP AND RELATION TO POPULATION

OCTOBER 2000 TABLE DL-20

AGE	MALE DRIVERS			FEMALE DRIVERS			TOTAL DRIVERS		
	NUMBER	PERCENT OF TOTAL DRIVERS	DRIVERS AS PERCENT OF AGE GROUP 1/	NUMBER	PERCENT OF TOTAL DRIVERS	DRIVERS AS PERCENT OF AGE GROUP 1/	NUMBER	PERCENT OF TOTAL DRIVERS	DRIVERS AS PERCENT OF AGE GROUP 1/
UNDER 16	17,543	0.0	0.4	15,706	0.0	0.4	33,248	0.0	0.4
16	753,624	0.8	37.3	704,633	0.8	37.0	1,458,257	0.8	37.2
17	1,200,327	1.3	57.9	1,130,122	1.2	58.2	2,330,449	1.2	58.0
18	1,434,671	1.5	72.1	1,332,849	1.4	70.7	2,767,520	1.5	71.4
19	1,563,198	1.7	74.3	1,457,470	1.6	72.6	3,020,668	1.6	73.5
(19 AND UNDER)	4,969,362	5.3	40.9	4,640,780	5.0	40.4	9,610,142	5.1	40.7
20	1,559,679	1.7	78.0	1,482,071	1.6	78.0	3,041,750	1.6	78.0
21	1,561,806	1.7	82.3	1,490,535	1.6	82.4	3,052,341	1.6	82.4
22	1,600,041	1.7	88.1	1,536,503	1.7	88.0	3,136,544	1.7	88.0
23	1,587,646	1.7	92.6	1,520,575	1.6	91.4	3,108,221	1.7	92.0
24	1,630,891	1.7	92.9	1,559,507	1.7	90.4	3,190,398	1.7	91.7
(20-24)	7,940,062	8.4	86.5	7,589,191	8.2	85.8	15,529,253	8.3	86.2
25-29	9,067,323	9.6	100.1	8,670,126	9.3	94.7	17,737,449	9.5	97.4
30-34	9,633,540	10.2	98.6	9,279,100	10.0	93.2	18,912,641	10.1	95.9
35-39	10,635,935	11.3	94.8	10,464,605	11.3	92.4	21,100,541	11.3	93.6
40-44	10,376,809	11.0	94.0	10,345,322	11.1	92.1	20,722,131	11.1	93.1
45-49	9,328,218	9.9	98.2	9,288,229	10.0	94.2	18,616,447	9.9	96.2
50-54	8,096,694	8.6	101.2	8,036,958	8.6	95.1	16,133,652	8.6	98.1
55-59	6,200,918	6.6	100.3	6,147,189	6.6	91.8	12,348,107	6.6	95.9
60-64	4,858,994	5.2	97.8	4,804,434	5.2	86.6	9,663,428	5.2	91.9
65-69	4,163,873	4.4	96.0	4,167,098	4.5	81.5	8,330,972	4.5	88.2
70-74	3,645,458	3.9	94.4	3,806,964	4.1	77.6	7,452,422	4.0	85.0
75-79	2,777,529	2.9	90.9	3,011,770	3.2	70.5	5,789,299	3.1	79.0
80-84	1,582,587	1.7	87.2	1,748,113	1.9	58.2	3,330,701	1.8	69.1
85 AND OVER	889,019	0.9	71.7	1,004,218	1.1	34.2	1,893,236	1.0	45.3
TOTAL	94,166,321	100.0	74.3	93,004,099	100.0	69.9	187,170,420	100.0	72.0

1/ These percentages are computed using population estimates of the Bureau of the Census. Under-16 age group is compared to 14 and 15-year-old population estimates; the other age brackets coincide with those from the Bureau of the Census.

Table 5-2: Test Driver Characteristics

Driver #	Age	Gender
1	23	Male
2	23	Male
3	27	Male
4	29	Male
5	31	Male
6	31	Male
7	33	Male
8	34	Male
9	35	Male
10	38	Male
11	45	Male
12	21	Female
13	22	Female
14	22	Female
15	22	Female
16	23	Female
17	23	Female
18	24	Female
19	30	Female
20	35	Female

5.4 Results

The Rakha model for predicting the maximum acceleration behavior of vehicles had been validated for the test vehicle, the 1999 Ford Crown Victoria, in the previous chapter. Figure 5-1 shows the strong correlation between the Rakha model and field data collected representing the maximum acceleration of the Crown Victoria. Note that this data was collected on a roadway with a substantial uphill grade. Because the Rakha model uses grade as an input parameter, it was recalibrated for a grade of 0% as shown in Figure 5-2 to account for the level grade used in this study. This model was used as a starting point and compared to the field results of each of the twenty drivers. Data was collected for the drivers, and plots of speed versus time, speed versus distance, acceleration versus time, acceleration versus distance, and acceleration versus speed were generated. Then, a reduction factor was introduced into the model for each driver until the model presented the best fit to the field data. The driver factor was multiplied by the predicted maximum acceleration to generate the actual acceleration at any time. Therefore, a driver factor of 1 would represent the maximum capability of the vehicle as shown in Figure 5-2, while a driver factor of 0.70 would signify that the driver accelerated at 70% of the maximum acceleration possible, for example.

The maximum acceleration behavior exhibited by the Crown Victoria and by other vehicles can be classified as starting at a maximum value at low speeds and gradually diminishing to lesser values as the speed of the vehicle increases, as demonstrated in the plot of acceleration versus speed in Figure 5-2. While it is clear that the typical acceleration behavior of drivers will reflect some value below the maximum vehicle capability, there is no guarantee that this lesser acceleration behavior will follow the same profile shape as the maximum behavior for every driver. Three types of driver behavior can therefore be observed. The first driver type can be classified as a Standard Accelerator. Drivers in this category will tend to follow the shape of the maximum acceleration profile, with the model simply shifted by some constant reduction factor throughout the run. A second driver classification is the Hard Accelerator. These drivers tend to accelerate from a stop at a high initial rate that is close to the maximum value and then decrease their acceleration rate as they approach their desired speed. A third group of drivers can be classified as Gradual Accelerators. These drivers are primarily concerned with passenger comfort, and accelerate at a relatively constant and moderate rate throughout the period of acceleration, despite the ability of the vehicle to accelerate more aggressively at low speeds. Figure 5-3 shows a sample test run for a driver in each of the three categories. Note that the final speed reached by each of the drivers is the same at the end of the test section. Therefore, these three drivers would have approximately the same driver reduction factor. However, Figure 5-3 clearly demonstrates three different approaches to obtaining the desired speed.

As will be discussed in the following section, the majority of the drivers observed in this research effort reflected the Standard Accelerator behavior. Because the Standard Accelerators follow the same trend as the maximum acceleration pattern, introducing a constant driver reduction factor to the model creates a good fit to the field data from their runs. Therefore, a constant reduction factor was applied to the maximum model to get

the best fit for each driver. The following section describes the breakdown for each of the drivers, grouped by their classification, and shows the fit of the model to each set of field data.

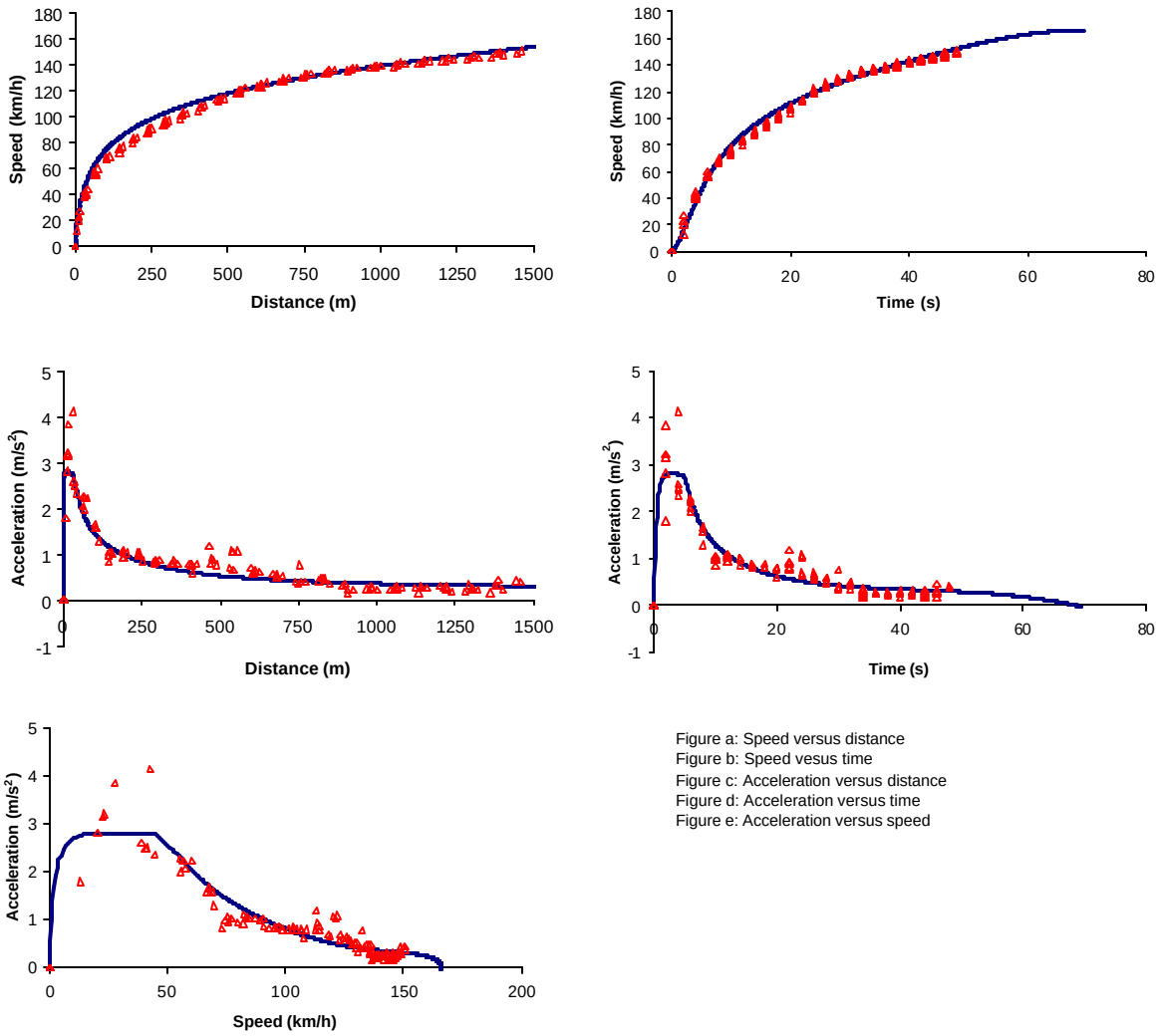

Figure 5-1: Crown Vic Maximum Acceleration Data on Smart Road with Rakha Model

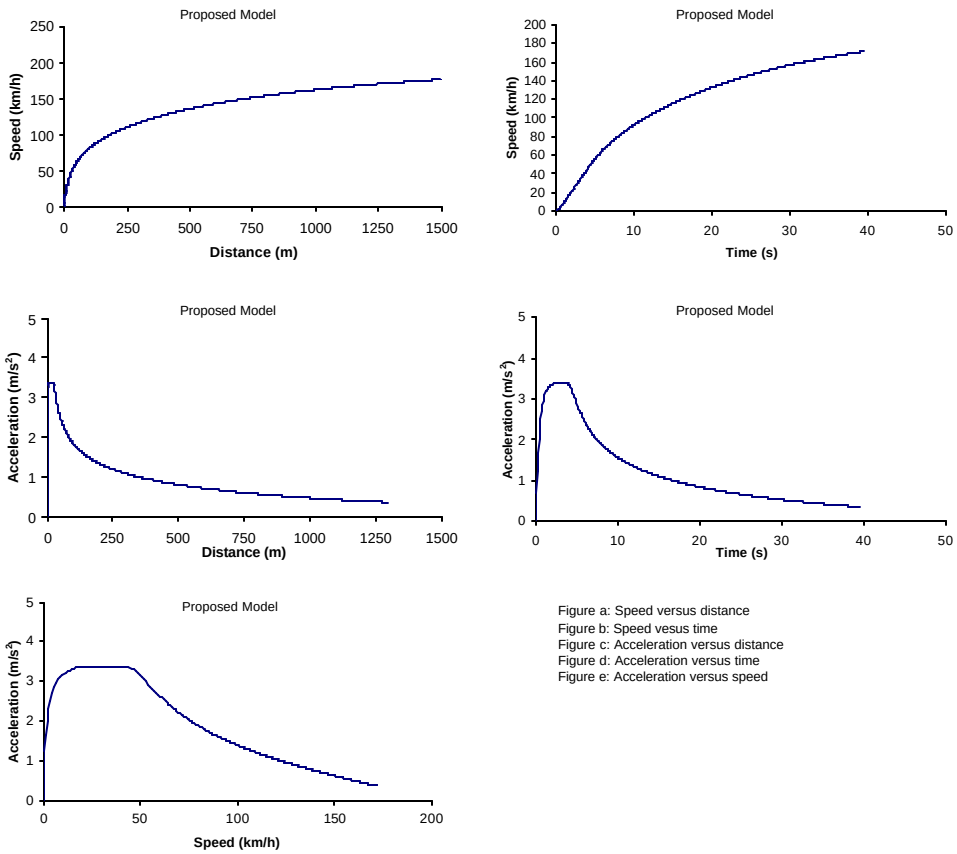

Figure 5-2: Rakha Model for Crown Vic Maximum Acceleration on Level Roadway

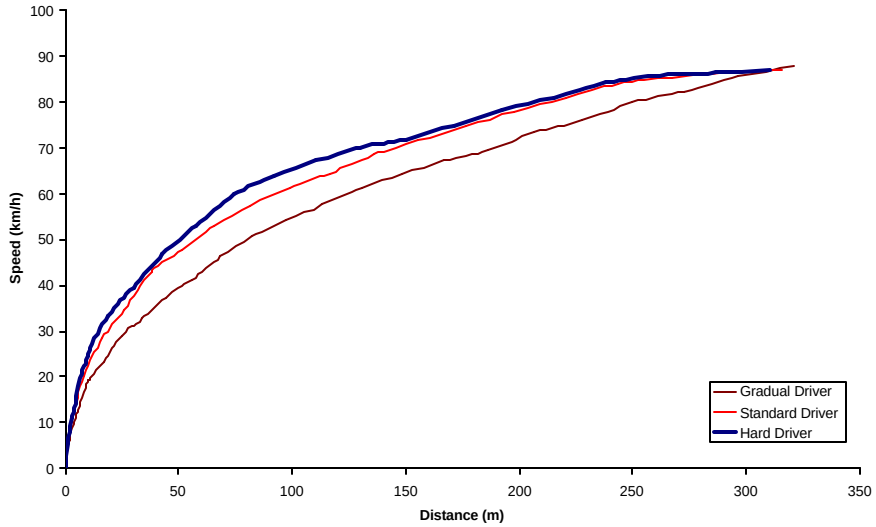

Figure 5-3: Example Profiles of Three Different Driver Types

5.4.1 *Driver Factors and Classification*

a. Standard Accelerators

The largest group of drivers observed in the study fell into the category of Standard Accelerators. The defining characteristic for this acceleration behavior is that they follow the pattern of maximum acceleration, only at a lower rate. Therefore, the acceleration profiles for these drivers are similar to the maximum acceleration profile that can be achieved by the vehicle, except that they are shifted by some constant reduction factor. Consequently, the data from these drivers shows the strongest correlation to the model. Figure 5-4 shows the effect of applying the driver factor to the acceleration versus speed plot. Note that the factor does not simply reduce the maximum acceleration rate by a certain percentage at a given speed. This is because the effect of the driver factor is cumulative throughout the acceleration, and therefore the plot is shifted towards the origin rather than just towards the x-axis. This enables the modified Rakha model to achieve a better fit to actual data than other models like the linear decay model, as will be discussed later in this report.

Fourteen of the twenty drivers (70%) fell into the standard accelerator category. Different driver factors were applied to the model for each driver to form the best fit to the field data. Larger driver factors indicate more aggressive driving. A good fit to the field data was achieved for each Standard Driver in all of the speed profiles. The trend in the acceleration plots also matches the model prediction for all of the drivers in this category. Please see Figures 5-5 through 5-18 for all plots of the different Standard Accelerators.

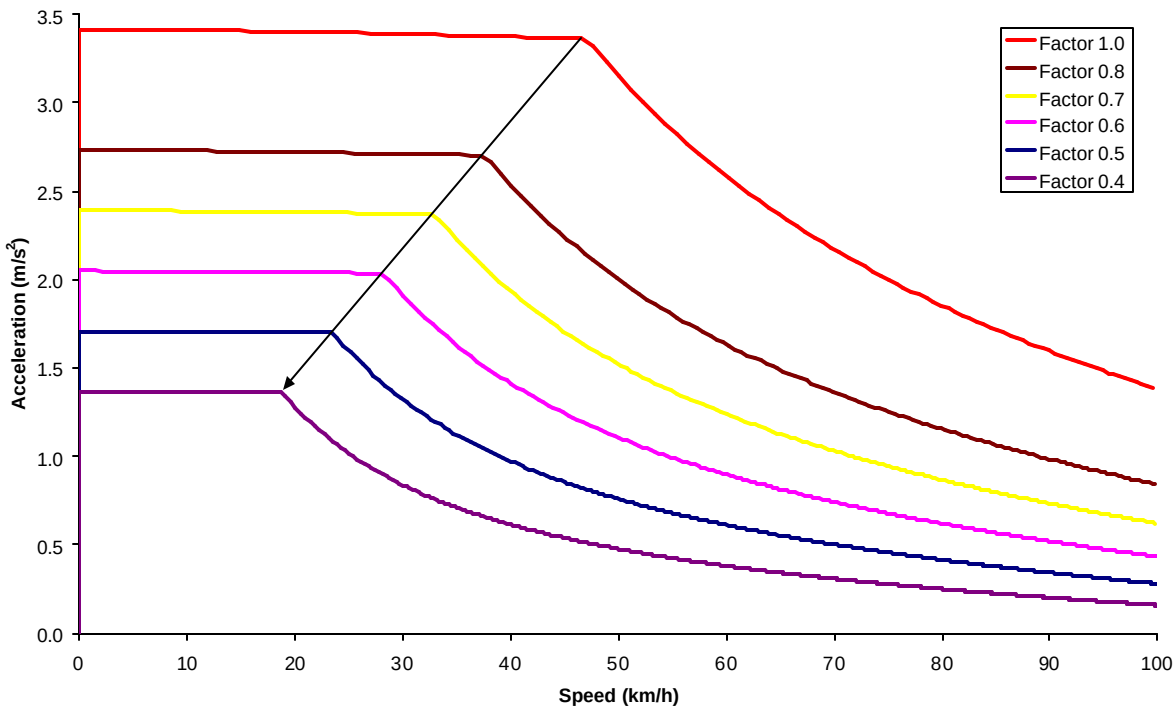

Figure 5-4: Example Effect of Driver Factors on Acceleration Profile

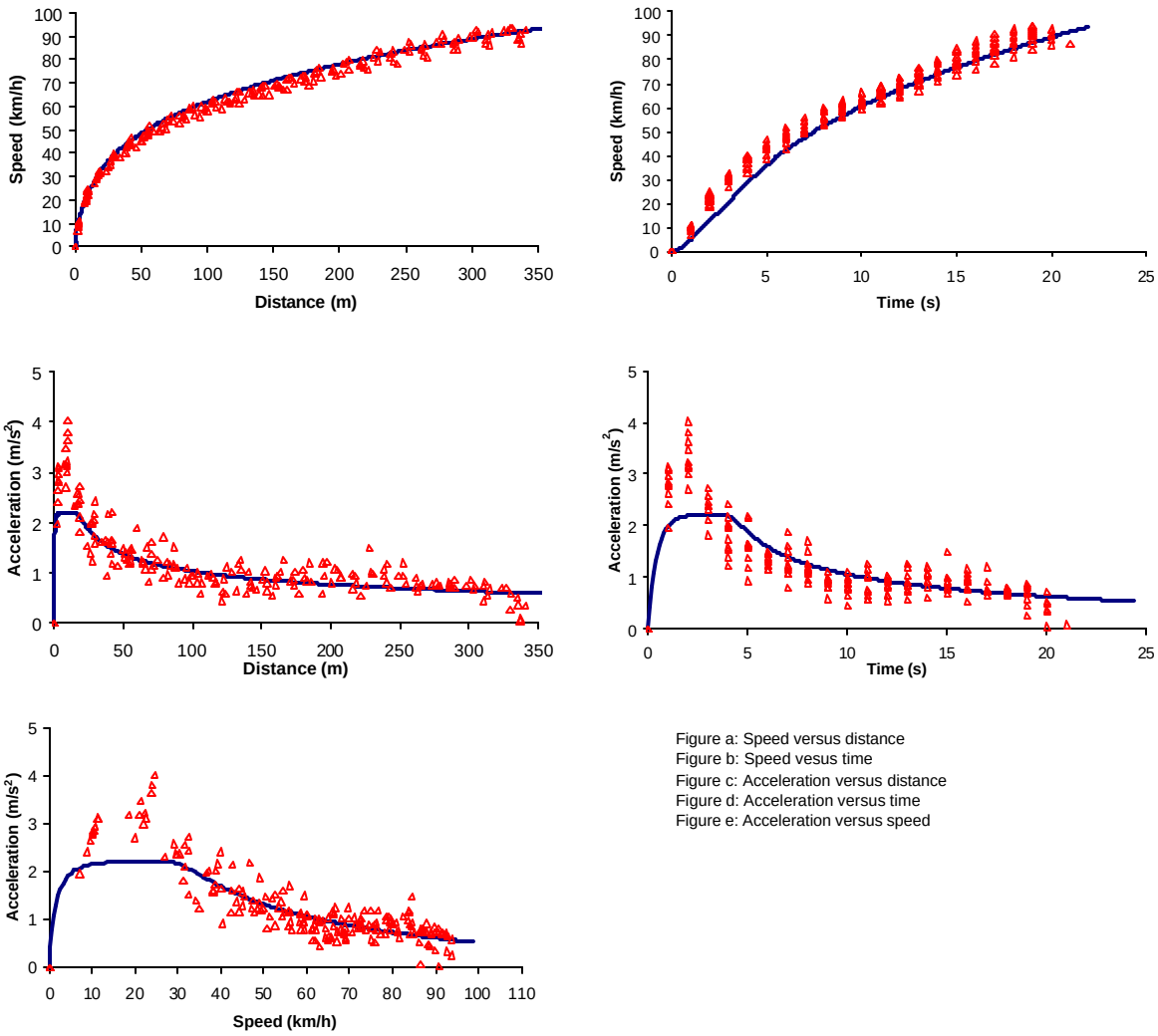

Figure a: Speed versus distance
Figure b: Speed vesus time
Figure c: Acceleration versus distance
Figure d: Acceleration versus time
Figure e: Acceleration versus speed

Figure 5-5: Driver #1 Data with Rakha Model, Reduction Factor = 0.65

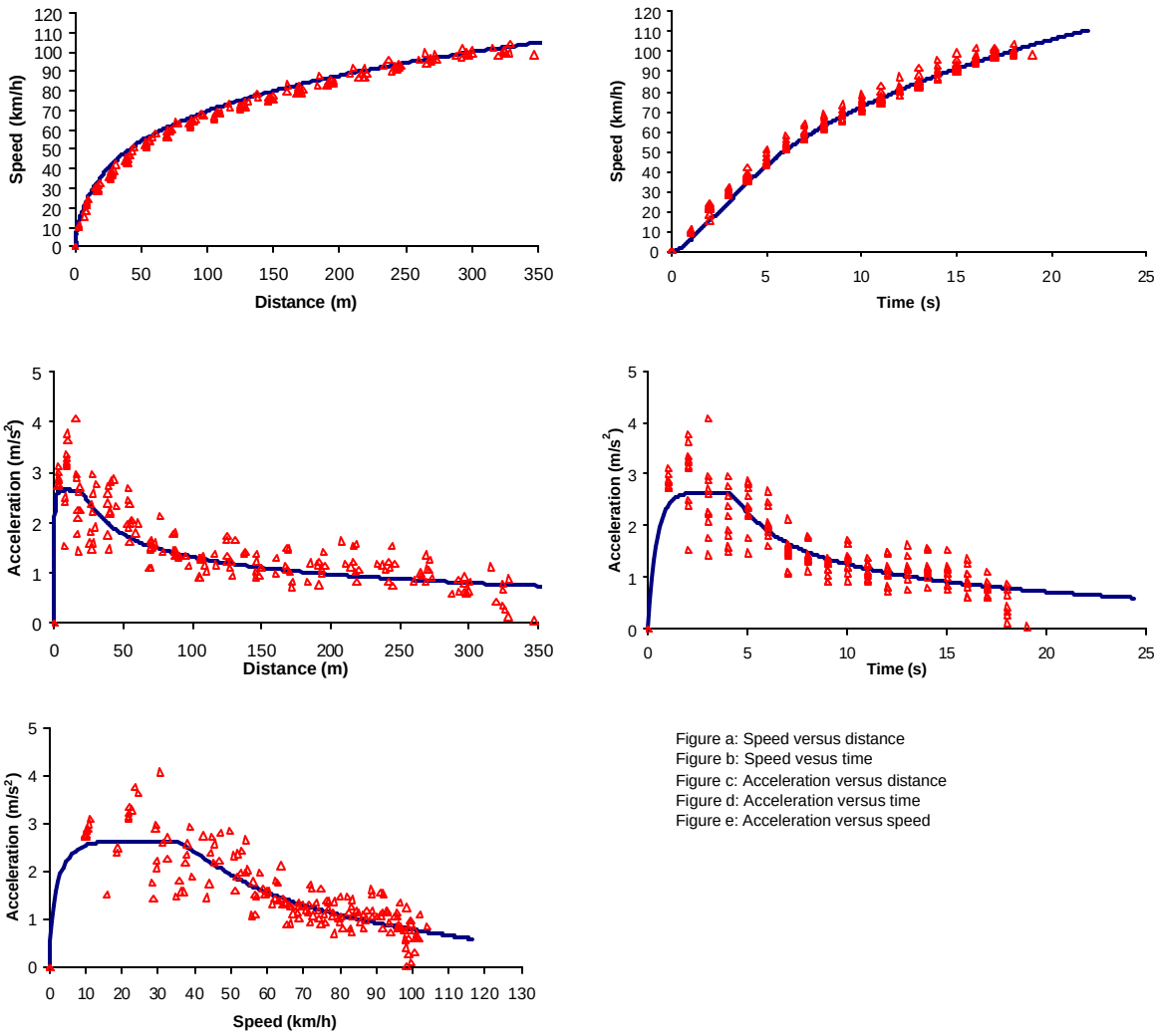

Figure a: Speed versus distance
Figure b: Speed vesus time
Figure c: Acceleration versus distance
Figure d: Acceleration versus time
Figure e: Acceleration versus speed

Figure 5-6: Driver #2 Data with Rakha Model, Reduction Factor = 0.78

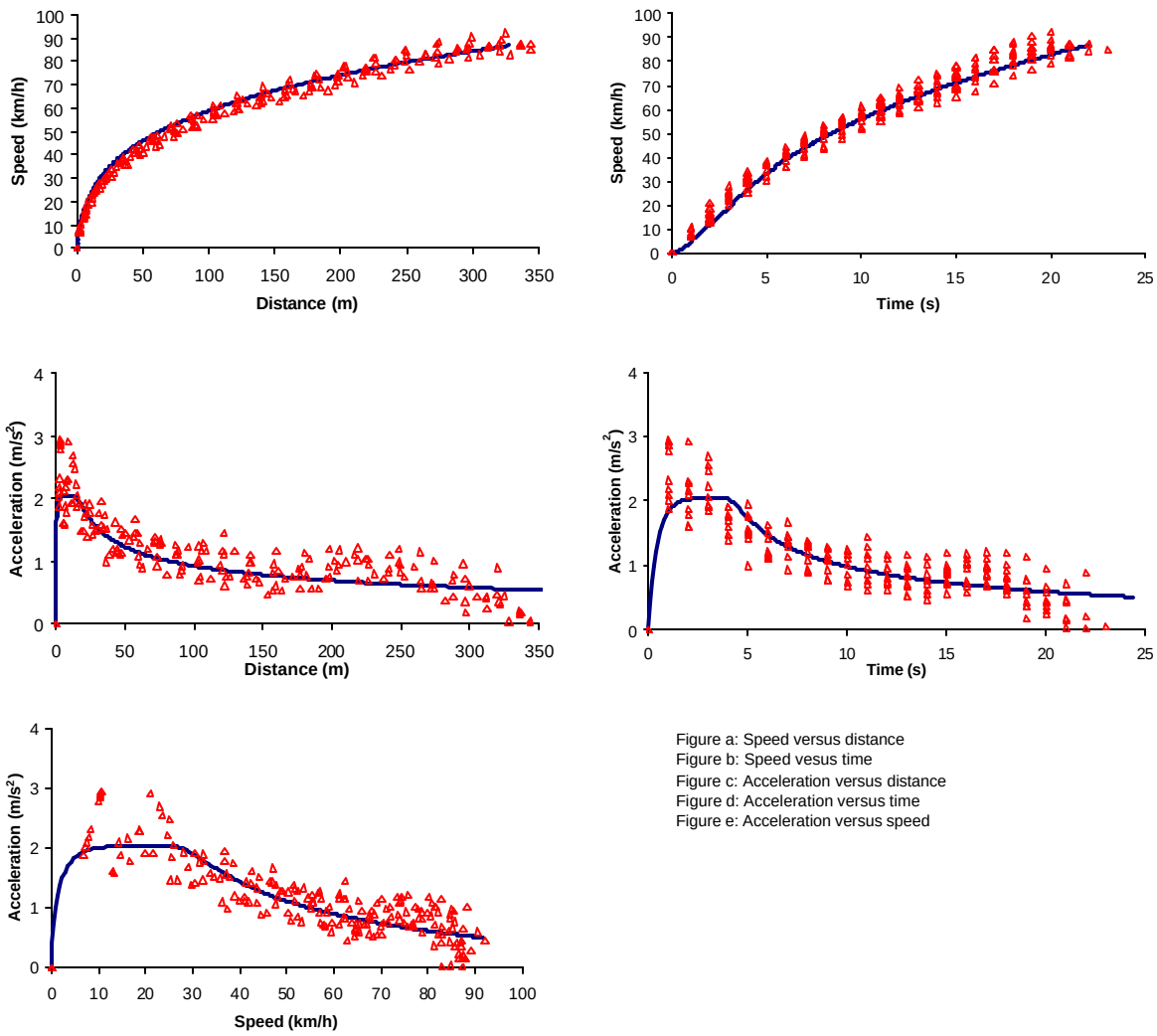

Figure a: Speed versus distance
Figure b: Speed vesus time
Figure c: Acceleration versus distance
Figure d: Acceleration versus time
Figure e: Acceleration versus speed

Figure 5-7: Driver #5 Data with Rakha Model, Reduction Factor = 0.60

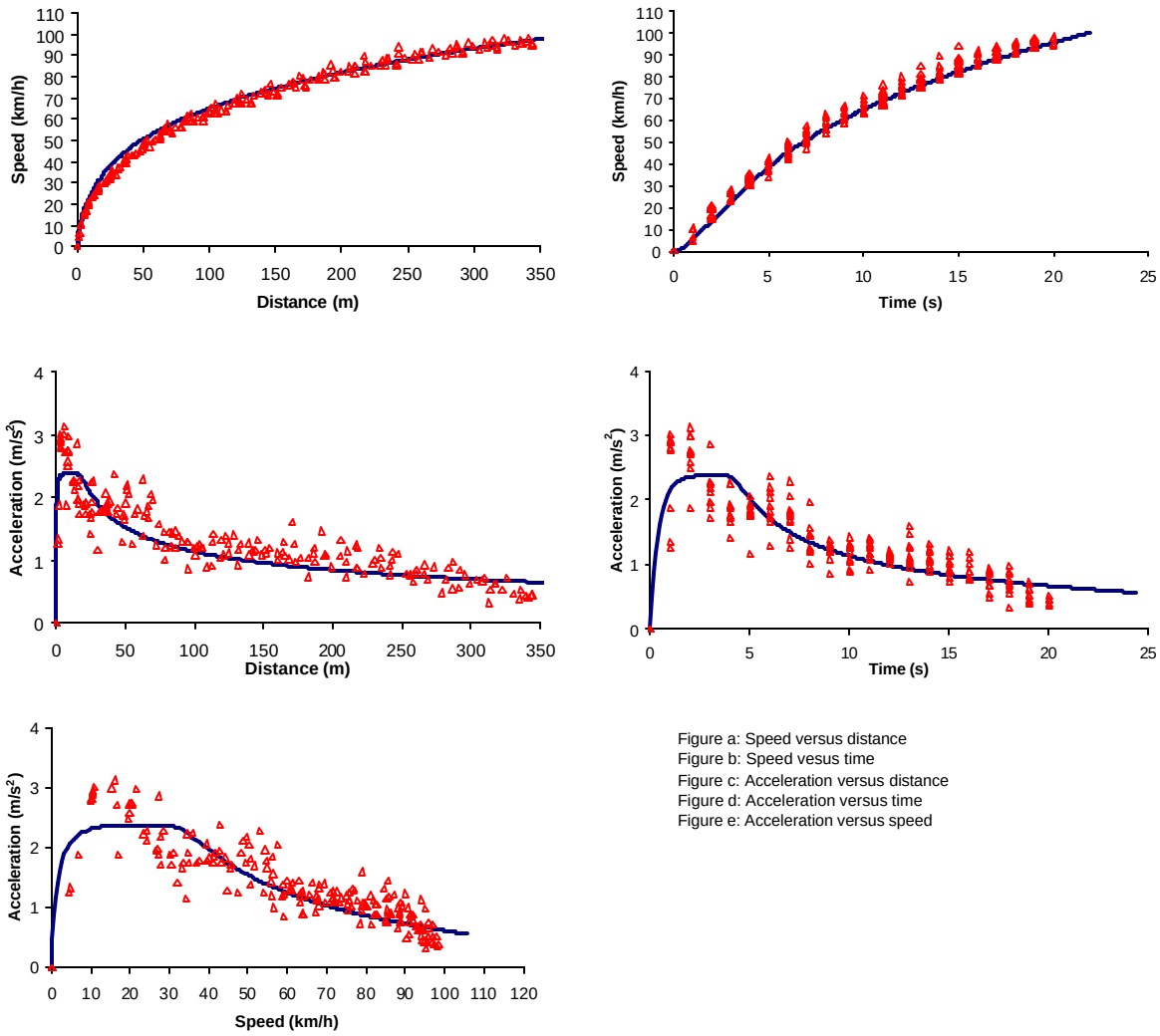

Figure 5-8: Driver #7 Data with Rakha Model, Reduction Factor = 0.70

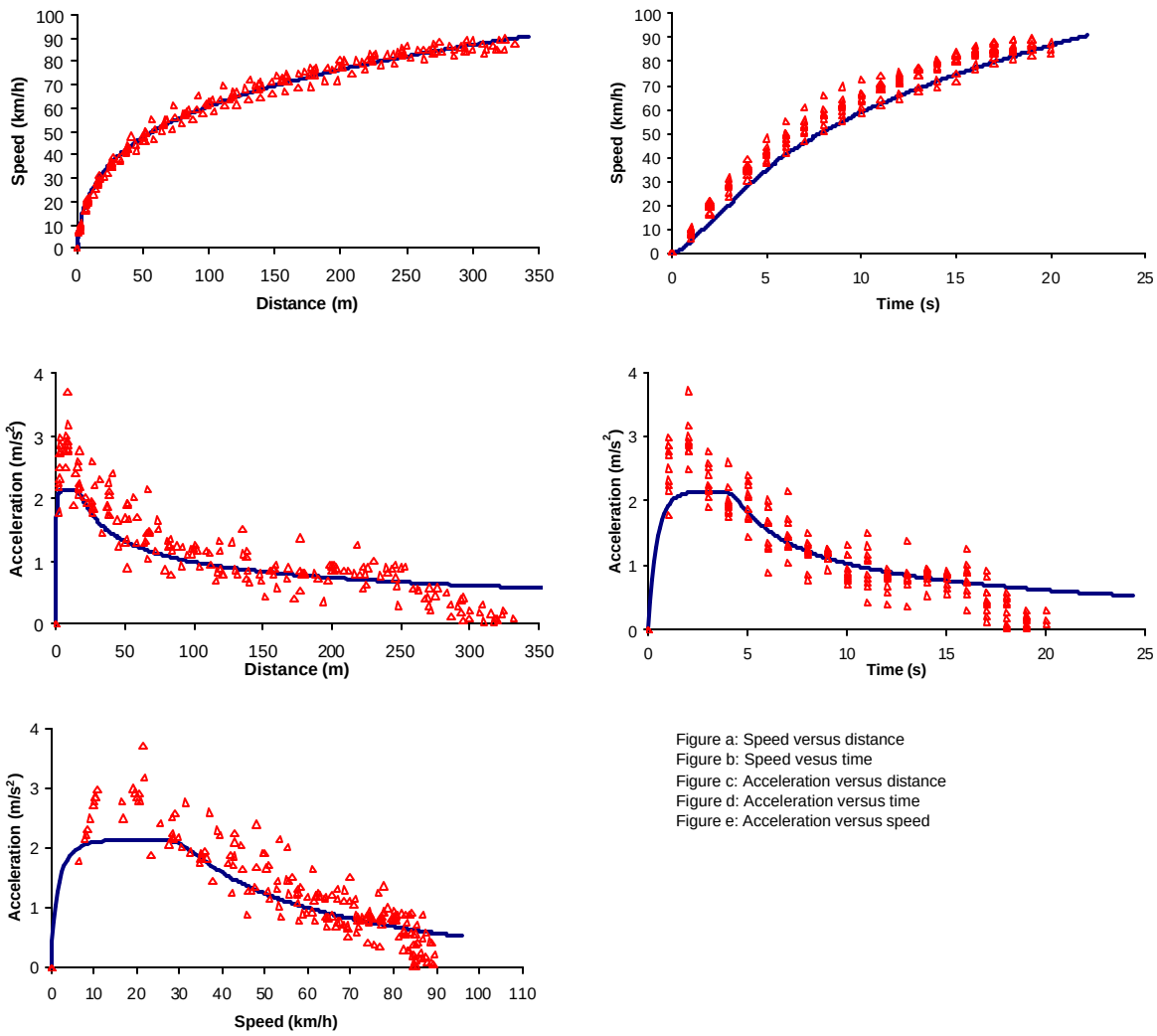

Figure a: Speed versus distance
Figure b: Speed vesus time
Figure c: Acceleration versus distance
Figure d: Acceleration versus time
Figure e: Acceleration versus speed

Figure 5-9: Driver #8 Data with Rakha Model, Reduction Factor = 0.63

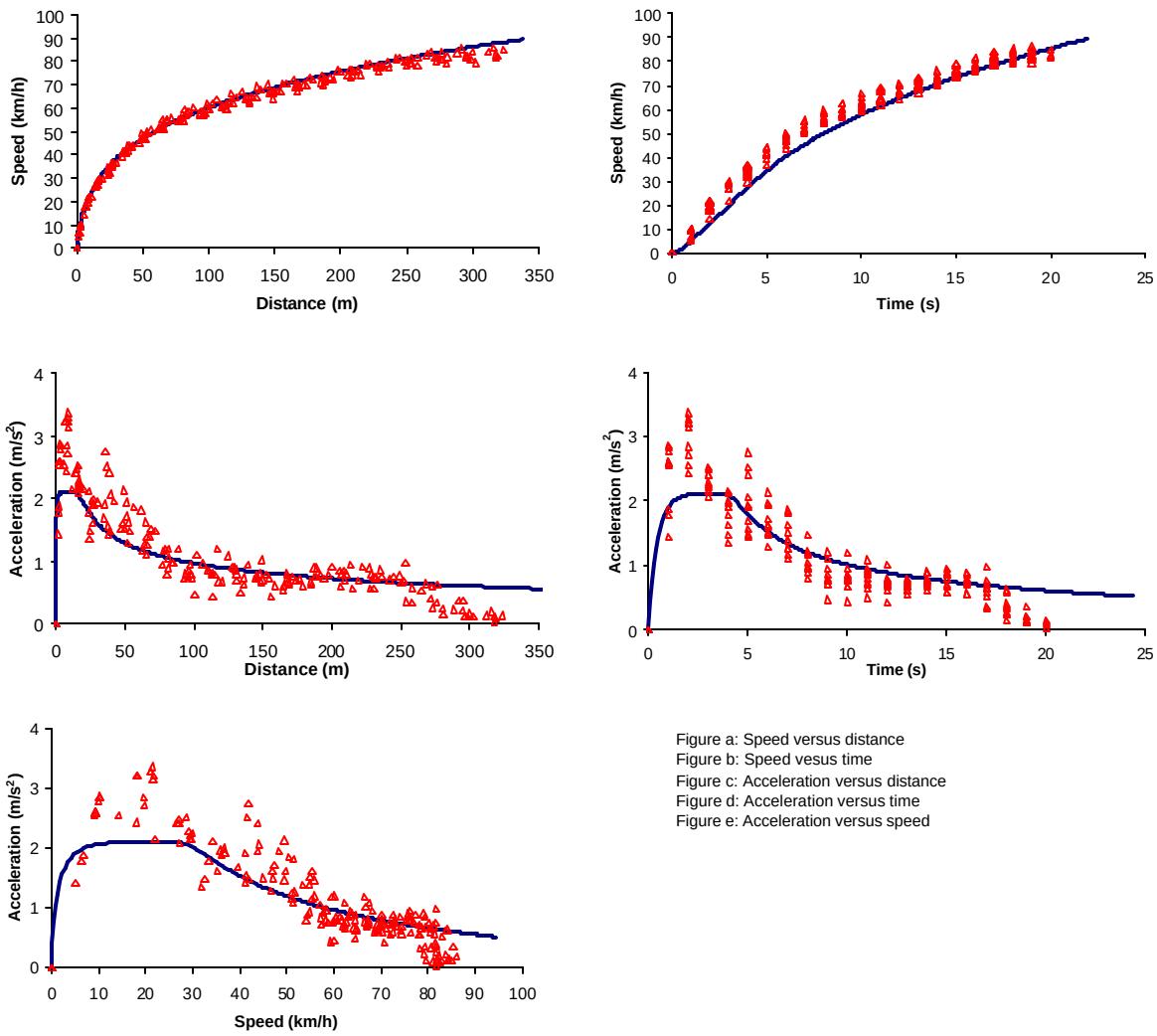

Figure a: Speed versus distance
Figure b: Speed vesus time
Figure c: Acceleration versus distance
Figure d: Acceleration versus time
Figure e: Acceleration versus speed

Figure 5-10: Driver #9 Data with Rakha Model, Reduction Factor = 0.62

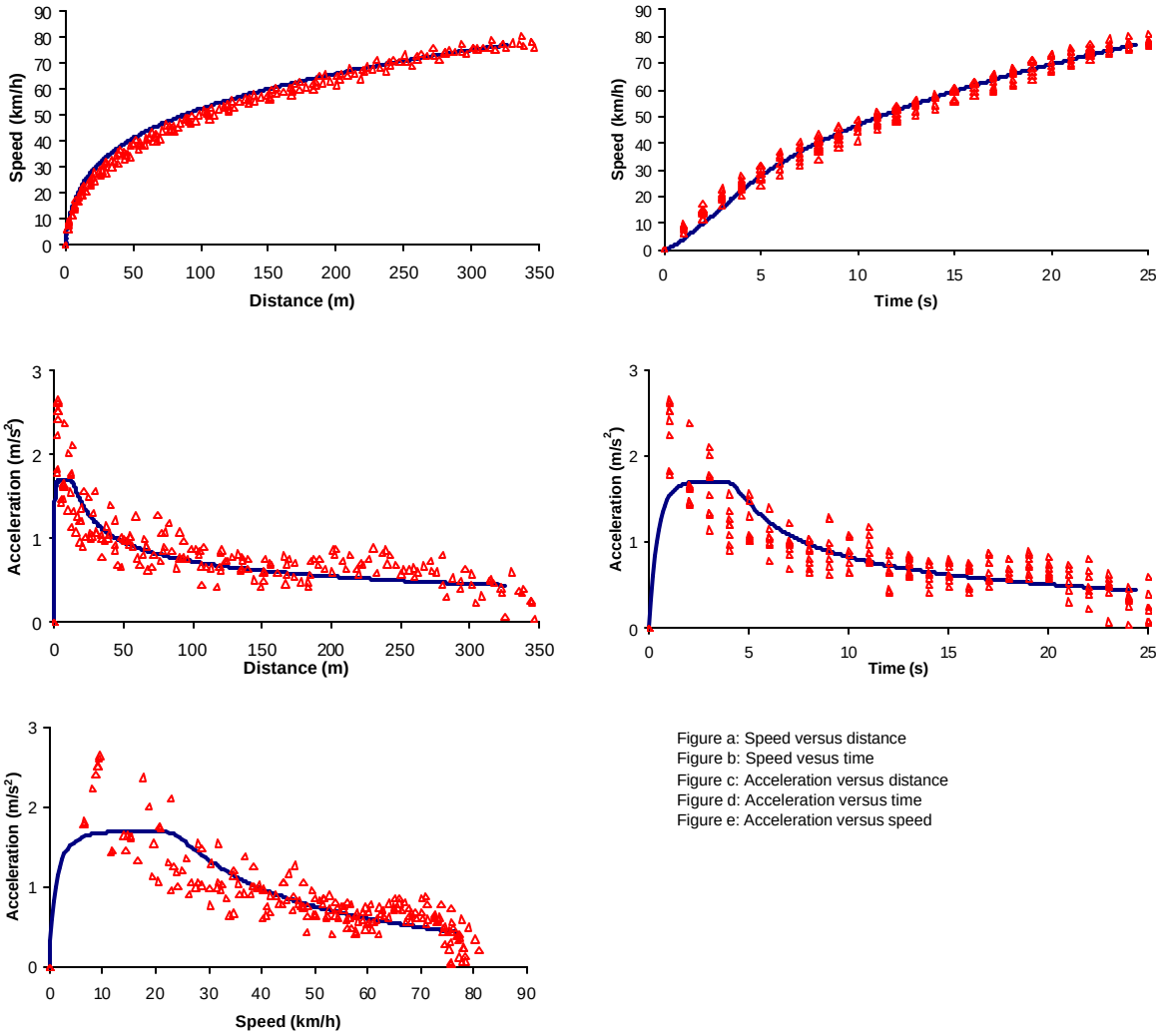

Figure a: Speed versus distance
Figure b: Speed vesus time
Figure c: Acceleration versus distance
Figure d: Acceleration versus time
Figure e: Acceleration versus speed

Figure 5-11: Driver #11 Data with Rakha Model, Reduction Factor = 0.50

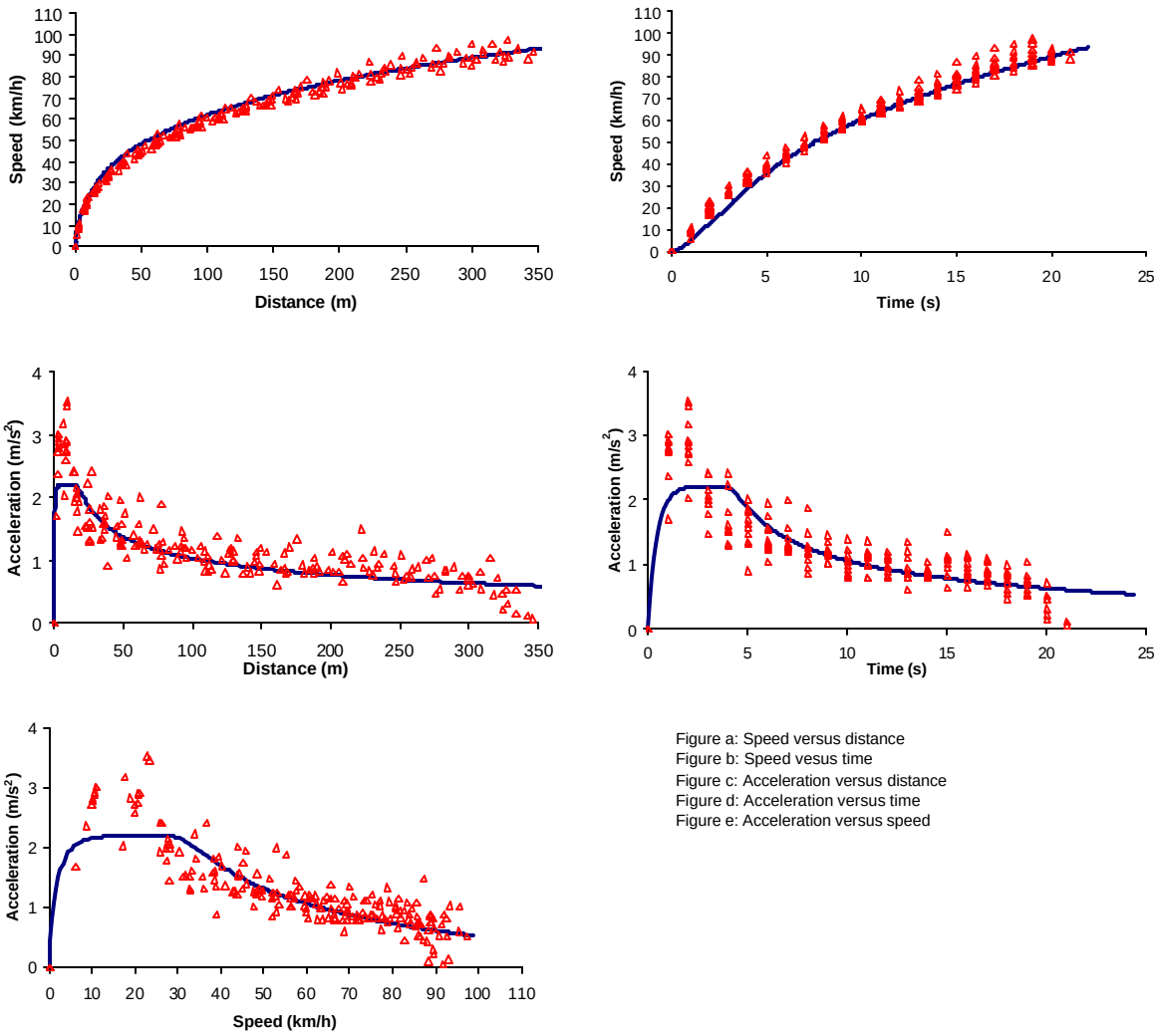

Figure a: Speed versus distance
Figure b: Speed vesus time
Figure c: Acceleration versus distance
Figure d: Acceleration versus time
Figure e: Acceleration versus speed

Figure 5-12: Driver #12 Data with Rakha Model, Reduction Factor = 0.65

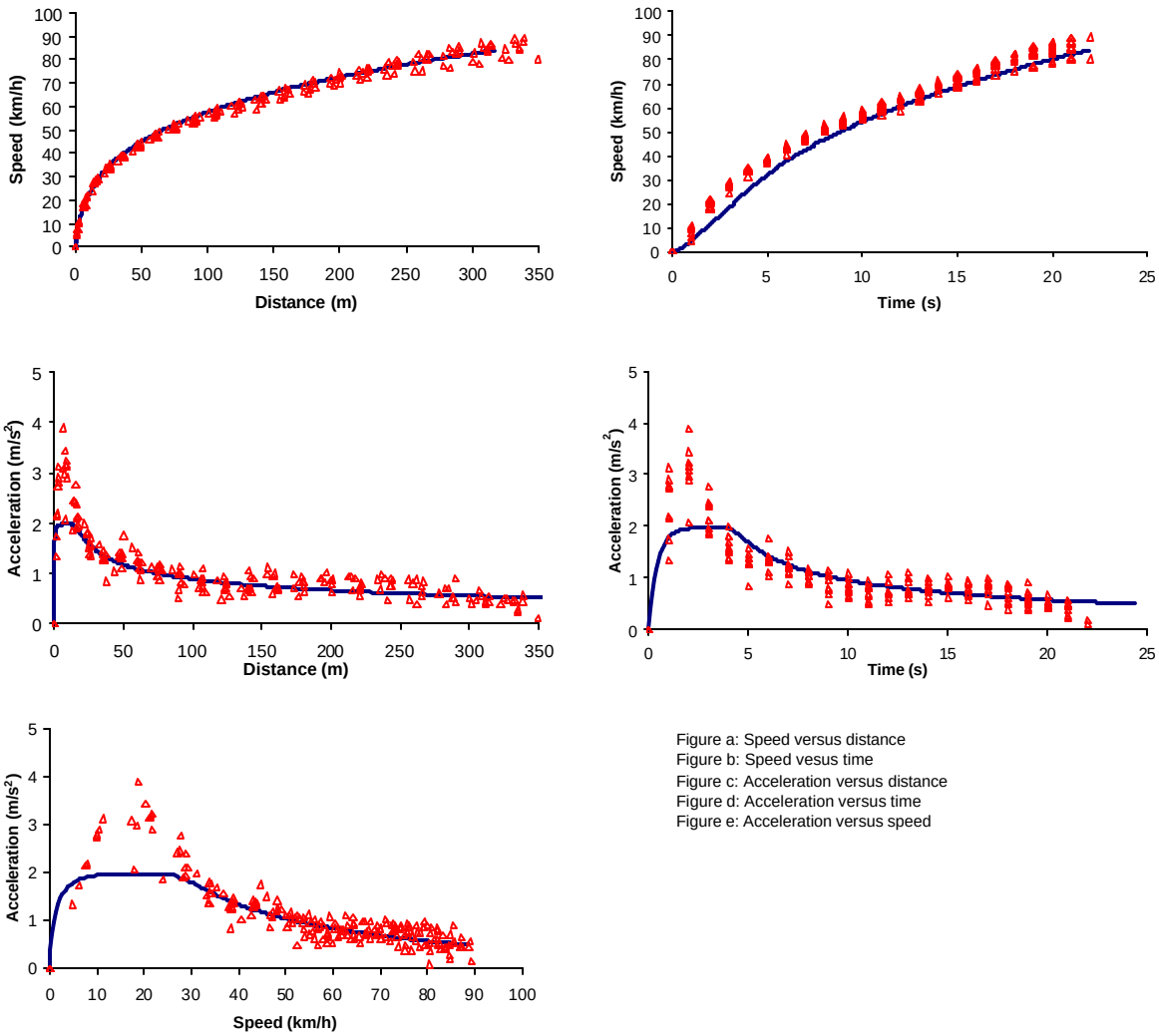

Figure a: Speed versus distance
Figure b: Speed vesus time
Figure c: Acceleration versus distance
Figure d: Acceleration versus time
Figure e: Acceleration versus speed

Figure 5-13: Driver #14 Data with Rakha Model, Reduction Factor = 0.58

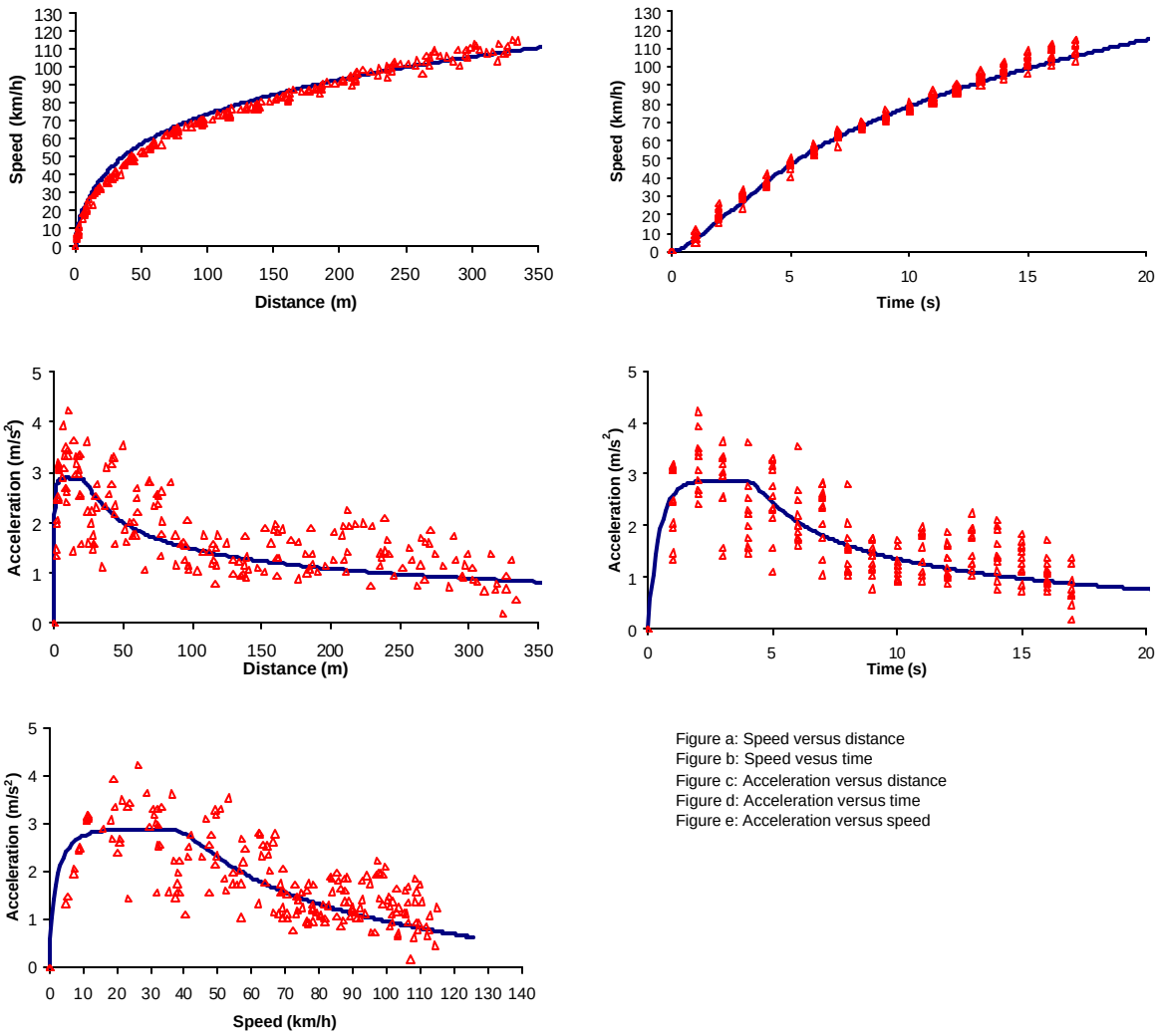

Figure a: Speed versus distance
Figure b: Speed vesus time
Figure c: Acceleration versus distance
Figure d: Acceleration versus time
Figure e: Acceleration versus speed

Figure 5-14: Driver #15 Data with Rakha Model, Reduction Factor = 0.85

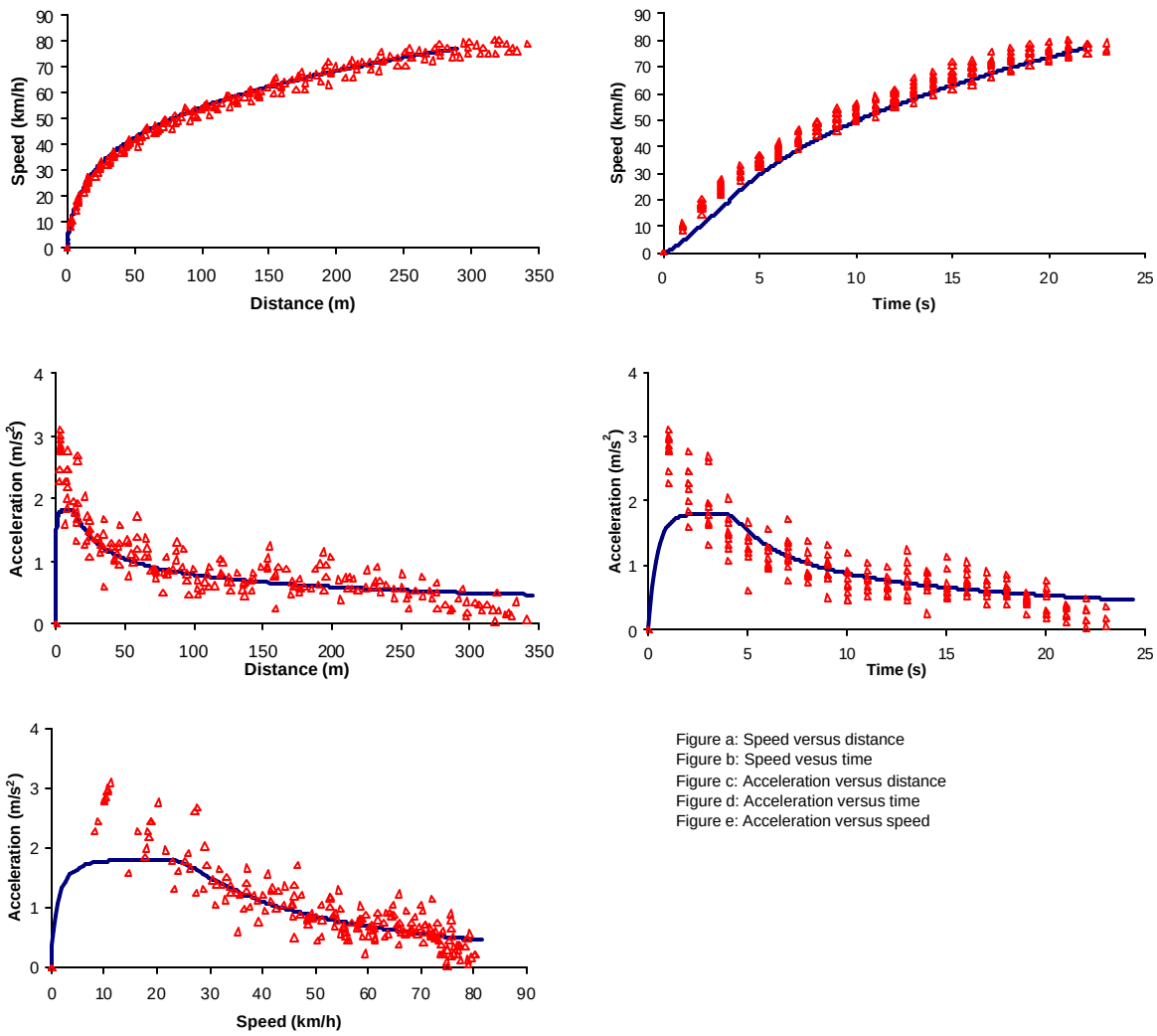

Figure a: Speed versus distance
Figure b: Speed vesus time
Figure c: Acceleration versus distance
Figure d: Acceleration versus time
Figure e: Acceleration versus speed

Figure 5-15: Driver #16 Data with Rakha Model, Reduction Factor = 0.53

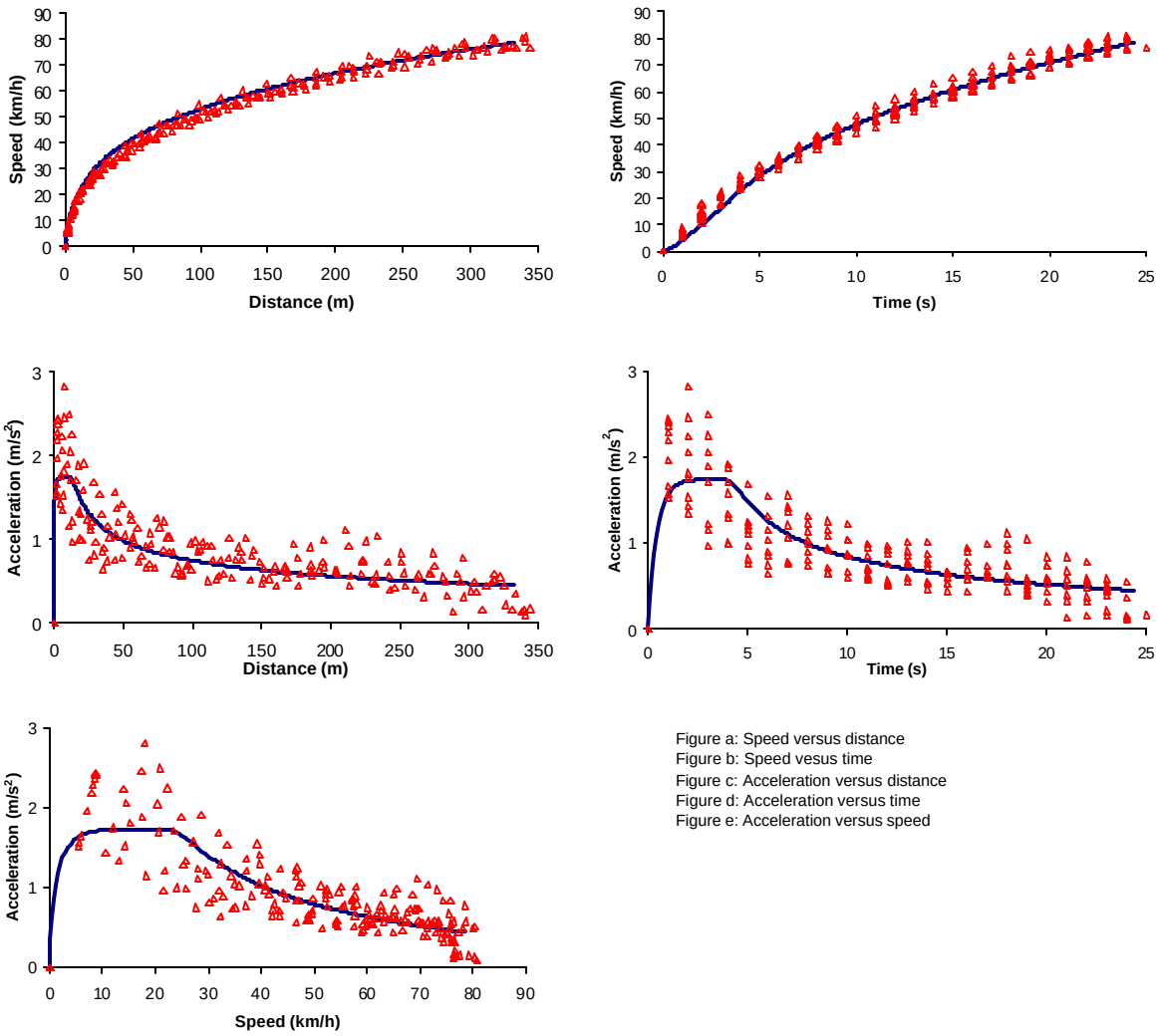

Figure a: Speed versus distance
Figure b: Speed vesus time
Figure c: Acceleration versus distance
Figure d: Acceleration versus time
Figure e: Acceleration versus speed

Figure 5-16: Driver #17 Data with Rakha Model, Reduction Factor = 0.51

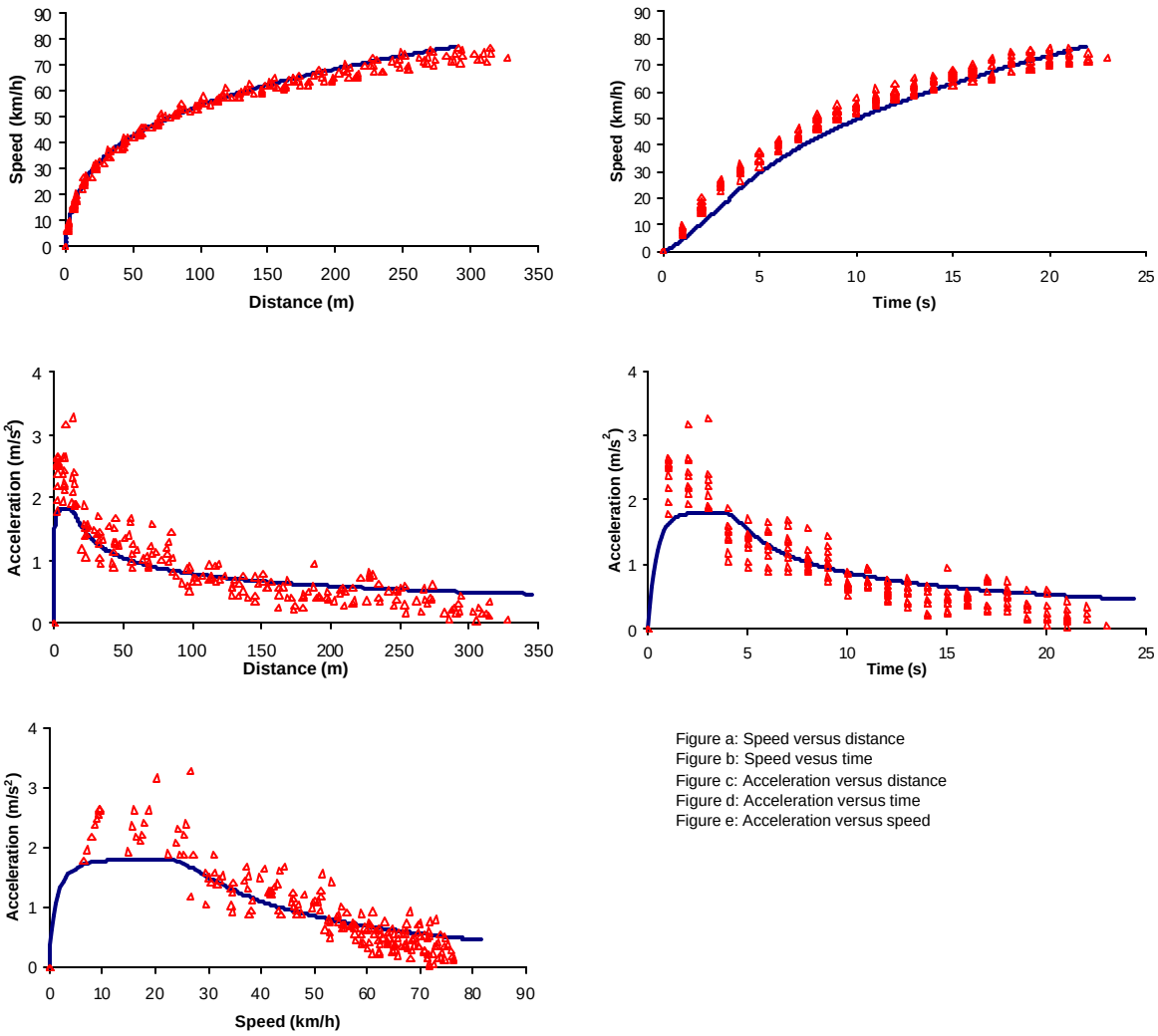

Figure a: Speed versus distance
Figure b: Speed vesus time
Figure c: Acceleration versus distance
Figure d: Acceleration versus time
Figure e: Acceleration versus speed

Figure 5-17: Driver #18 Data with Rakha Model, Reduction Factor = 0.53

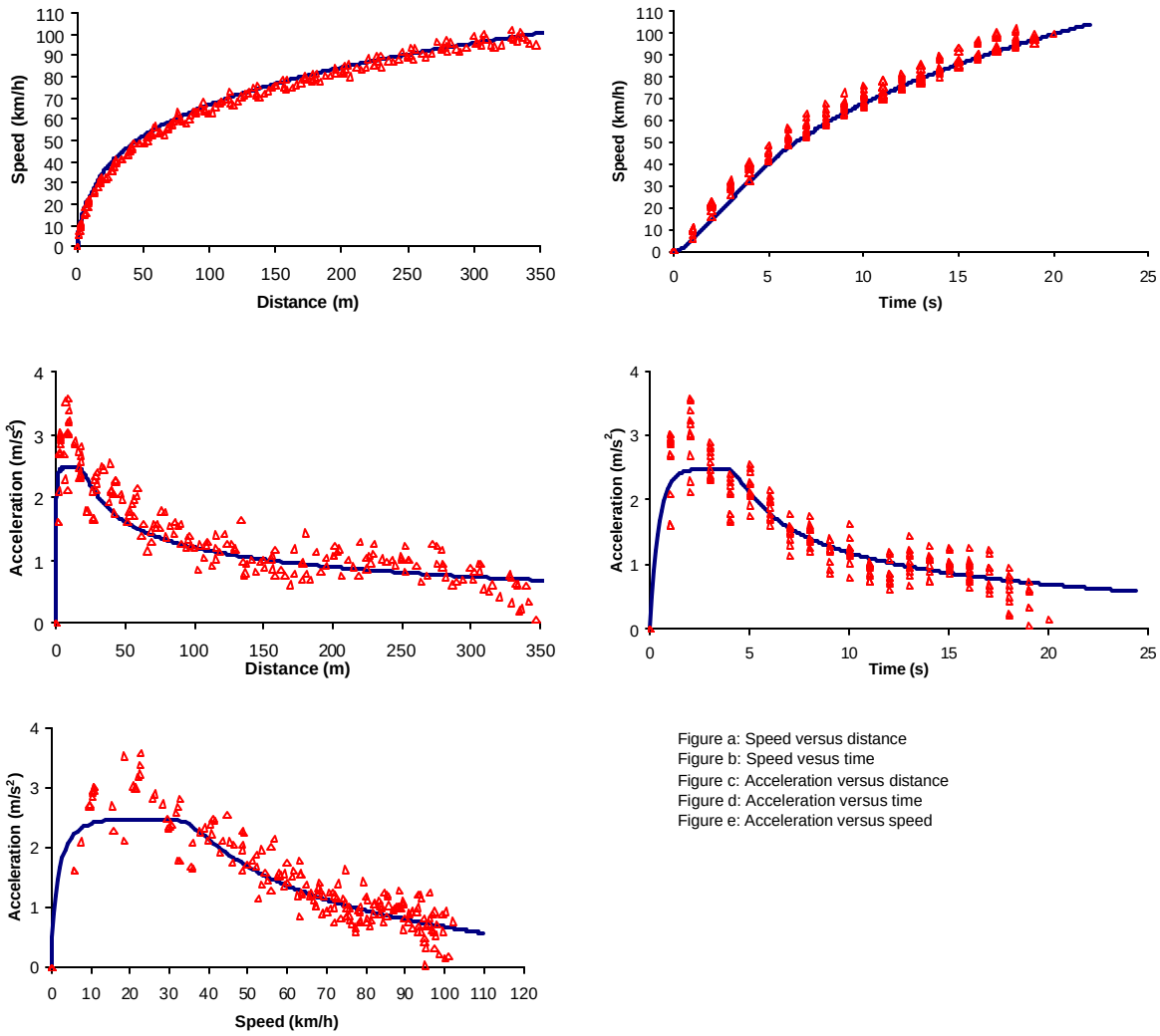

Figure a: Speed versus distance
Figure b: Speed vesus time
Figure c: Acceleration versus distance
Figure d: Acceleration versus time
Figure e: Acceleration versus speed

Figure 5-18: Driver #19 Data with Rakha Model, Reduction Factor = 0.73

b. Gradual Accelerators

Three individuals tested exhibited gradual acceleration behavior. These drivers tended to accelerate at a lower rate than the Standard Accelerators at the beginning of the run. Therefore, there are several indicators of Gradual Accelerator behavior that can be observed in the plots of Figures 5-19 through 5-21. For the Gradual Accelerators, the model tends to overestimate speeds towards the beginning of the run. The model also overestimates accelerations at low speeds for this driver type. Finally, the slopes of acceleration versus time plots for these drivers appear to be less severe than the model predicts. Overall, however, the model predicts reasonable speed profiles, even for drivers in this category. Only in the most extreme case of gradual acceleration behavior (Driver #20, Figure 5-21) does the model provide somewhat inaccurate results.

c. Hard Accelerators

Three individuals exhibited hard acceleration behavior. These drivers accelerate very aggressively initially, when the acceleration capability of the vehicle is greatest, but rapidly decrease their acceleration once higher speeds are achieved. Figures 5-22 through 5-24 show the plots of the drivers in this category. The speed versus distance plots show that the model overestimates speeds towards the end of the run for these drivers because the model is fit to the beginning of the run when the acceleration is more aggressive. The acceleration versus speed plots also show that the model underestimates acceleration slightly at low speeds. The model also underestimates speed for these drivers in the speed versus time plot. Despite these minor errors, the model still provides a reasonable approximation of the speed profiles for these drivers.

5.4.2 *Driver Summary*

A wide range of driver factors was observed in this study, from a highly aggressive value of 0.85 to a very non-aggressive value of 0.40. The observed speed profiles are shown in Figure 5-25. The distribution of driver factors is analyzed in the following section. Three driver types were observed – Gradual Accelerator, Standard Accelerator, and Hard Accelerator. Standard Accelerators accounted for 14 of the drivers, while only 3 examples of Gradual Accelerators and Hard Accelerators were observed. The assumption of applying a constant reduction factor to the maximum acceleration model throughout the run creates a good fit for the Standard Accelerators. Since this group represents the vast majority of driver types, this assumption is valid. In fact, the constant reduction factor also enabled a reasonable fit for most of the Gradual and Hard Accelerators. Only the extreme examples of these driver classifications resulted in data inconsistent with the model predictions. It would be unreasonable to develop a model for these extreme situations, and we can therefore conclude that the model effectively represents the range of typical driver behavior.

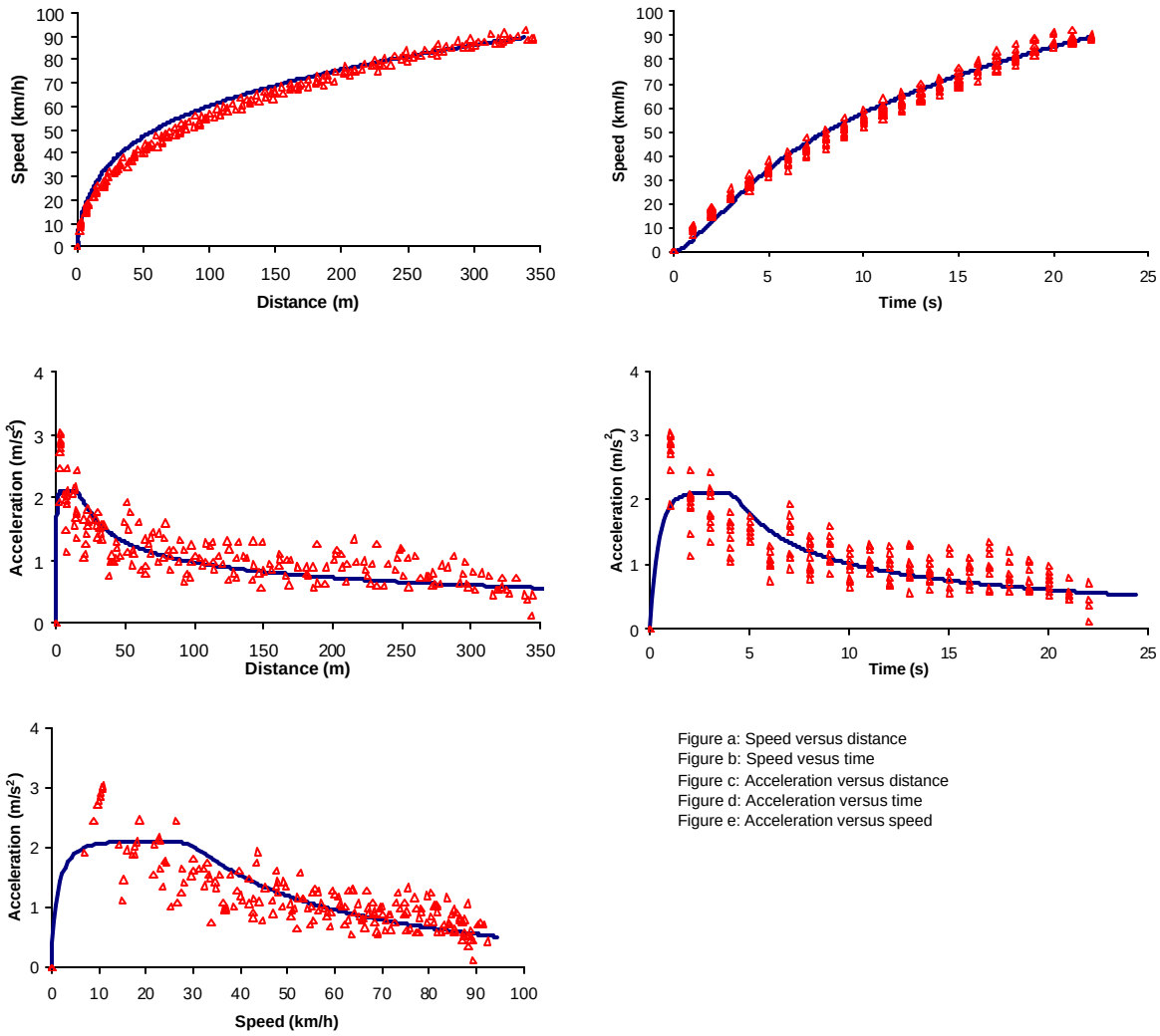

Figure a: Speed versus distance
Figure b: Speed vesus time
Figure c: Acceleration versus distance
Figure d: Acceleration versus time
Figure e: Acceleration versus speed

Figure 5-19: Driver #10 Data with Rakha Model, Reduction Factor = 0.62

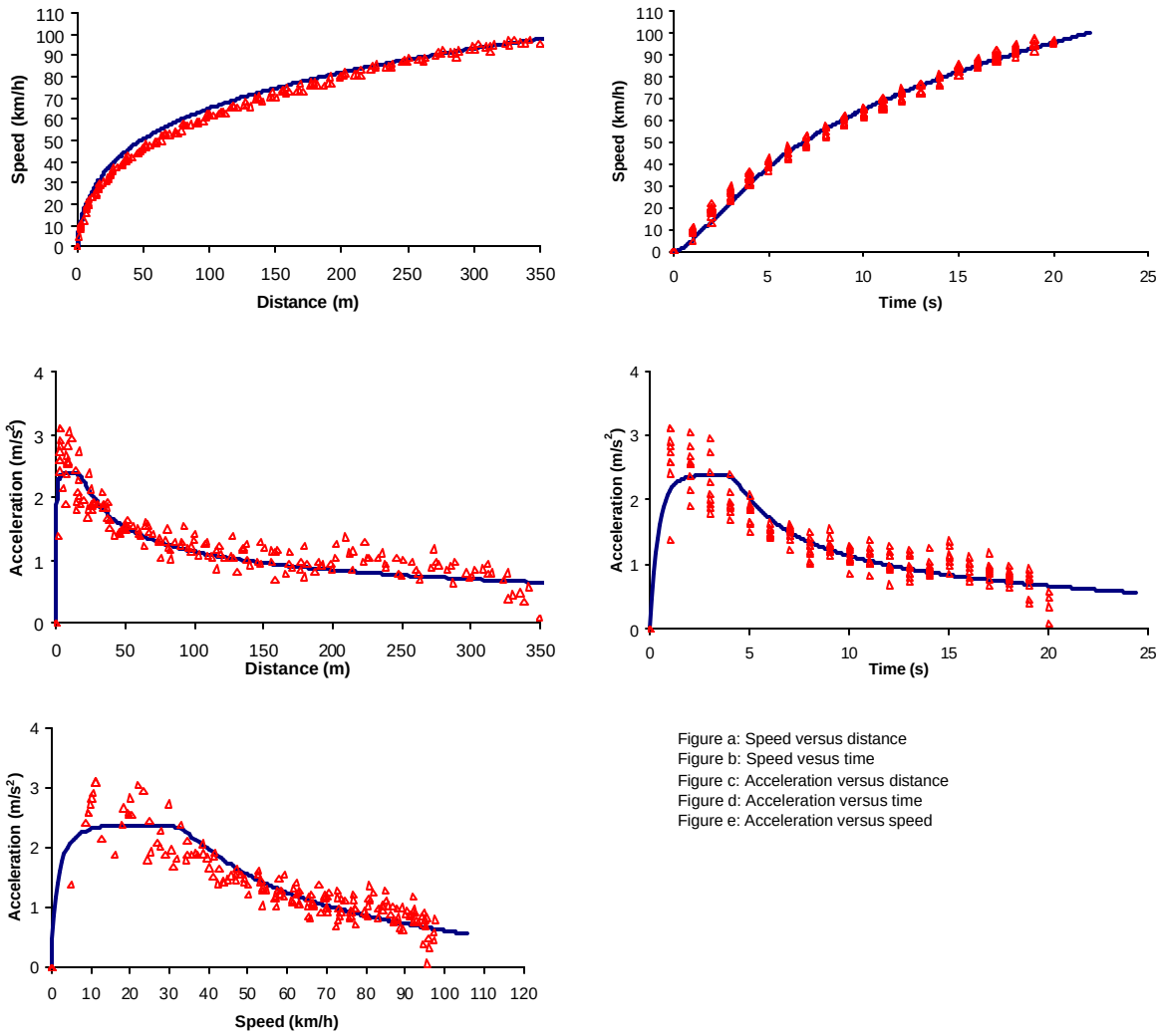

Figure a: Speed versus distance
Figure b: Speed vesus time
Figure c: Acceleration versus distance
Figure d: Acceleration versus time
Figure e: Acceleration versus speed

Figure 5-20: Driver #13 Data with Rakha Model, Reduction Factor = 0.70

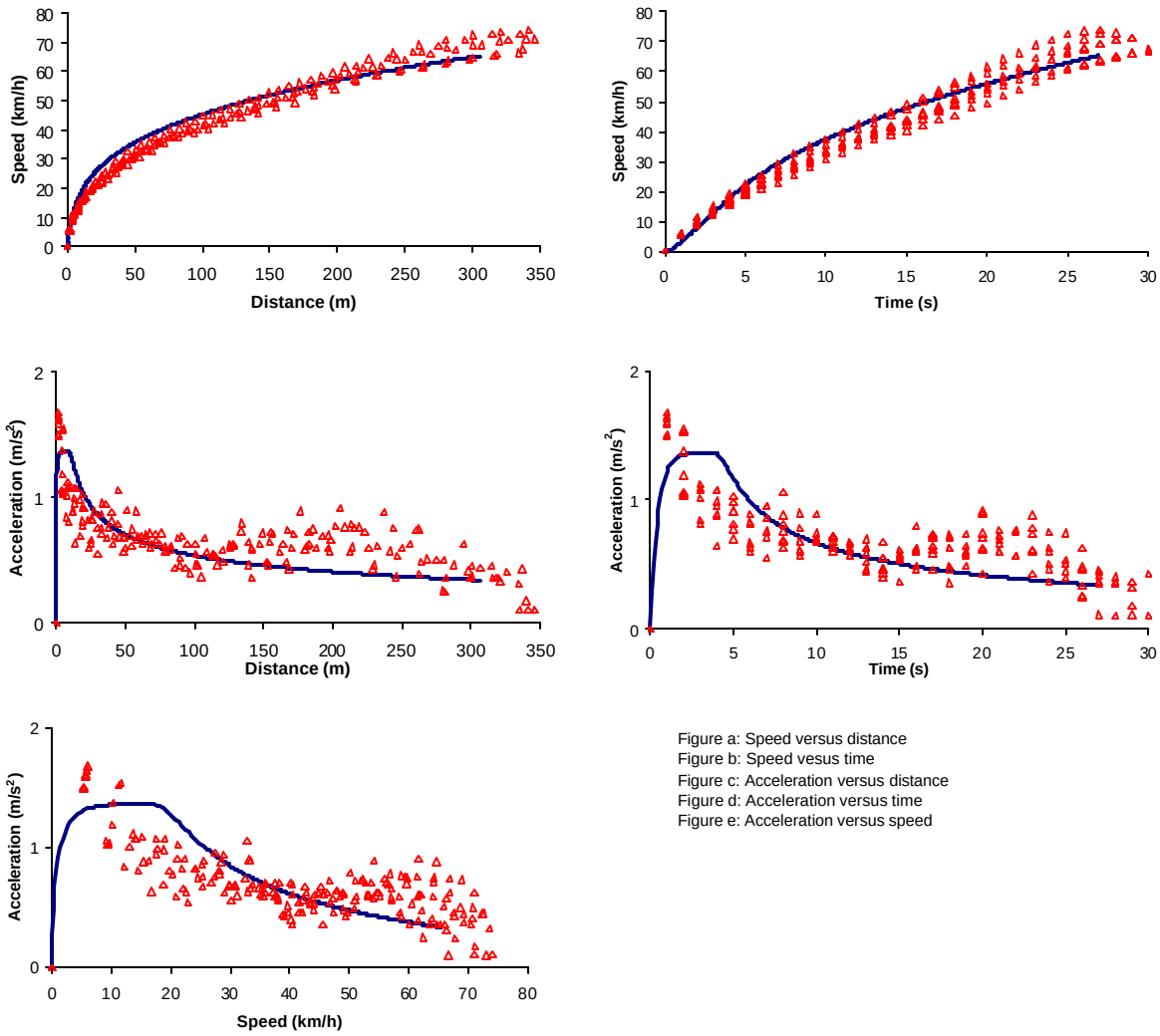

Figure a: Speed versus distance
Figure b: Speed vesus time
Figure c: Acceleration versus distance
Figure d: Acceleration versus time
Figure e: Acceleration versus speed

Figure 5-21: Driver #20 Data with Rakha Model, Reduction Factor = 0.40

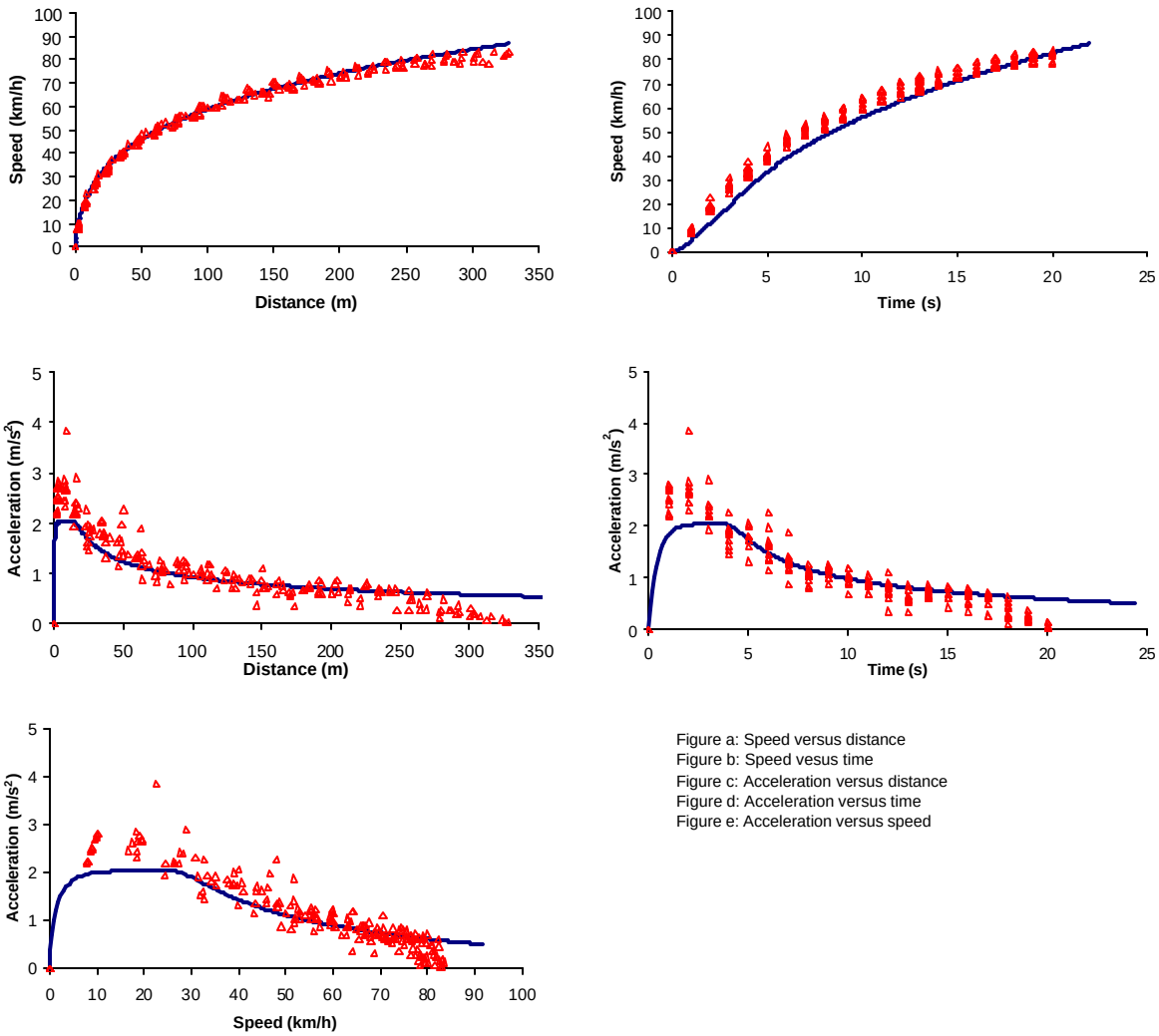

Figure a: Speed versus distance
Figure b: Speed vesus time
Figure c: Acceleration versus distance
Figure d: Acceleration versus time
Figure e: Acceleration versus speed

Figure 5-22: Driver #3 Data with Rakha Model, Reduction Factor = 0.60

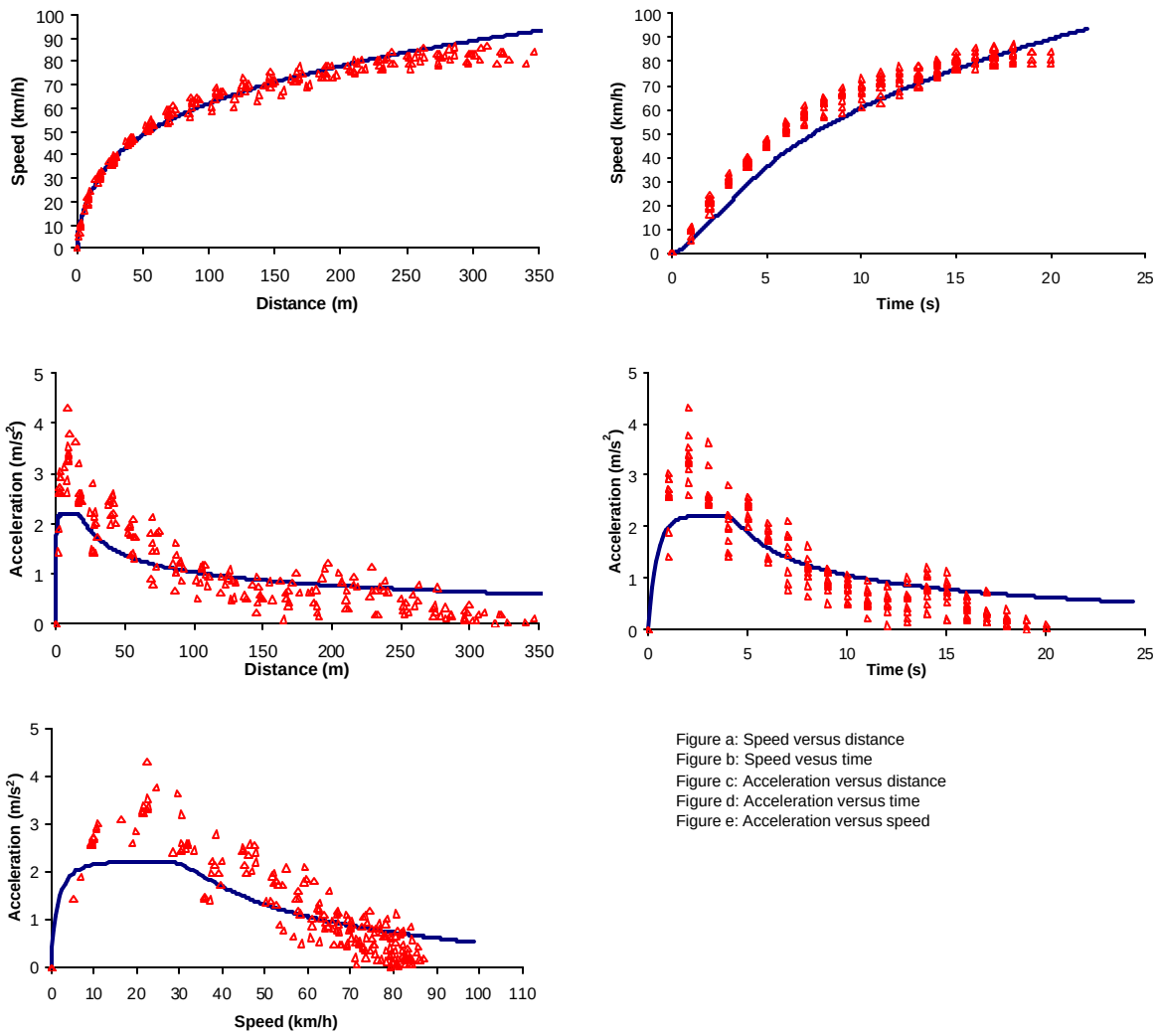

Figure a: Speed versus distance
Figure b: Speed vesus time
Figure c: Acceleration versus distance
Figure d: Acceleration versus time
Figure e: Acceleration versus speed

Figure 5-23: Driver #4 Data with Rakha Model, Reduction Factor = 0.65

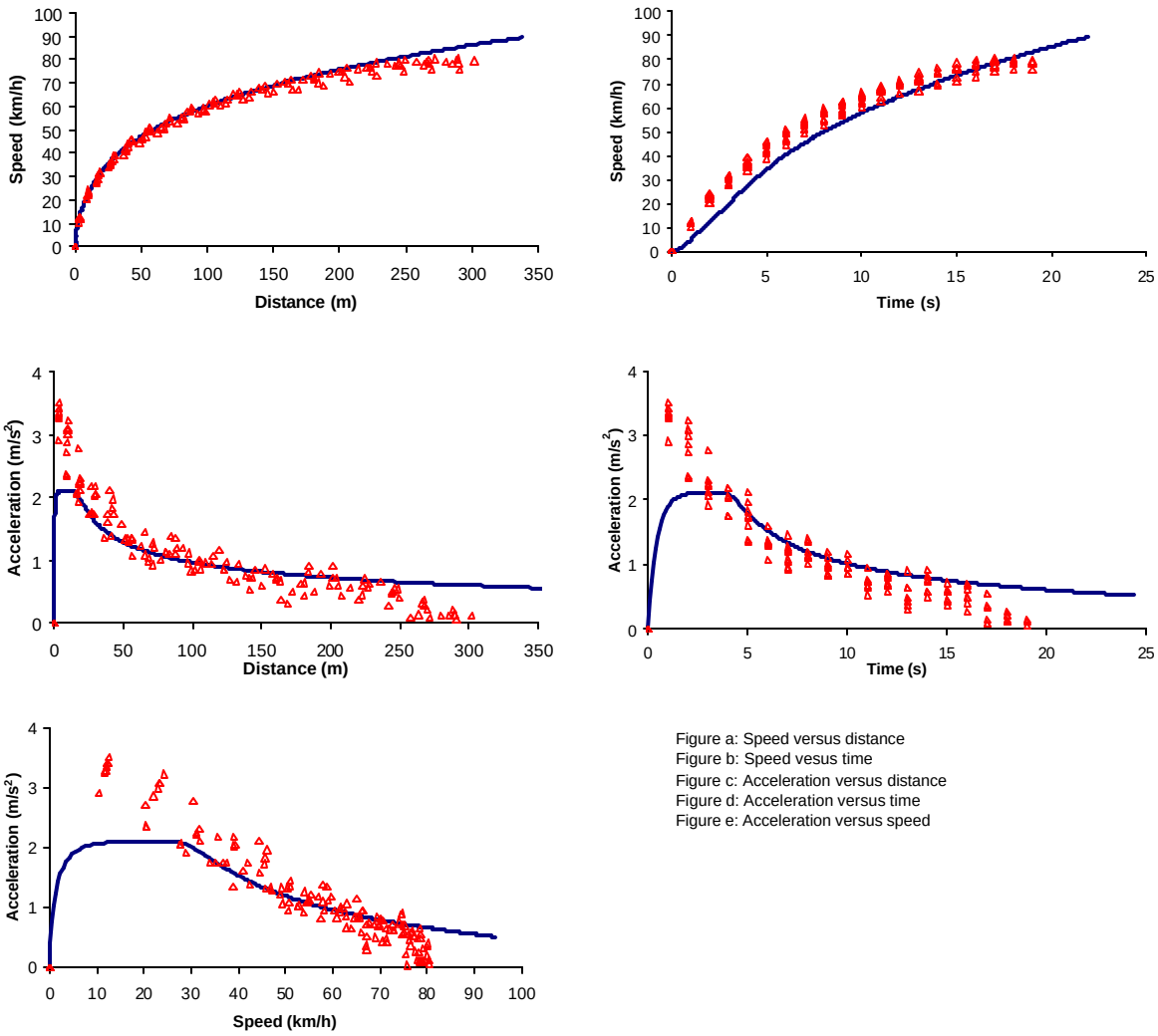

Figure a: Speed versus distance
Figure b: Speed vesus time
Figure c: Acceleration versus distance
Figure d: Acceleration versus time
Figure e: Acceleration versus speed

Figure 5-24: Driver #6 Data with Rakha Model, Reduction Factor = 0.62

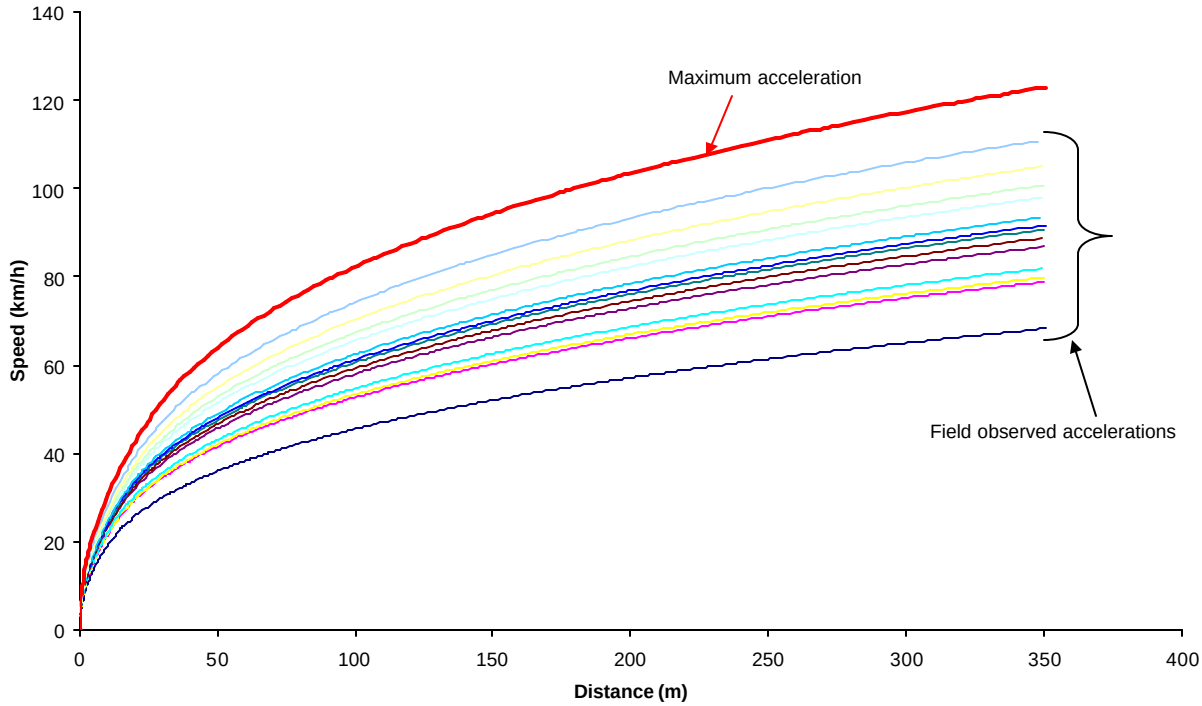

Figure 5-25: Observed Typical Speed Profiles Versus Maximum Profile

5.4.3 *Distribution*

This research has shown that a model for typical acceleration behavior can be generated for any driver by applying a certain reduction factor to the maximum acceleration Rakha model. Obviously, every driver on the road cannot be tested to obtain his or her factor. However, a statistical distribution of driver factors can be generated based on the drivers studied in this paper.

With that in mind, the reduction factors for each of the twenty drivers in this study were grouped into bins and plotted as shown in Figure 5-26. Based on Figure 5-26 and common sense, a reasonable assumption can be made that the driver factors could be fit to a normal statistical distribution. This would mean that the majority of drivers would exhibit some average driver factor, and the probability of observing different factors would reduce as values moved away from the average. A normal distribution was therefore fit to the data as shown in Figure 5-27. Figure 5-28 shows a good fit between the cumulative normal distribution and the one observed during the field tests. The best-fit normal distribution of driver factors had a mean of 0.60 and a standard deviation of 0.08. The actual mean value observed for the 20 drivers was 0.62.

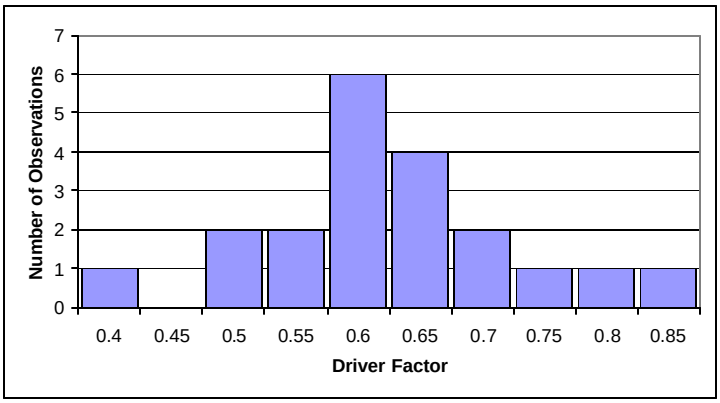

Figure 5-26: Distribution of Observed Driver Factors

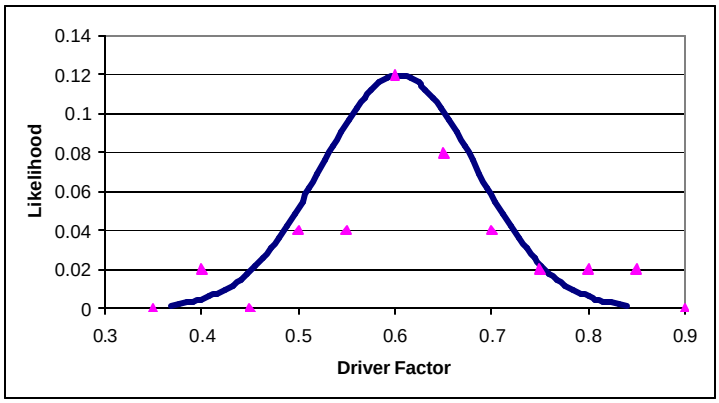

Figure 5-27: Normal Distribution Fit to Observed Driver Factors

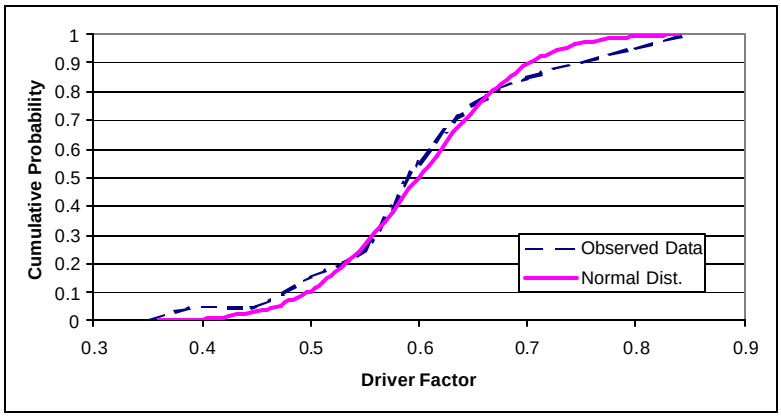

Figure 5-28: Cumulative Normal Distribution Fit to Data

To test the validity of applying the normal distribution to the set of observed factors, a chi-squared test was performed. The factors were grouped into three bins – less than 0.55, between 0.55 and 0.65, and greater than 0.65. This insured that each bin would have at least five observations, as required for the chi-squared test. Table 5-3 shows the number of observed and expected observations for each bin, as well as the deviation. A chi-squared value of 0.082 was calculated from the data. This value is well below the critical value of 5.99. Therefore, this data set shows a strong correlation to the normal distribution at the 5% confidence limit. Further evidence of the strong correlation between the normal distribution and the test data is shown in Figure 5-29. This figure shows the data points from all runs for each of the twenty drivers. The speed profile for the mean driver factor as well as for the 5% and 95% confidence limits are also depicted on the graph. Several observations can be made from this graph. The first observation is that a large percentage of the runs are grouped near the mean, which should be expected. Also, the plot shows that data points from one driver are below the 5% confidence limit and data points from one driver are above the 95% confidence limit. This should be expected because this represents 5% (1 of 20) of the test subjects at either end of the spectrum.

Table 5-3: Chi Squared Test Calculation

Class	Observed	Expected	Deviation	d squared	d2/e
< 0.55	5	5.32	0.32	0.1024	0.019248
0.55-0.65	10	9.36	-0.64	0.4096	0.043761
> 0.65	5	5.32	0.32	0.1024	0.019248

Chi Squ	0.082257

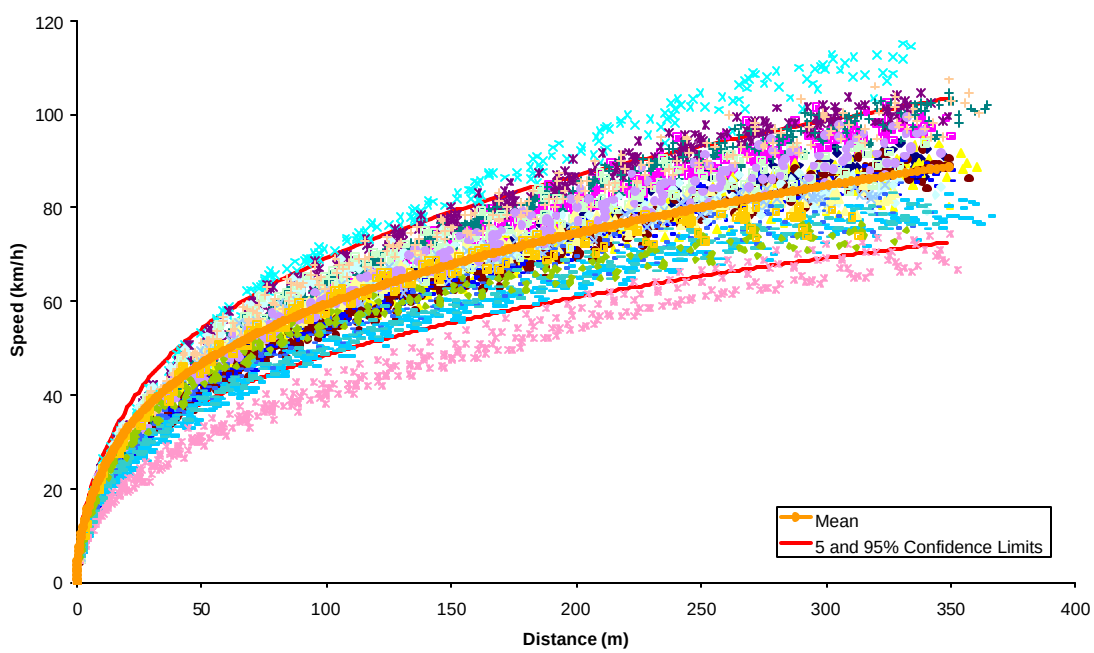

Figure 5-29: Driver Run Data with Distribution Mean and Selected Percentiles

5.4.4 *Age and Gender Variability*

In addition to developing a distribution of driver factors, tests were done to see if age or gender affected the observed driver factors. As might have been expected, the mean driver factor for men was higher than for women (0.634 to 0.609) and the mean driver factor for ages 20-29 was higher than for ages 30 and above (0.639 to 0.602). An analysis of variance test was performed on the data to determine if these means were statistically different. Table 5-4 shows the computed values for the gender comparison, while Table 5-5 shows the values for the age comparison. An analysis of variance was also performed for both factors simultaneously, as shown in Table 5-6. The results of these tests showed that there was no statistical difference in the means at the 5% confidence limit that could be attributed to age or gender. Therefore, we can conclude that the normal distribution with a mean of 0.60 and a standard deviation of 0.08, as determined earlier in this report, does not need to be modified for driver populations of different ages or genders.

Table 5-4: ANOVA Table, Male versus Female

Anova: Single Factor

SUMMARY

Groups	*Count*	*Sum*	*Average*	*Variance*
Female	9	5.48	0.608889	0.018686
Male	11	6.97	0.633636	0.004705

ANOVA

Source of Variation	*SS*	*df*	*MS*	*F*	*P-value*	*F crit*
Between Groups	0.003032	1	0.003032	0.277639	0.604686	4.413863
Within Groups	0.196543	18	0.010919			
Total	0.199575	19				

Table 5-5: ANOVA Table, Young versus Old

Anova: Single Factor

SUMMARY

Groups	*Count*	*Sum*	*Average*	*Variance*
20-29	11	7.03	0.639091	0.011389
Over 30	9	5.42	0.602222	0.009869

ANOVA

Source of Variation	*SS*	*df*	*MS*	*F*	*P-value*	*F crit*
Between Groups	0.006729	1	0.006729	0.628031	0.438399	4.413863
Within Groups	0.192846	18	0.010714			
Total	0.199575	19				

Table 5-6: ANOVA Table, Both Factors

Terms:

	Sex	Age	Sex:Age	Residuals
Sum of Squares	0.0030316	0.013264	5E-07	0.183279
Deg. Of Freedom	1	1	1	16

Residual standard error: 0.1070276

	Df	Sum of Sq	Mean Sq	F Value	Pr(F)
Sex	1	0.0030316	0.003032	0.264652	0.613975
Age	1	0.0132644	0.013264	1.157964	0.297847
Sex:Age	1	0.0000005	4.9E-07	0.000043	0.994849
Residuals	16	0.1832786	0.011455		

5.5 Linear Decay Model Comparison

The model presented in this paper has been shown to provide a good fit for each driver in the domains of speed versus time, speed versus distance, acceleration versus time, acceleration versus distance, and acceleration versus speed. For comparison, the linear decay model recommended in the literature (Long, 2000) was applied to the data sets collected for this study to determine their fit. The results of this effort are discussed in the following paragraphs.

The first task was to calibrate the linear decay model to fit the maximum acceleration profile of the Ford Crown Victoria. This was accomplished by setting the maximum acceleration at a value of 2.5 m/s^2 and by setting the maximum speed to 160 km/h. This resulted in alpha and beta values of 2.5 and 0.05625, respectively. Using these values, the linear decay model showed an excellent fit to the maximum acceleration field data collected in a prior research effort. The next step was to apply the driver factors determined in this report to the linear decay model for each driver and compare the results to the typical acceleration field data. One example of a gradual acceleration driver, a standard acceleration driver, and a hard acceleration driver were chosen for illustration purposes in this report.

Figure 5-30 shows the fit of the linear decay model to a driver classified as a gradual accelerator. The model demonstrates a good fit in all domains for this driver, and even captures the slope of the acceleration versus speed plot better than the model developed in this paper for this particular driver. This demonstrates that using a reduction factor along with the linear decay model is effective in modeling drivers that exhibit gradual acceleration tendencies. However, only 15% of the drivers studied in this test exhibited this behavior.

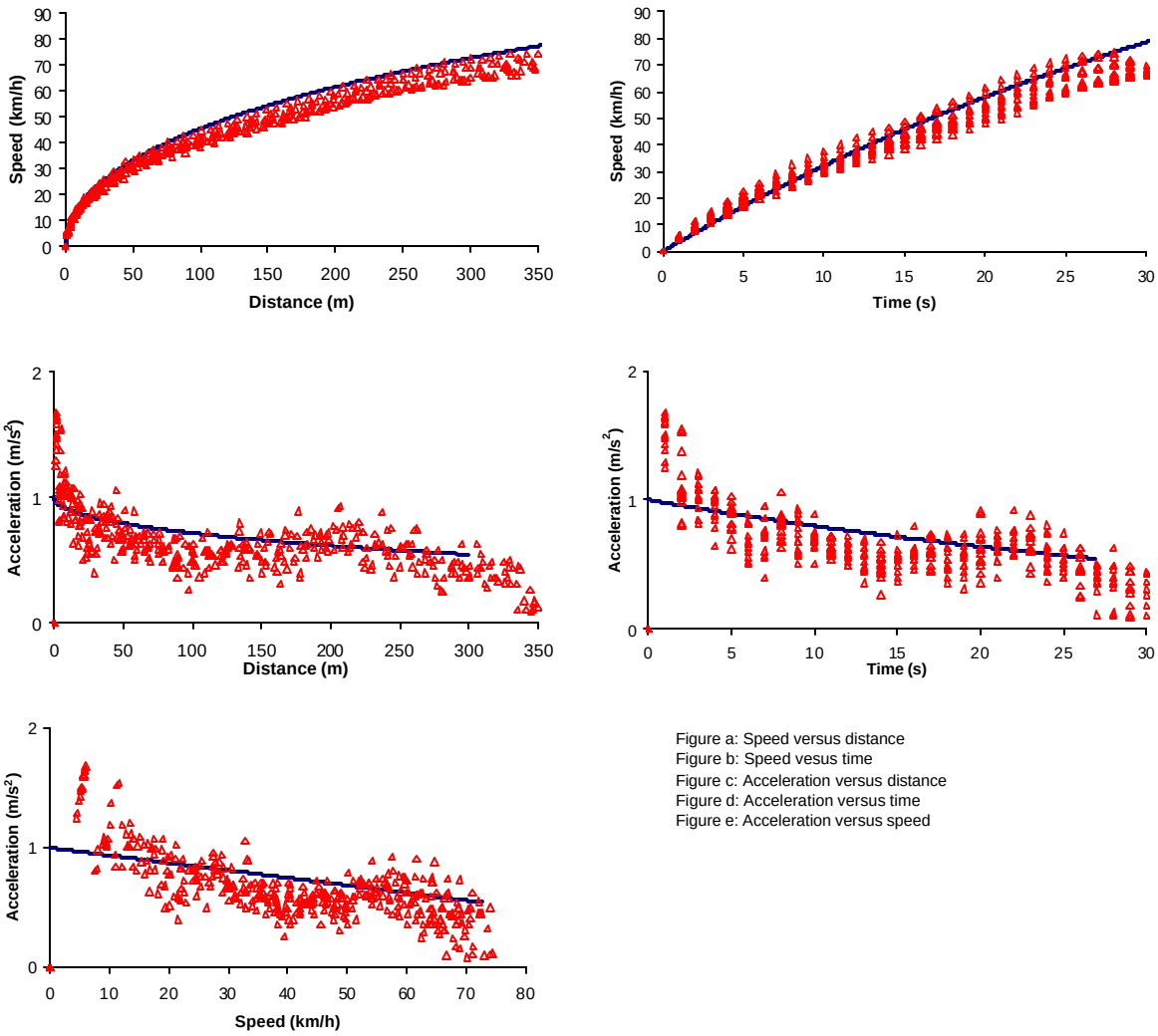

Figure a: Speed versus distance
Figure b: Speed vesus time
Figure c: Acceleration versus distance
Figure d: Acceleration versus time
Figure e: Acceleration versus speed

Figure 5-30: Sample Gradual Acceleration Driver versus Linear Decay Model

Figure 5-31 shows the plots of a standard accelerating driver versus the linear decay model. The speed versus distance plot shows a reasonable fit, which indicates that the driver factor used was appropriate. However, the linear decay model seems to underestimate the driver acceleration for the first half of the run. The model does not seem to capture the appropriate slope in the acceleration versus speed domain for the standard accelerators. This is a major limitation of the linear decay model, because the majority of drivers in this study – 70% - were classified in this group. Therefore, the linear decay model would not accurately describe the acceleration behavior of most of the drivers on the road. This is consistent with the findings of Long (2000), who found that the slope of the acceleration versus speed plot was too flat when a reduction factor was applied to the linear decay model to predict typical acceleration behavior.

Figure 5-32 demonstrates that the fit of the linear decay model to individuals classified as hard accelerators is even worse. In addition to the slope being erroneous in the acceleration versus speed plot, the speed profiles predicted by the linear decay model are also flawed for the hard accelerators.

We can conclude that using a reduction factor with the linear decay model to predict typical acceleration rates generates a profile that is consistent with the gradual accelerator driver type. Because only a small percentage of drivers exhibit this behavior, it is not recommended to use the model in this fashion to predict typical behavior. The Rakha model provides a good fit for all driver types, particularly those in the standard accelerator category. Since this group makes up the largest percentage of drivers, the Rakha model is more effective at predicting typical acceleration behavior using driver reduction factors than the linear decay model.

5.6 Importance of Modeling a Range of Typical Behavior

This paper has shown that typical driver behavior varies greatly from driver to driver. It has also shown that a good fit to field data can be generated by applying various driver factors to the maximum acceleration capabilities of vehicles predicted by the Rakha model. A normal distribution of driver factors was determined with a mean of 0.60 and a standard deviation of 0.08 that represents the driver population on the road. However, a question remains; is it really necessary to use the driver distribution in simulation models, or is it sufficient to use the mean value for all drivers?

To answer this question, a simple test was conducted. The Rakha model was used to predict the speed profiles of a simulated vehicle driven by five different drivers with reduction factors ranging from 0.4 to 0.8. The 0.4 factor represented a driver with a low aggressiveness, while the 0.8 factor represented a highly aggressive driver. The driver factor of 0.6 represents average driver aggressiveness. The speed profile for each driver was determined over an 850-meter distance on a road with a speed limit of 55 mph (88.5 km/h). Each driver was simulated to accelerate from a stop to the speed limit, and then continue traveling at the speed limit until the end of the 850-meter section. Figure 5-33 shows the corresponding speed profiles in this simulation for the different driver types.

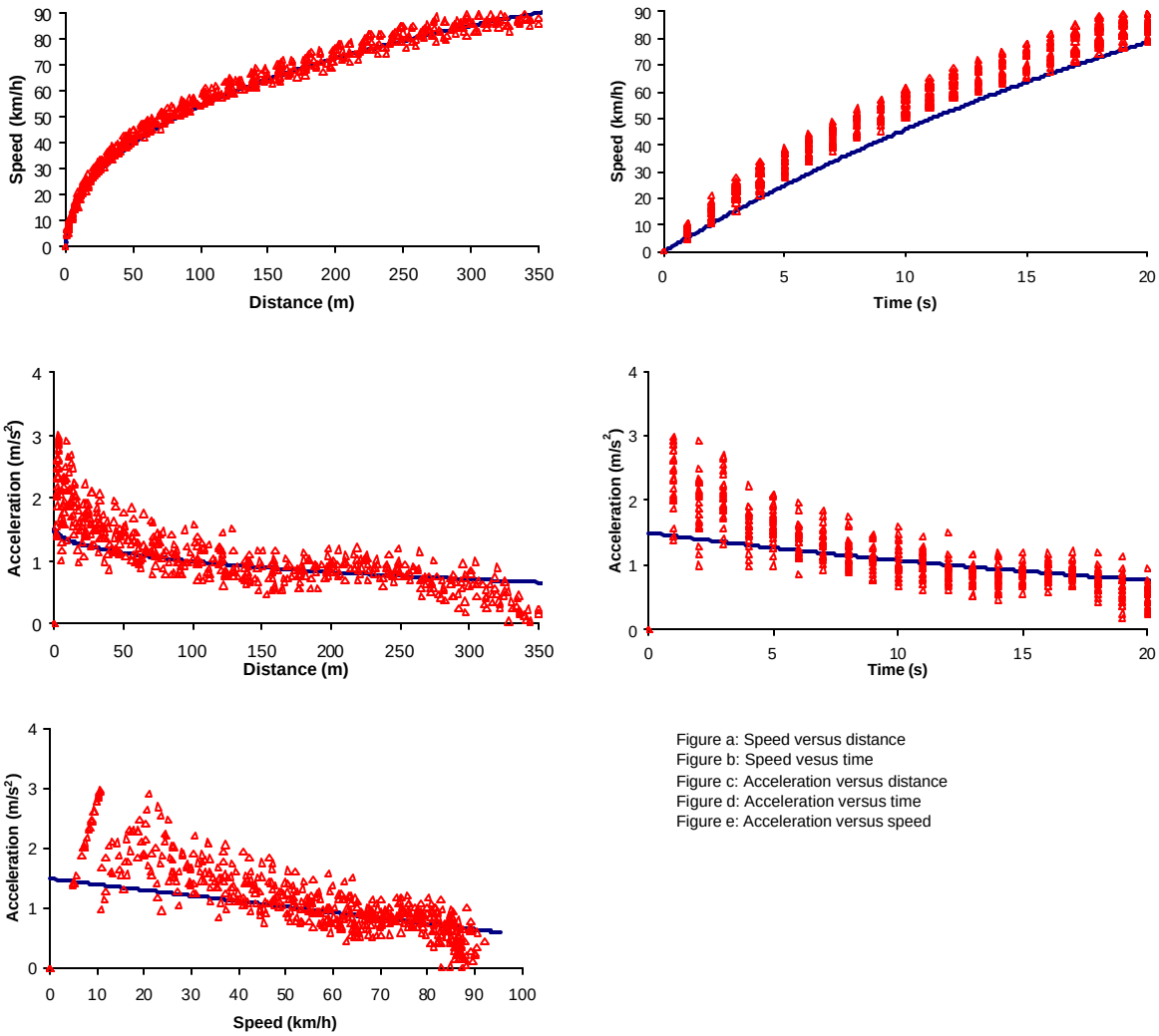

Figure a: Speed versus distance
Figure b: Speed vesus time
Figure c: Acceleration versus distance
Figure d: Acceleration versus time
Figure e: Acceleration versus speed

Figure 5-31: Sample Standard Acceleration Driver versus Linear Decay Model

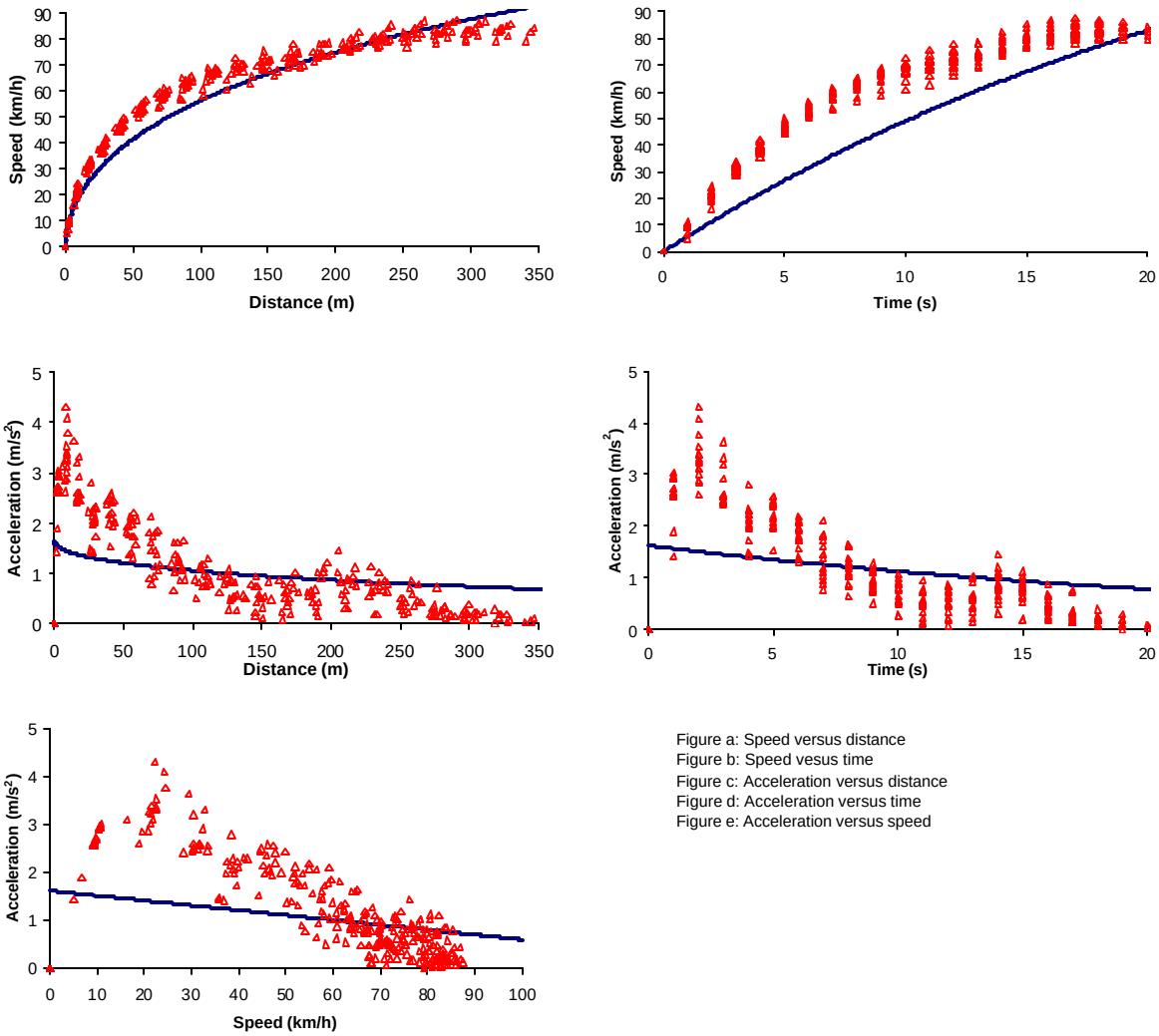

Figure a: Speed versus distance
Figure b: Speed vesus time
Figure c: Acceleration versus distance
Figure d: Acceleration versus time
Figure e: Acceleration versus speed

Figure 5-32: Sample Hard Acceleration Driver versus Linear Decay Model

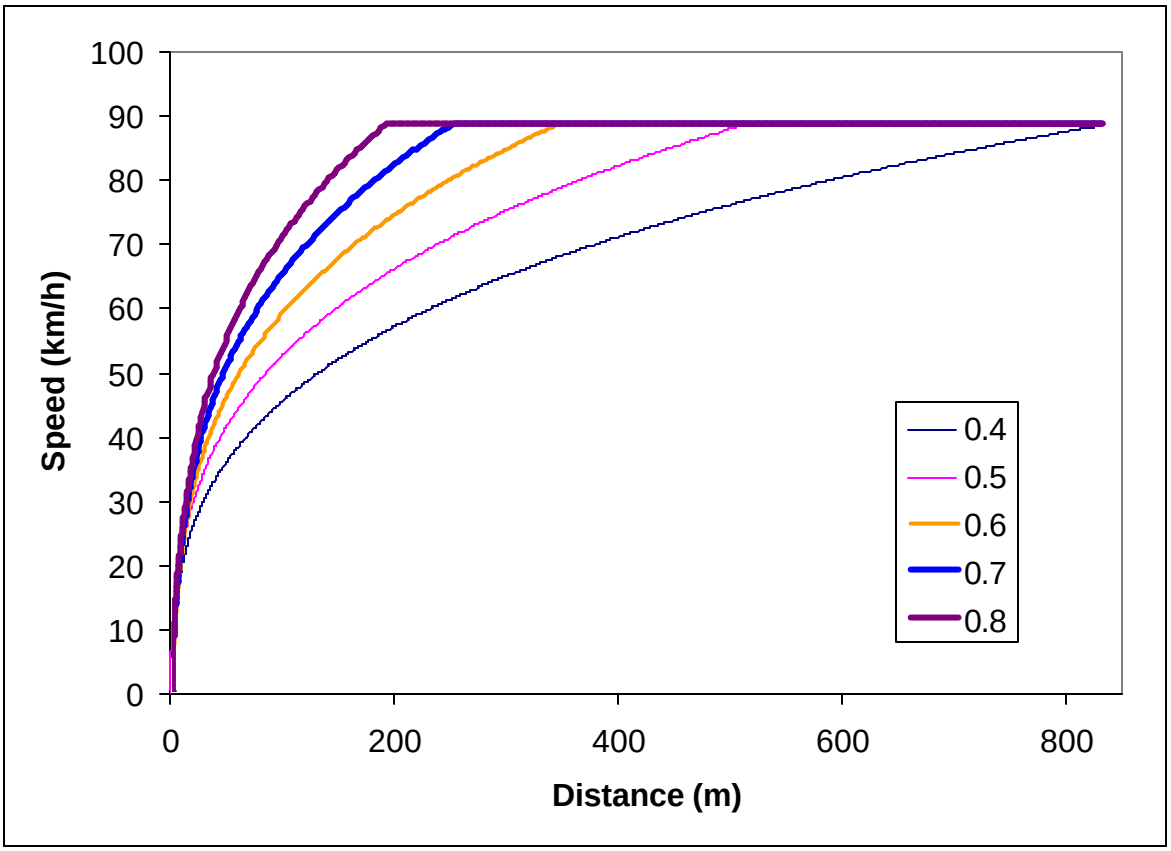

Figure 5-33: Sample Speed Profiles for Different Driver Factors

The simulation was performed to illustrate the difference in vehicle behavior between an aggressive driver, an average driver, and a passive driver. The first thing to note is the amount of time required to obtain the speed limit. The average driver takes 22.5 seconds to accelerate up to a speed of 55 mph, and accomplishes this over a distance of about 345 meters. A highly aggressive driver can reach the same speed in only 13.2 seconds in a distance of 190 meters, while a non-aggressive driver requires 51.0 seconds and 830 meters to reach 55 mph. These differences in actual driver performance are significant and could change the results of a simulation model, especially when accumulated throughout the network over time. If only average drivers are modeled in the simulation, actual roadway conditions will not be observed. This could result in the model generating inappropriate signal timings, for example.

In addition to vehicle behavior varying greatly from driver to driver, other factors related to the acceleration profile of the vehicles, including fuel consumption and emissions, can vary as well. To test the significance, the five vehicle profiles for the 850-meter simulation were input into the VT-Micro model. This model can determine the fuel consumption and emissions for any speed profile (Rakha and Ahn, 2002). The results are shown in Table 5-7. The table indicates that modeling all vehicles using the average driver behavior may overestimate fuel consumption, as the fuel consumption is lower for

both very aggressive drivers and very non-aggressive drivers. The emissions produced by the vehicle also vary greatly depending on driver aggressiveness. A highly aggressive driver emits nearly double the amount of carbon monoxide as a typical driver. This further demonstrates the need to model a distribution of drivers in the simulation.

Table 5-7: Fuel Consumption and Emissions Rates for Various Driver Types

Unit: fuel (grams), HC, CO, NOx (grams)

	Fuel Consumption	HC	CO	NOx
Factor 0.4	87.11067692	0.175094	1.186048	0.509914
Factor 0.5	90.96896729	0.17257	1.308218	0.57115
Factor 0.6	90.76632661	0.170953	1.477122	0.598116
Factor 0.7	89.39008278	0.174112	1.853774	0.585632
Factor 0.8	88.31145741	0.185001	2.846411	0.525558

Variation from Mean

	Fuel Consumption	HC	CO	NOx
Factor 0.4	-4%	2%	-20%	-15%
Factor 0.5	0%	1%	-11%	-5%
Factor 0.6	0%	0%	0%	0%
Factor 0.7	-2%	2%	25%	-2%
Factor 0.8	-3%	8%	93%	-12%

5.7 Conclusions and Recommendations

This paper has presented a modification to the Rakha vehicle dynamics model for predicting the acceleration behavior of vehicles. The modification involves applying a reduction factor to the value of maximum acceleration to account for the typical behavior of a given driver. Field data was collected for twenty drivers operating the same test vehicle. The drivers included men and women and ranged from age 21 to 45. Driver factors were observed that fit a normal distribution with a mean of 0.6 and a standard deviation of 0.08. A constant driver reduction factor throughout the run was shown to generate a good fit to the field data for most of the drivers. Males and younger drivers tended to be more aggressive in this study, but the statistical means of these groups did not vary significantly when an analysis of variance was applied. The distribution of driver reduction factors can be used with the Rakha model and incorporated into simulation models to reflect the population of drivers on the roadway more accurately.

The following recommendations for future research action are proposed to enhance the capabilities of the updated acceleration model:

1. Tests should be performed with teenage drivers and older drivers. As mentioned in the report, drivers outside the range of ages studied in this research account for nearly half the drivers on the road. These groups need to be included in future data collection to enhance the accuracy of the model. It is of particular importance to study these two groups because teenagers generally represent an aggressive group and older drivers

generally reflect more conservative driving behavior. Therefore, the statistical means of these two groups may be different from the means for the 20-45 age group.

2. Testing should be performed with other vehicles. It is unclear from this testing whether the driver factor would change based on the capability of the vehicle. For example, would the same driver accelerate more rapidly in a vehicle with more horsepower, or would the acceleration profile for a given driver be similar regardless of vehicle?

3. Testing should be done on a vehicle with manual transmission. The test vehicle used in this study was automatic transmission and therefore may have limited the ability of the drivers to accelerate at their normal levels.

4. Testing should be performed in real on-road driving conditions. The point of this research was to compare driver behavior to maximum vehicle capability in an unconstrained testing environment. Research needs to be done to determine how the typical acceleration rate varies in normal driving conditions, where car following is present.

Chapter Six:
Summary, Conclusions, and Recommendations

6.1 Summary

The paper first constructed a database of unconstrained maximum vehicle acceleration data for thirteen light duty vehicles and trucks. In addition, the paper validated a vehicle dynamics model for predicting maximum light duty vehicle acceleration rates. The model was compared to four of state-of-art acceleration models using the developed data set. Advantages of the vehicle dynamics model were presented, including its ability to accurately predict vehicle behavior with readily available input parameters and its flexibility in estimating acceleration rates of both large and small vehicles on varied terrain.

This paper then presented a modification to the vehicle dynamics model in order to predict the typical acceleration behavior of drivers. The modification involved applying a reduction factor to the value of maximum acceleration to account for the typical behavior of a given driver. Field data was collected for twenty drivers operating the same test vehicle. The drivers included men and women and ranged from age 21 to 45. Driver factors were observed that fit a normal distribution with a mean of 0.6 and a standard deviation of 0.08. A constant driver reduction factor throughout the run was shown to generate a good fit to the field data for most of the drivers. Males and younger drivers tended to be more aggressive in this study, but the statistical means of these groups did not vary significantly when an analysis of variance was applied. The distribution of driver reduction factors can be used with the Rakha model and incorporated into simulation models to reflect the population of drivers on the roadway more accurately.

6.2 Conclusions

The vehicle dynamics model proposed originally by Rakha *et al.* (2001) to predict the maximum acceleration behavior of trucks can be applied successfully to predict the maximum acceleration behavior of a variety of passenger vehicles, ranging from small subcompact cars, to larger vans, sport utility vehicles, and pickup trucks. While a variable power modification to the model is necessary to account for the build-up of power through gear shifting in trucks, this modification is not necessary when modeling cars because they have fewer gears and generally use automatic transmission. Therefore, the more-basic constant power model can be applied successfully when simulating passenger vehicles.

This vehicle dynamics model was shown to outperform other similar acceleration models recommended in the literature. The model is able to generate a good fit to field data in all possible speed profile domains, including speed versus time, speed versus distance, acceleration versus time, acceleration versus distance, and acceleration versus speed. Several limitations of existing models were found, including their reliance on field data,

and their tendency to only provide a reasonable fit to field data for the domain in which they were calibrated.

Based on a comparison study, three primary advantages of the Rakha dynamics model were observed:

1. Good Fit in all Domains: The vehicle dynamics model offers a good fit to field data in each of the domains, namely speed versus distance, speed versus time, acceleration versus speed, acceleration versus time, and acceleration versus distance. Alternatively, the other models, especially the empirical models, are designed to fit a single domain, and therefore do not fit well over all domains.

2. Model Flexibility: The vehicle dynamics model is able to adapt to different vehicle types, different pavement conditions, and travel over different terrain.

3. Simple Calibration: Another advantage of the vehicle dynamics model is that it does not require field data sets to calibrate input parameters. Specifically, input parameters can be obtained from vehicle manuals, car magazines, and/or the World Wide Web. Alternatively, the other models require field data for the calibration of input parameters.

The Rakha model can also be applied to typical driver behavior by introducing a reduction factor to the maximum acceleration model for each driver. A different factor can be chosen for each driver that will enable the model to provide a good fit to field data in each domain. The distribution of observed driver factors fit a normal distribution with a mean of 0.60 and a standard deviation of 0.08. This distribution can be used to model the driver population in simulation situations. The Rakha model was shown to be superior to similar typical acceleration models because of its ability to properly predict the acceleration profiles of the majority of drivers. Three driver types were identified, including Standard Accelerators, Gradual Accelerators, and Hard Accelerators. The Rakha model was most successful in modeling the behavior of Standard Accelerators, which comprised 70% of those tested.

6.3 Recommendations

The following recommendations for future action are suggested to further enhance the capabilities of the models presented in this paper for predicting maximum and typical acceleration levels:

1. Testing should be performed in real on-road driving conditions. The point of this research was to observe driver behavior and maximum vehicle capability in an unconstrained testing environment. Research needs to be done to determine how the typical acceleration rate varies in normal driving conditions, where car following is present.

2. Data are also required on typical vehicle acceleration during critical events, including merging with freeway traffic at an on-ramp and accelerating to overtake a vehicle. For all these scenarios vehicle acceleration models should be developed to capture driver behavior in the non-steady state car-following mode of operation.

To expand the capabilities of the typical acceleration model presented in Chapter 5, the following actions are recommended:

1. Tests should be performed with teenage drivers and older drivers. As mentioned in the report, drivers outside the range of ages studied in this research account for nearly half the drivers on the road. These groups need to be included in future data collection to enhance the accuracy of the model. It is of particular importance to study these two groups because teenagers generally represent an aggressive group and older drivers generally reflect more conservative driving behavior. Therefore, the statistical means of these two groups may be different from the means for the 20-45 age group.

2. Testing should be performed with other vehicles. It is unclear from this testing whether the driver factor would change based on the capability of the vehicle. For example, would the same driver accelerate more rapidly in a vehicle with more horsepower, or would the acceleration profile for a given driver be similar regardless of vehicle?

3. Testing should be done on a vehicle with manual transmission. The test vehicle used in this study was automatic transmission and therefore may have limited the ability of the drivers to accelerate at their normal levels.

References

1. Akcelik, R. and Biggs, D.C. (1987) *Acceleration Profile Models for Vehicles in Road Traffic*. Transportation Science, Vol. 21, No. 1.
2. Archilla, A.R., and De Cieza, A.O.F. (1999). *Truck Performance on Argentinean Highways*. Transportation Research Record 1555, Transportation Research Board, Washington, D.C.
3. Bham, G.H. and Benekohal, R.F. (2002) *Development, Evaluation, and Comparison of Acceleration Models*, Paper No. 02-3767, CD-ROM, 81st Annual Meeting of the Transportation Research Board, Washington, D.C.
4. Dockerty, A. (1966) *Accelerations of Queue Leaders from Stop Lines*. Traffic Engineering and Control. Vol. 8, No. 3.
5. Drew, D.R. (1968) *Traffic Flow Theory and Control*. McGraw-Hill.
6. Fitch, J.W. (1994). *Motor Truck Engineering Handbook*. Society of Automotive Engineers, 4th Edition.
7. Lee, C., and T. Rioux (1977), *The TEXAS Model for Intersection Traffic – Development Research Report*. University of Texas at Austin.
8. Long, G. (2000) *Acceleration Characteristics of Starting Vehicles*. Transportation Research Record, No. 1737.
9. Loutzenheiser, D.W. (1938) *Speed-Change Rates of Passenger Vehicles*. HRB Proc., Vol. 18.
10. Mannering, F.L. and Kilareski, W.P. (1990). Principles of Highway Engineering and Traffic Analysis. John Wiley & Sons.
11. *A Policy on Geometric Design of Highways and Streets* (1994). AASHTO, Washington, D.C.
12. *A Policy on Geometric Design of Rural Highways* (1954). AASHTO, Washington, D.C.
13. Rakha H. and K. Ahn (2002), "The INTEGRATION Framework for Estimating Mobile Source Emissions," Submitted for publication in the *Journal of Advanced Transportation*.
14. Rakha H. and B. Crowther (2002), *A Comparison of the Greenshields, Pipes, and Van Aerde Car-Following and Traffic Stream Models*, Accepted for publication in the Transportation Research Record.
15. Rakha H., Lucic I., Demarchi S., Setti J., and Van Aerde M. (2001) *Vehicle Dynamics Model for Predicting Maximum Truck Acceleration Levels*. Journal of Transportation Engineering, Vol. 127, No. 5.
16. Rakha H., and Lucic I. (2002) *Variable Power Vehicle Dynamics Model for Estimating Maximum Truck Acceleration Levels*, Accepted for publication in the Journal of Transportation Engineering.

17. Searle, J. (1999) *Equations for Speed, Time and Distance for Vehicles Under Maximum Acceleration*. Advances in Safety Technology, Society of Automotive Engineers Special Publications, No. 1433.

18. Society of Automotive Engineers (SAE). (1996). *Commercial Truck and Bus SAE Recommended Procedure for Vehicle Performance Prediction and Charting*. SAE Procedure J2188. Warrendael, PA.

19. Varat, M.S. and Husher, S.E. (2000), *Vehicle Impact Response Analysis Through the Use of Accelerometer Data.* Accident Reconstruction: Analysis, Simulation, and Visualization, SP-1491, Society of Automotive Engineers, Inc., Warrendale, PA.

20. Watanada, T., et al. (1987). Description of the HDM-III Model. The Highway Design and Maintenance Standard Model, Vol. 1, Johns Hopkins University, Baltimore.

Vita

Matt Snare was born in Phillipsburg, New Jersey to Parker and Sherryl Snare. He later moved to Easton, Pennsylvania with his family and went on to graduate from Easton Area High School as the salutatorian of the Class of 1997. Matt attended Virginia Tech after high school and he received a Bachelor of Science degree in Civil Engineering in 2001. Matt elected to stay at Virginia Tech for his graduate work, and he received the Charles Edward Via fellowship to pursue his graduate studies. At Virginia Tech, Matt became the president of the university chapter of the Institute of Transportation Engineers and also served as a teaching assistant. Matt will be married on September 1, 2002 to his fiancée Miriam, and the couple will be relocating to Cockeysville, Maryland where Matt will work as a traffic engineer with the consulting firm of Rummel, Klepper, and Kahl in Baltimore.